DISS. ETH NO. 22105

ROLE OF THE NOGO-A PROTEIN IN THE MATURATION AND PLASTICITY OF THE MOUSE VISUAL SYSTEM

A thesis submitted to attain the degree of

DOCTOR OF SCIENCES of ETH ZURICH

(Dr. sc. ETH Zurich)

presented by

ANNA GUZIK-KORNACKA

M.Sc., Warsaw University of Life Sciences

born on *27.10.1983*

citizen of Poland

accepted on the recommendation of

Prof. Dr. Martin E. Schwab
Prof. Dr. Stephan Neuhauss
Prof. Dr. Ulrich Suter

2014

TABLE OF CONTENT

Summary

The role of the myelin-associated protein Nogo-A, as a neurite growth inhibitor after CNS injury has been well described. However, much less is known about its physiological functions in the maturing and adult brain. Nogo-A is thought to stabilize neuronal circuits and restrict synaptic plasticity, and accordingly, has been shown to limit the experience-dependent plasticity in the visual cortex beyond the developmental critical period. In my thesis, I investigated the role of Nogo-A protein in the developmental refinement of retinal terminals and in the anatomical and the functional plasticity of the subcortical visual system in mice.

In the first part of my thesis, I analyzed the expression pattern of Nogo-A in the retina and in the subcortical and the cortical visual system as well as the expression of the two main Nogo-A receptors, Nogo-66 receptor 1 (NgR1) and sphingosine 1-phosphate receptor 2 (S1PR2). NgR1 was strongly expressed in the retinal ganglion cell (RGC) bodies and axons whereas Nogo-A was complementarily expressed in in the Müller glia in the retina, and in oligodendrocytes and neurons in the brain. In the same chapter, I examined the developmental refinement of retinal terminals, which was not affected by systemic Nogo-A deletion in knock-out (KO) mice.

In the second part of this thesis, I addressed the function of Nogo-A in the visual system plasticity using functional and anatomical readouts. Eye-specific terminal segregation in the dorsal lateral geniculate nucleus (dLGN) of adult Nogo-A KO mice was decreased as compared to wild type (WT) controls. To test the hypothesis, that this result could be attributed to a lower stability of the circuits in the Nogo-A KO mice we induced experience-dependent plasticity by right eye closure (monocular deprivation, MD). In the absence of Nogo-A, an additional desegregation of eye-specific retinogeniculate terminals occurred in the left dLGN and ectopic open-eye terminals in the right dLGN were observed. Interestingly, on the functional level,

Nogo-A KO mice exhibited increased spatial frequency sensitivity as tested by the optokinetic tracking response (OKR) test. Upon MD, the spatial frequency and contrast sensitivity of the open eye increased stronger in the Nogo-A deficient mice than WT controls.

In conclusion, the work presented in this thesis indicates that the functional and anatomical plasticity of the subcortical visual system can be restricted in the adult brain by the Nogo-A protein.

Zusammenfassung

Das myelin-assoziierte Protein Nogo-A ist in seiner Rolle als Wachstumshemmer für Neuriten gut beschrieben. Im Gegensatz dazu ist über die physiologische Funktion von Nogo-A im sich entwickelnden und im adulten Gehirn wenig bekannt. Es wird angenommen, dass Nogo-A neuronale Netzwerke stabilisiert und synaptische Plastizität einschränkt. Dementsprechend wurde gezeigt, dass Nogo-A erfahrungsabhängige Plastizität im visuellen Kortex nach der entwicklungsphysiologischen kritischen Periode limitiert.

In meiner Arbeit habe ich die Rolle des Proteins Nogo-A für die entwicklungsbedingte Verfeinerung retinaler Nervenendigungen im dorsalen Corpus geniculatum laterale (dCGL, engl. dLGN) und für die anatomische und funktionale Plastizität des subkortikalen visuellen Systems von Mäusen untersucht.

In Kapitel 2 meiner Arbeit, habe ich die Expressionsmuster von Nogo-A und den zwei Hauptrezeptoren von Nogo-A, Nogo-66 Rezeptor 1 (NgR1) und Sphingosin 1-Phosphat Rezeptor 2 (S1PR2), in der Retina und im subkortikalen sowie dem kortikalen visuellen System analysiert. NgR1 war stark in den Zellkörpern der retinalen Ganglienzellen und Axonen exprimiert, während Nogo-A komplementär in den Müller Gliazellen der Retina und in Oligodendrozyten und Neuronen des Gehirns exprimiert war. In demselben Kapitel konnte ich zeigen, dass die entwicklungsbedingte Verfeinerung retinaler Nervenendigungen im dCGL nicht durch systemische Deletion von Nogo-A in Knockout (KO)-Mäusen beeinflusst war.

Im zweiten Teil meiner Arbeit habe ich die Rolle von Nogo-A für neuronale Schaltkreis-Plastizität im visuellen System auf funktioneller und anatomischer Ebene untersucht. Im Vergleich zu Wildtyp-Mäusen war die augenspezifische Segregation von Nervenendigungen im

dCGL in Nogo-A KO Mäusen vermindert. Dies könnte auf eine verminderte Stabilität der neuronalen Schaltkreise in Abwesenheit von Nogo-A zurück zu führen sein. Um diese Hypothese zu testen induzierten wir aktivitätsabhängige Plastizität mittels einer monokularen Deprivation (MD) des rechten Auges. In Abwesenheit von Nogo-A konnte eine zusätzliche Desegregation der augenspezifischen Projektionen der Retina in den linken dCGL und ektopische Endigungen des geöffneten Auges im rechten dCGL beobachtet werden. Zusätzlich beobachteten wir auf funktioneller Ebene eine erhöhte Sensitivität für die räumliche Frequenzwahrnehmung im optokinetischen Bewegungstest. Nach MD erhöhte sich die Frequenz- und die Kontrastsensitivität stärker in Mäusen ohne Nogo-A als in WT-Kontrolltieren.

Zusammenfassend zeigen diese Resultate, dass Nogo-A einen einschränkenden Einfluss auf die funktionelle und anatomische Plastizität im adulten subkortikalen visuellen System hat.

CHAPTER 1

INTRODUCTION: MATURATION AND PLASTICITY OF THE MOUSE VISUAL SYSTEM AND THE PHYSIOLOGICAL FUNCTIONS OF THE NOGO-A PROTEIN

1. Maturation and plasticity of the mouse subcortical visual system

The precise organization of the adult brain requires activity-based rearrangements of neuronal circuits during brain maturation and later on mechanisms that can maintain the refined circuits during adulthood. The mouse visual system serves as an excellent model to study different aspects of these processes. The subcortical visual system is often used as a model system to study developmental refinement of the retinal fiber projections, whereas adult experience-dependent plasticity is usually studied in the binocular visual cortex. In the experimental part of this thesis I investigated, whether the growth inhibitory protein Nogo-A affects anatomical refinement and the adult structural and functional plasticity in the subcortical visual system. In this chapter I summarize the anatomical organization of the subcortical visual system, the mechanisms of the developmental refinement of retinal projections and the models of experience-dependent plasticity. Furthermore, I will briefly introduce Nogo-A downstream signaling and its known physiological functions.

1.1 The mouse visual system

Mice, being nocturnal animals with rather poor vision, were for long time neglected for studies of the visual system. However the basic organization of the mouse visual system has many similarities with that of higher mammalian species. Moreover, mice are born with closed eyes, and therefore the development and maturation of the visual system occurs in large part postnatally, making it accessible for experimental manipulations. The powerful genetic tools available for mice help to answer questions about the development, maturation and plasticity of the visual system which would be difficult to address in other animal models. Retinal ganglion cells (RGCs) are the only retinal neurons projecting their axons to the brain. The main visual pathway processing conscious vision consist of retinal projections to the dorsal lateral geniculate

nucleus (dLGN) in the thalamus which further relays visual information to the primary visual cortex (V1) and then to secondary visual areas [1, 2]. Retinal ganglion cells (RGCs) project also to other areas such as the superior colliculus (SC) in the midbrain, important for eye and head movement coordination, but also for other sensory and motor functions [3]. Retinal projections to the brain are retinotopically organized: adjacent neurons in the retina innervate adjacent regions in the SC and the dLGN, which further relays the topographic organization to the visual cortex. Mechanisms of the retinotopic map formation, which involve i.a. ephrin signaling, were intensively studied in the mouse visual system [4-7]. After initial targeting of visual targets based on molecular cues [4], retinal terminals undergo extensive pruning, which can be investigated in the early postnatal (P4-P8) mouse retinogeniculate and retinocollicular pathways [8, 9]. It is well established that map refinement is driven by the spontaneous retinal activity [10] but sensory experience also influences its maturation and plasticity. Monocular eye closure or rearing animals in a darkness leads to functional [11, 12] and anatomical [13] changes in the visual cortex, especially in juvenile mice during a critical period lasting from P19-32 [11]. One of the factors shown to limit visual cortex plasticity after the critical period is the myelin Nogo-A protein and its receptor NgR1 [14]. Nogo-A [15] and NgR1 [16] are also expressed in the subcortical visual system, making them plausible regulators of subcortical visual system maturation and plasticity.

1.2 Mouse subcortical visual system

Mouse eyes are positioned laterally and the region of visual space seen by both eyes comprises only the central 30-40° of the upper visual field [17]. Therefore, the majority of retinal ganglion cell axons cross at the optic chiasm, innervating the contralateral hemisphere, and only 2-3% of axons which originate from the ventrotemporal retina project ipsilaterally [18].

Figure 1 Retinal projections from the two eyes to the main retinorecipient brain areas

Retinal projections from two eyes were anterogradely traced by intraocular injection of cholera toxin β-subunit (CTb) tracers; CTb-594 (red) was injected to left eye and CTb-488 (green) to right eye. **a-d** coronal brain sections from adult C57BL/6 mouse containing main retinorecipient areas are presented in the caudal-to-rostral direction. **a** Section through the rostral region of the superior colliculus (**SC**) in the midbrain; the main target of mouse RGC axons. Retinal terminals innervate 3 superficial layers of the SC: **Zo** zonal, **SuG** superficial gray and **Op** optic layer. The superior colliculus receives mainly retinal projections from the contralateral eye, and the ipsilateral eye projections terminate in the deeper superficial gray and in the optic layer. The dorsal terminal nucleus (**DTN**) of the accessory optic system lies in a groove at the ventral end of the brachium of the SC. **b** Section through the midbrain containing pretectal nuclei: nucleus of the optic tract (**NOT**), olivary pretectal nucleus (**OPT**), posterior pretectal (**PPT**) and medial (**MPT**) pretectal nuclei. At the ventral side of the midbrain lies the medial terminal nucleus (**MTN**) of the accessory optic system. **c** Section through the rostral end of the midbrain containing rostral part of the OPT innervated at this region by both eyes. In the thalamus, there is also visible caudal end of the dorsal lateral geniculate nucleus (**dLGN**). **d** Section through the thalamus containing the dorsal (**dLGN**) and ventral (**vLGN**) lateral geniculate nuclei and the intergeniculate leaflet (**IGL**). The dLGN receives projections from the contralateral (**contra**) and ipsilateral (**ipsi**) eye reaching the thalamus through the optic tract (**OT**). **e** The first target of retinal axons after optic chiasm is the suprachiasmatic nucleus (**SCN**) in the hypothalamus; **OT** optic tract, **3V** third ventricle. Scale bar is the same for **a-e**: 500 μm.

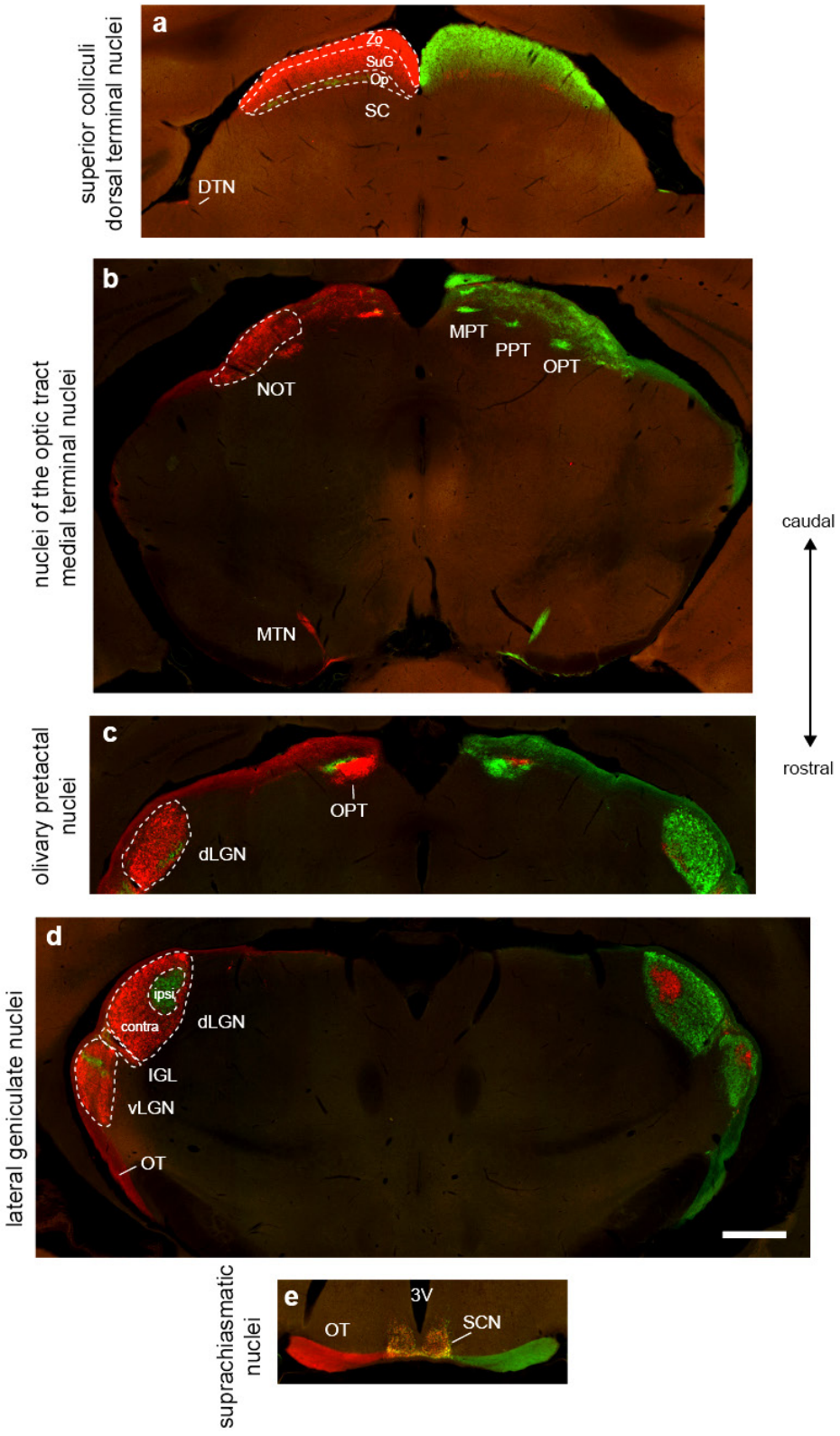
a
Zo
SuG
Op
SC
DTN
superior colliculi
dorsal terminal nuclei
b
MPT
PPT
OPT
NOT
MTN
nuclei of the optic tract
medial terminal nuclei
caudal
rostral
c
OPT
dLGN
olivary pretactal
nuclei
d
ipsi
contra
dLGN
IGL
vLGN
OT
lateral geniculate nuclei
e
3V
OT
SCN
suprachiasmatic
nuclei

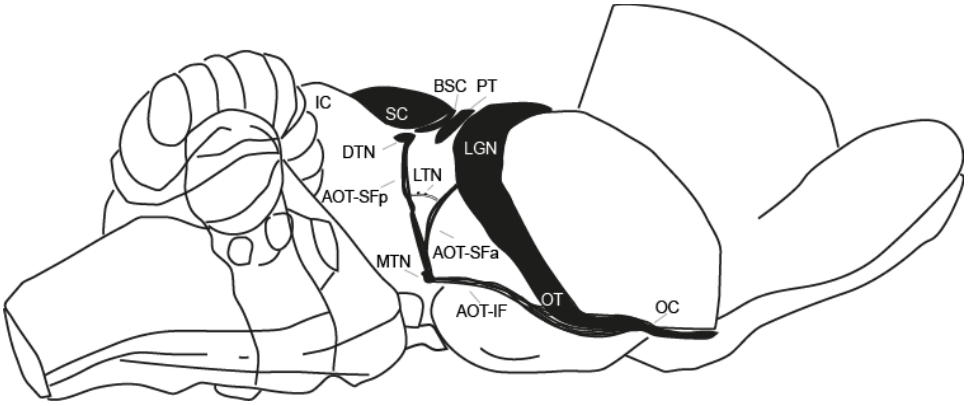

Figure 2 Organization of the retinal projections in the mouse brain including the inferior and superior fascicles of the accessory optic tract which innervate accessory optic nuclei

Accessory optic system nuclei (MTN, DTN, LTN), which are involved in optokinetic tracing responses, are innervated by retinal axons that diverge from the optic tract (**OT**) at tree main locations: at the midhypothalamus forming inferior fascicule of the accessory optic tract (**AOT-IF**), later at the level of the ventral LGN leave the anterior fibers of the superior fascicle of AOT (**AOT-SFa**) and at the brachium of superior colliculus (**BSC**) the posterior fibers superior fascicle (**AOT-SFp**). Medial terminal nucleus (**MTN**) is innervated by fibers from AOT-IF and AOT-SF. Dorsal terminal nucleus (**DTN**) is innervated by AOS-SFp and the lateral terminal nucleus (**LTN**), which is not very defined in mouse, lies in between anterior and posterior fibers of AOT-SF. Abbreviations: **OC** optic chiasm, **PT** pretectum, **SC** superior colliculus, **IC** inferior colliculus. Modified from Hayhow et al. 1960 [19] based on Yonehara et al. 2009 [20].

The first retinorecipient target after the optic chiasm is the suprachiasmatic nucleus (SCN) in the hypothalamus (Fig. 1e), which is involved in circadian responses to light [21]. The SCN is bilaterally innervated by intrinsically photosensitive RGCs (ipRGCs) expressing the photopigment melanopsin [21]. Further caudally in the thalamus lies the lateral geniculate nucleus (LGN; Fig. 1d), which is subdivided into dorsal (dLGN) and ventral (vLGN) nuclei separated by intergeniculate leaflet (IGL). The dLGN is a relay nucleus to the primary visual cortex and receives contralateral and ipsilateral eye projections in distinct domains. The vLGN and IGL are innervated by melanopsin ipRGCs and are involved in the circadian clock regulation [22, 23]. Another nucleus which is innervated by ipRGCs [23], the olivary pretectal nucleus (OPT) in the dorsal midbrain (Fig. 1c), is responsible for the pupillary light reflex. Further caudally in the midbrain lie other pretectal nuclei: the nucleus of the optic tract (NOT) as well as the medial (MPT) and the posterior (PPT) pretectal nuclei and the caudal end of the olivary pretectal nucleus (Fig. 1b). The NOT together with the dorsal terminal nucleus (DTN) of the accessory optic system (AOS), which lies ventrally from the superior colliculus (Fig.1 a), are involved in the optokinetic reflex induced by stimuli moving in the temporal-to-nasal direction [24]. At the same level as pretectal nuclei, at the ventral part of the midbrain, lies the medial terminal nucleus (MTN) of the AOS (Fig. 1b) which is responsible for the optokinetic reflex in response to upward and downward moving stimuli. The accessory optic system takes its name from the fact that the retinal axons innervating it diverge from the main optic tract, forming inferior and superior fascicle of the accessory optic tract (AOT-IF and AOT-SF; Fig. 2). AOS nuclei are innervated exclusively by the crossed projections [24, 25]. Further caudally lies the main target of RGC axons, the superior colliculus (SC) (Fig. 1a). In the mouse, virtually all RGCs project to the superior colliculus [26], which corresponds to the optic tectum in lower vertebrates, whereas in primates the dLGN is the main target of RGCs and less than 10% of

fibers project to the SC [27]. The SC consists of seven layer from which tree superficial layers, the zonal (Zo), the superficial gray (SuG) and the optic layer (Op), are innervated by the retina [26]. The superior colliculus is mainly innervated by the contralateral eye, while sparse ipsilateral eye projections go to the deeper SuG and Op layers in the rostral and medial part of the SC (Fig. 1a) [28].

1.3 Establishment of the retinotopic maps

Mechanisms of the correct retinotopic map establishment, which involve mainly Eph and ephrin signaling, have been intensively studied in the developing chick optic tectum and the mouse superior colliculus [29, 30]. At perinatal ages, EphA receptors, including EphA5 and 6, are expressed in the mouse RGCs in the temporal-to-nasal (T-N) high-to-low gradient, whereas the ephrin-A ligands, mainly A2 and A5, are highly expressed at the posterior end of the SC (Fig. 3a; reviewed in [4, 31]). Temporal and nasal RGC axons terminate along the anterior-posterior (AP) axis of the SC. Mediolateral targeting is mediated by EphBs, including B1-B4, expressed in the RGCs in a ventral-to-dorsal gradient and by Ephrin-B1 expressed highly in the medial SC, which acts as a branch attractant [32]. Therefore, RGC axons from the ventral retina with high EphBs expression, preferentially terminate in the medial SC, whereas dorsal RGC axons in the lateral SC. Apart from ephrins, Wnt-Ryk signaling is involved in the mediolateral SC targeting [33]. The mechanisms of the dLGN map formation are less investigated but Eph-As and ephrin-As are also involved in this process [5, 34]; for details see Fig. 3a. RGC axons initially overshoot their proper termination zones (TZ) and then form interstitial branches preferentially close to their future TZ. The mechanisms by which branch formation is biased towards the appropriate location are not fully understood; however TrkB-BDNF signaling was proposed to be involved in this process [30].

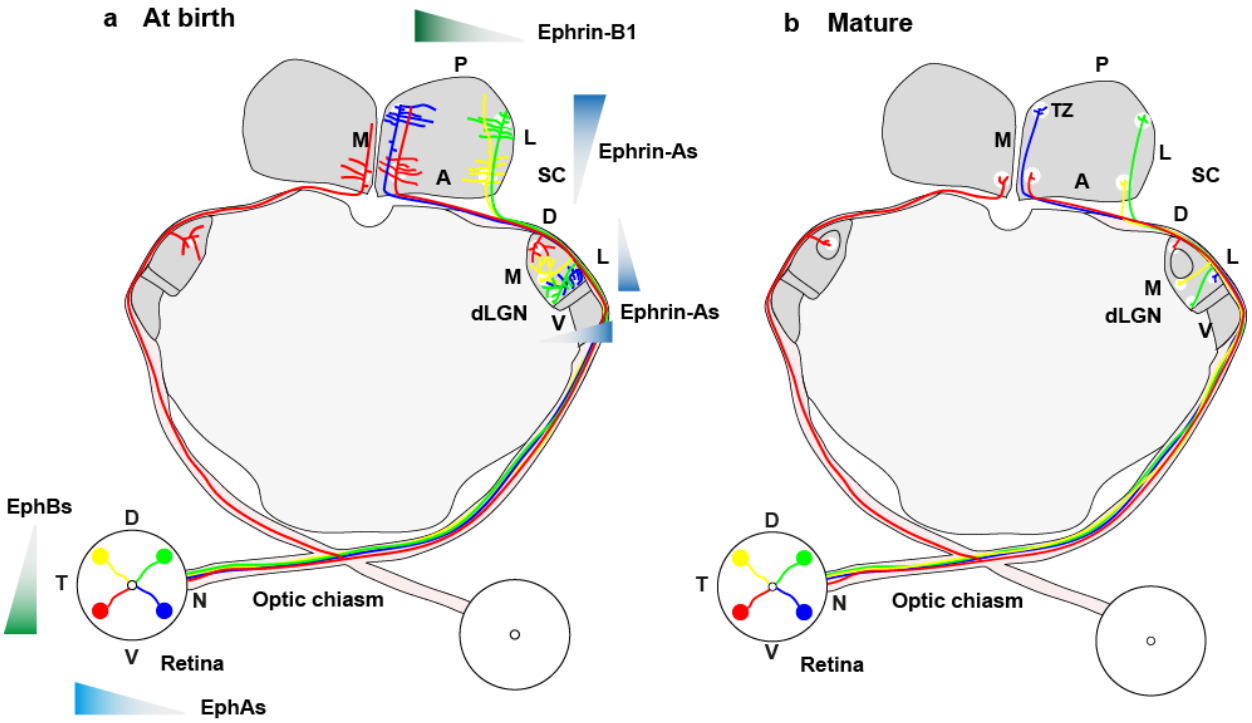

Figure 3 Development of the retinotopic maps in the mouse dorsal lateral geniculate nucleus (dLGN) and the superior colliculus (SC)

a At birth, retinal ganglion cells (RGCs) project to the dLGN and the SC based on the complementary expression of the Eph receptors in the retina and the ephrins in the target structures. Several EphA receptors are expressed in the RGCs in the temporal-to-nasal (**T-N**) high-to-low gradient. In the **SC**, ephrin-As, including ephrin-A2 and A5 are expressed in the anterior-to-posterior (**A-P**) low-to-high gradient. RGCs from temporal retina, with high **EphAs** receptor expression, are more sensitive to their repulsive ligands **ephrin-As**, and therefore project to the anterior SC, whereas RGCs from N retina project to the posterior SC. Targeting along the mediolateral axis (**M-L**) of the SC is determined by the **EphBs** ventral-to-dorsal (**V-D**) high-to-low expression gradient in the retina and by the M-L high-to-low expression of **ephrin-B1** in the SC, which acts as a branch attractant. Axons from the ventral retina project therefore medially and those from the dorsal retina more laterally in the SC. In the **dLGN**, ephrin-A2 and A5 are expressed in the anterior-ventral-lateral (high) to posterior-dorsal-medial (low) gradient. The dLGN is a three-dimensional structure; therefore not all projections shown on the scheme are located in the same A-P plane. In the dLGN, **NV** axons (**blue**) terminate in the most anterior part of the nucleus, near the optic tract at the ventral side. **ND** axons (**green**) project to posterior half of the nucleus to the ventromedial location. **TV** axons (**red**), apart from projecting ipsilaterally, in the contralateral dLGN terminate in the middle of the A-P axis in the most dorsal part of the nucleus. **TD** axons (**yellow**) project the posterior half of the nucleus just below the ipsilateral-eye area. **a** At birth in the SC and the dLGN, RGC axons overshoot their proper termination zones (**TZ**; white circles) and form several branches with a bias towards the TZ. Axonal overshoots and inappropriate branches are eliminated during first postnatal week based on the spontaneous retinal activity, leading to the precise innervation of the mature SC and the dLGN **b**.

The refinement of the imprecise retinotopic maps is mediated by the spontaneous retinal activity, and in the SC and the dLGN occurs ~P4-P8 [9]. The most widely used model system to study this process is the segregation of the eye-specific retinal projections in the dLGN [35] which I will summarize in the next paragraph.

1.4 Eye-specific segregation of the retinal input in the dorsal lateral geniculate nucleus

Retinal projections which cross at the optic chiasm innervate the dLGN at embryonic day 15-16, whereas the ipsilateral projections arrive on postnatal day 0-2 and occupy the dorsal half of the nucleus [28]. This initial targeting is influenced by the complementary pattern of Eph receptors and ephrin expression in the RGC axons and the LGN as described in the previous paragraph [5, 7], but might also be influenced by the spontaneous retinal activity which occurs even during embryonic development (Fig. 4d) [29]. At postnatal days 2-4, the terminals from the two eyes are widely distributed throughout the dLGN in overlapping territories (Fig. 4a',a'',b) and each LGN neuron receives many weak synaptic contacts from both eyes (Fig. 4c) [30]. During the first postnatal days, cholinergic starburst amacrine cells generate retinal activity waves [31] (Fig. 4d) which are relatively slow and therefore not correlated between two eyes; they allow for specific strengthening of terminals from only one eye (Fig. 4c) [32, 33]. This spontaneous retinal activity leads to the coarse-scale refinement of retinal terminals and to the segregation of eye-specific domains in the dLGN by P10 (Fig. 4a''',b) [34, 35]. The weak synaptic terminals are further eliminated and the remaining ones strengthened by a mechanism depending on the stage III glutamatergic retinal waves, which are generated by retinal bipolar cells (Fig. 4c,d) [36, 37]. Disruption of the stage III waves with the pharmacological blocker APB [36] or in mutant mice in which stage III waves are abnormally frequent and persistent [37], leads to desegregation of segregated eye-specific projections in the dLGN. After eye opening, occurring in mice ~ P12-14,

stage III waves are blocked by the maturing retinal inhibitory circuits [38, 39], and retinal activity starts being driven by the visual experience. A recent study, using electrophysiological recordings in the LGN slice preparation, indicated that visual experience plays a crucial role in the maintenance of retinogeniculate synapses [40]. Dark rearing after initial visual experience led to the weakening and increase in the number of retinogeniculate synapses. The effect of dark rearing was limited to a restricted sensitive period, finishing at the end of the first postnatal month [41]. Whether this kind of plasticity is paralleled by structural plasticity of retinal terminals and potential desegregation of eye-specific domains in the dLGN is unknown. Furthermore, the molecular mechanisms by which the plasticity of the retinogeniculate pathway is restricted in the adult brain were not investigated.

1.5 Experience dependent plasticity of the visual system

1.5.1. Ocular dominance plasticity

Ever since the landmark study of Torsten Wiesel and David Hubel [42] on the role of experience in the preferential responses of neurons in the cat binocular visual cortex to one or the other eye, ocular dominance (OD) serves as a model to study the mechanisms of experience–dependent brain plasticity. In this work, monocular eye-closure (monocular deprivation, MD) in juvenile kittens led to weakening of the responses from the deprived eye and strengthening of the open eye responses in the binocular visual cortex. Further work determined that the OD plasticity was limited to the critical period ending in cats around the third postnatal month [43]. Since then, many studies confirmed these results in other mammalian species including mouse in which 4 days of MD during the critical period (P19-32) leads to pronounce OD shift [10, 38].

Figure 4 Eye-specific segregation of retinal terminals in the dorsal lateral geniculate nucleus

a Tracing of retinal projections from both eyes to the LGN using cholera toxin β-subunit tracers (CTb, left eye CTb-594, red; right eye CTb-488, green). **a'** At postnatal day 2 (P2), retinal terminals from both eyes strongly overlap in the dorsal part of the dLGN (ipsilateral green, contralateral red). **a''** At P4, retinal terminals from the ipsilateral eye are more restricted to the dorso-medial part of the dLGN but they are still strongly overlapping with the contralateral eye projections. **a'''** By 10 postnatal day, retinal projections from the ipsi- (green) and contralateral eye are well segregated into eye-specific domains; scale bar 200 μm. **b** Scheme showing that the eye-specific projections in the dLGN are strongly overlapping during first postnatal days (P1-P4) but the coarse-scale refinement is finished by postnatal day 10. **c** Example of the synaptic refinement on one dLGN neuron from the right eye ipsilateral domain. Early postnatally, the LGN neuron is contacted by many weak synapses from both eyes. By P10, based on the spontaneous activity (stage II waves) projections from the right eye are eliminated and afterwards the remaining left eye synapses are further strengthened (fine-scale refinement). In adult animals LGN neurons receive 1-3 retinal inputs. **d** Developmental phases of retinal activity: Before birth, mouse retina spontaneously generates slow cholinergic waves called stage I waves which are propagated through gap junctions. Postnatally, stage II cholinergic waves mediate coarse-scale refinement of retinal terminals. Stage III glutamatergic waves are important for the maintenance of retinal terminals. Recent studies indicate that sensory experience also plays a role in the maintenance process. **c** and **d** are based on drawings from [44, 45].

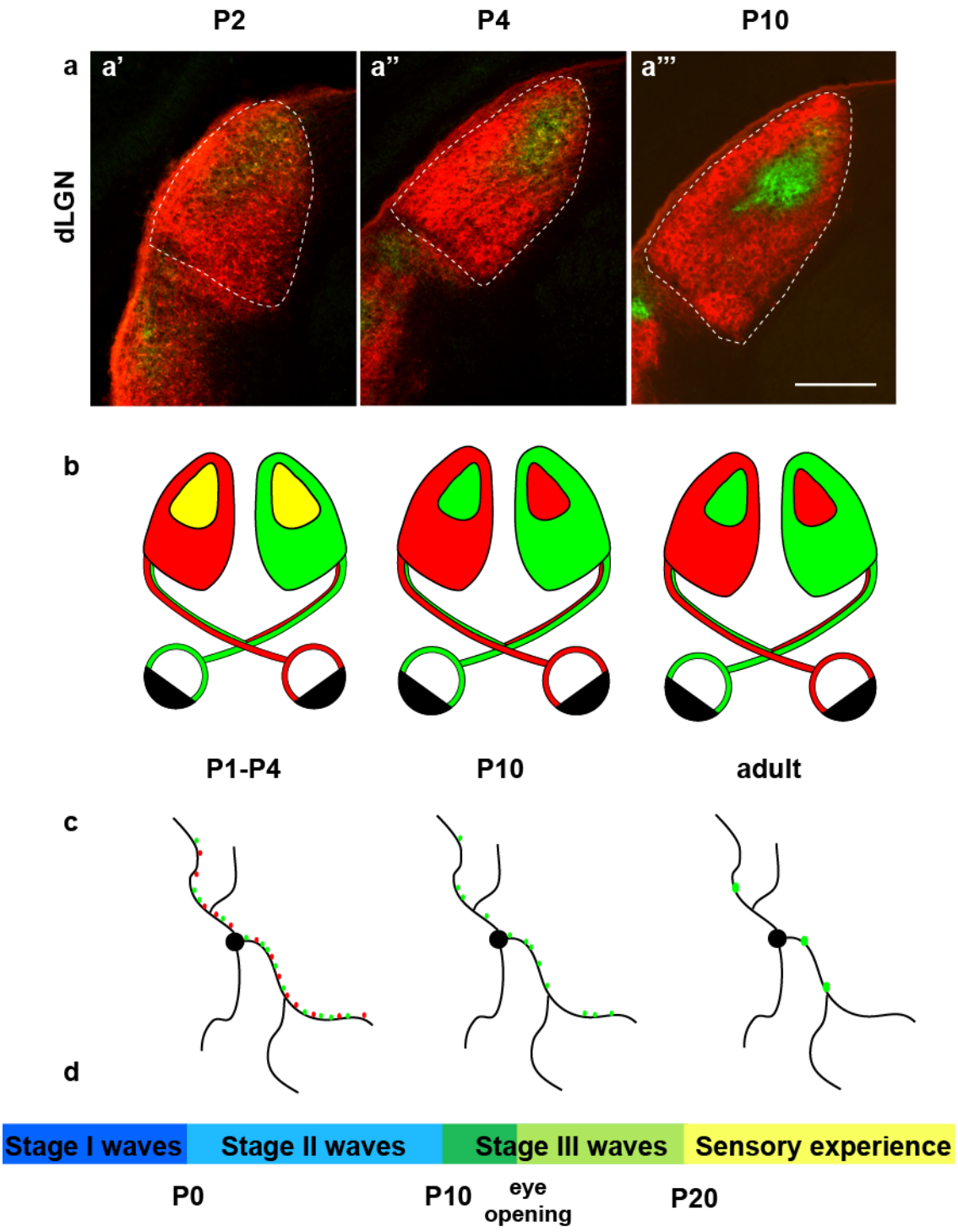
P2
P4
P10
a
a'
a''
a'''
dLGN
b
P1-P4
P10
adult
c
d
Stage I waves
Stage II waves
Stage III waves
Sensory experience
P0
P10
eye opening
P20

However, recent research in mice indicated that the OD plasticity is not strictly limited to the critical period and can also occur in adult animals after longer periods of deprivation or after repeated MD [39-41]. Mechanisms of juvenile and adult OD plasticity differ from each other [39]. During the critical period, there is first pronounced weakening of the closed-eye synapses followed by the strengthening of the open-eye synapses [42]. In adult animals, however, the NMDA-receptor dependent strengthening of open-eye synapses is more apparent than closed-eye input weakening and therefore the effects of MD probably need a longer time to be manifested [39, 42, 43]. Molecular and cellular mechanisms governing the OD plasticity are not fully understood. It is known that the maturation of the inhibitory circuit in the visual cortex is essential for the initiation of the OD plasticity during the critical period. In mice deficient in the GAD65 enzyme, important for GABA synthesis, MD does not cause any OD shift but local restoration of inhibition by diazepam can rescue the phenotype [46]. Several studies addressed also factors that limit OD plasticity during adulthood. Cortical inhibition is also involved in the closure of the critical period and reducing it locally with pharmacological blockers (MPA or picrotoxin) [47], affecting neuromodulation with fluoxetine [48] or by enriched environment housing [49, 50] can increase OD plasticity in adult animals. Structural factors such as myelin and perineuronal nets (PNNs) are also involved in the decreased plasticity during adulthood. PNNs, the extracellular matrix structures compose of chondroitin sulfate proteoglycans (CSPGs), mature around the end of critical period and are enriched around cortical interneurons. They are involved in the synapse stabilization as shown by the effects of their local digestion in the visual cortex: chondroitinase ABC enzyme increases adult OD plasticity [51]. Myelin in the visual cortex also matures around the end of critical period and systemic deletion of the myelin protein Nogo-A or its receptor NgR1 [14] restored juvenile-like plasticity in adult mice, which suggests that the Nogo-A deficient myelin provided less inhibitory environment. However, Nogo-A

protein is also expressed by neurons and therefore the observed plasticity might be mediated directly by neuronal Nogo-A [52, 53].

1.5.2. Plasticity of optokinetic reflexes

Eye movements can be divided into two broad categories: movements that stabilize the retina in respect to the visual world and movements that shift the retina in respect to the world. Gaze-shifting movements are important to adjust the position of the fovea, the region in the central retina with high density of photoreceptors. Mice lack a fovea and therefore they do not display apparent gaze-shifting movements. In contrast, as other afoveate animals, mice exhibit robust behaviors that stabilize the retina in respect to the world. One type of those compensatory gaze-stabilizing eye movements is the vestibular-ocular reflex (VOR), which generates compensatory eye movements in opposite direction during head rotation or translation to maintain the gaze on a stationary object. On the other hand, the large-field movements in the visual surround trigger spontaneous, compensatory eye and head movements, which follow the stimulus, known as the optokinetic response (OKR). When the animal is unrestrained, the motion of visual field triggers not only eye but also reflexive head and neck movement which can be easily monitored by the observer [54]. The OKR is triggered by stimuli moving slowly in three main directions: temporal-to-nasal, upward and downward [25]; they are detected by the On direction-selective ganglion cells (DSGCs) [55], but On-Off DSGCs may also contribute to the OKR [56, 57]. On and On-Off DSGCs project to the pretectal nucleus of the optic tract (NOT) and the terminal nuclei of the accessory optic system (AOS) [56]. The horizontal OKR is mediated by the NOT and the dorsal terminal nucleus (DTN). The OKR is usually tested by presenting to animals rotating sine wave black and white gratings and monitoring the evoked eye or head movements [54, 58]. By increasing the spatial frequency of the grating or decreasing contrast one can determine the

spatial frequency and the contrast sensitivity threshold. The head OKR spatial frequency threshold for adult C57BL/6 mice is approximately 0.4 cycles per degree (c/d) [54] which is a bit lower than the cortical visual acuity approaching 0.6 c/d [59]. The horizontal head OKR is triggered by a stimulus moving in the temporal-to-nasal direction whereas the nasal-to-temporal direction does not induce head tracking behavior. Therefore, it is possible to test spatial frequency and contrast sensitivity independently for both eyes, simply by changing the direction of the stimulus. It has also been described that the OKR can undergo plastic changes. Upon monocular deprivation, the spatial frequency and contrast sensitivity of the open eye increases over time, whereas the performance of the closed eye is not affected after eyelid reopening [60]. The mechanism of the OKR plasticity after MD is not fully understood. It has been suggested that the visual cortex is responsible for the increased visual performance after MD and accordingly, pharmacological cortex inactivation blocked the MD effect [60]. However, after bilateral visual cortex aspiration, MD still led to a moderate increase in spatial frequency sensitivity [60], suggesting that other circuits including possibly indirect efferent projections from NOT and DTN to the oculomotor and vestibular regions of cerebellum [61] might be involved in this visual improvement. The molecular bases of this plasticity have not been addressed so far, and therefore in chapter 3, we investigated whether Nogo-A protein restricts this type of plasticity similarly to its role in the cortical OD plasticity.

2. The Nogo-A protein in the CNS

2.1 Nogo-A signaling pathways

Nogo-A is well known as a myelin-associated protein, inhibiting neurite growth after spinal cord injury or stroke [62]. However, it is also endogenously expressed in myelin and neurons under physiological conditions [63]. In the intact CNS, it plays a role in the stabilization of neuronal circuits [64] and restriction of synaptic plasticity [52]. Nogo-A protein contains two main inhibitory domains: the C-terminal Nogo-66 domain and the Nogo-A Δ20 domain in the middle of the Nogo-A-specific, extracellular region [65]. Nogo-66 binds to the Nogo-66 receptor 1 (NgR1) [66], whereas the Nogo-A Δ20 domain binds to the newly identified G-protein coupled receptor sphingosine 1-phosphate receptor 2 (S1PR2) [67] (Fig. 4). Both domains, Nogo-66 and Δ20, activate the small GTPase RhoA (Fig. 5a). Downstream signaling modulates actin and microtubule cytoskeleton dynamics: RhoA activates its effector ROCK which further transduces growth inhibitory signals through cofilin or myosin light chain 2 (MLC2) to F-actin and through collapsin response mediator protein 2 (CRMP2) to microtubules. Apart from the main signaling pathway, the Nogo-A Δ20 region has been shown to be internalized (Fig. 5b) together with its receptor, forming signaling endosomes transported retrogradely from the growth cone to the cell body where they lower the phosphorylation state of the cyclic AMP response element binding protein (CREB) transcription factor and thereby possibly inhibit growth-related gene expression [62, 67]. However, the mechanisms by which the Δ20 fragment could be cleaved off from full length Nogo-A protein are not clear yet. Recently, Δ20 but not Nogo-66 mediated growth cone collapse has been shown to be dependent on mammalian target of rapamycin (mTOR) pathway-activated protein translation [68] (Fig. 5c). Apart from Nogo-A, two other myelin inhibitory proteins, myelin-associated glycoprotein (MAG) and Oligodendrocyte-myelin glycoprotein

Figure 5 Nogo-A signaling pathways

Nogo-A exerts its inhibitory action mainly through two domains, the Nogo-66 (red) and the Nogo-A Δ20 region (green). Nogo-66 binds to the GPI-anchored NgR1 receptor which forms a complex with two co-receptors Lingo1 and p75 or Troy enabling signal transduction. The NgR1 signaling complex activates RhoA-GTPase which regulates cytoskeleton dynamics and mediates growth inhibitory action of Nogo-A. The Nogo-A Δ20 domain binds to sphingosine 1-phosphate receptor 2 (S1PR2) activating G_{13} protein and further LARG protein which also activates RhoA. Therefore, signaling from both Nogo-A inhibitory domains converge on the RhoA pathway. **a** RhoA activates ROCK protein which phosphorylates several protein involved in actin and microtubule dynamics. Phosphorylated LIM kinase phosphorylates and thereby inactivates cofilin, an F-actin-severing protein. Inactive cofilin attenuates F-actin reorganization. ROCK may also activate slingshot phosphatase (SSH) which activates cofilin and therefore increases F-actin depolymerization at the minus end of filaments, thereby preventing their reassembly. ROCK may activate also myosin light chain 2 (MLC2) which induces actomyosin contraction promoting filopodia retraction. Phosphorylation and thereby inactivation of the collapsin response mediator protein 2 (CRMP2) destabilizes microtubules. **b** The Nogo-A Δ20 fragment has been shown to be internalized together with its receptor S1PR2 by pincher mediated endocytosis forming signaling endosomes. Signalosomes can be retrogradely transported along the axon to the cell body and modulate growth related gene expression by decreasing CREB phosphorylation. **c** Recently, Δ20 but not Nogo-66 mediated growth cone collapse has been shown to be dependent on the protein synthesis involving the mTOR pathway. The Δ20 region has also been shown to activate indirectly integrin signaling.

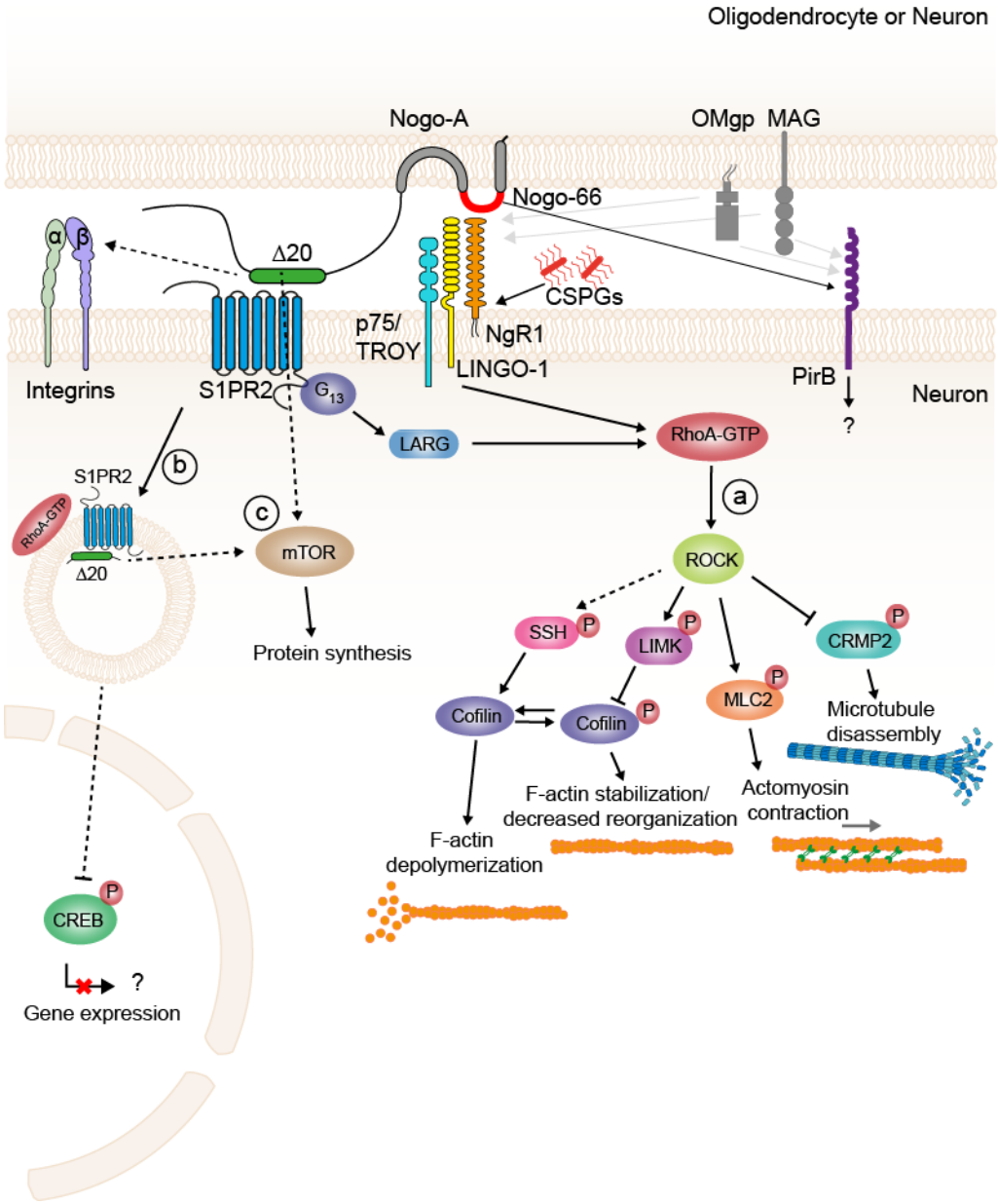
Oligodendrocyte or Neuron
Nogo-A
OMgp
MAG
Nogo-66
α
β
Δ20
CSPGs
p75/
TROY
NgR1
LINGO-1
PirB
Neuron
?
Integrins
S1PR2
G13
LARG
RhoA-GTP
b
S1PR2
RhoA-GTP
Δ20
c
mTOR
a
ROCK
Protein synthesis
SSH
P
LIMK
P
CRMP2
P
Cofilin
Cofilin
P
MLC2
P
Microtubule
disassembly
F-actin stabilization/
decreased reorganization
Actomyosin
contraction
F-actin
depolymerization
CREB
P
?
Gene expression

(OMgp), and chondroitin sulfate proteoglycans (CSPGs) have been shown to bind to the NgR1 receptor and to activate RhoA-ROCK pathway [76, 77]. Nogo-66, MAG and OMgp also bind to the paired immunoglobulin-like receptor B (PirB) but its downstream signaling is less well understood [78]. The temporal and spatial pattern of expression of different Nogo-A signaling components may be crucial for the final signaling outcome.

2.2 Physiological functions of the Nogo-A protein in the CNS

Nogo-A has been discovered as a main component of differentiated oligodendrocytes and myelin which inhibits neurite growth, neuroblast migration and fibroblast spreading and migration [77]. Studies using Nogo-A blocking antibodies in vivo confirmed it relevance as an inhibitor of neurite sprouting: suppression of Nogo-A after spinal cord injury and stroke enhanced axonal sprouting and regeneration and was accompanied by functional recovery [78, 79]. Since the observation that acute Nogo-A neutralization can induce sprouting of the non-injured axons in the cerebellum [64] it has been hypothesized that Nogo-A may restrict structural plasticity in the intact CNS. Several studies confirm this hypothesis; for review see [69]. Nogo-A has been also shown to limit dendritic complexity and synaptic transmission of Purkinje cells in cerebellum [70]. Apart from neurite growth, Nogo-A was shown to stabilize dendritic spines in the hippocampus [71], where Nogo-A neutralization and to the lesser extent its genetic deletion leads to more immature spine morphology. This effect seems to be mediated by NgR1, since single cell knock-down of NgR1 reproduced the Nogo-A neutralization phenotype. These results are in line with recent findings that Nogo-A limits synaptic long term potentiation (LTP) in the CA3-CA1 pathway of hippocampus and motor cortex [52, 53]. The synaptic plasticity function might be at least partially mediated by neuronal Nogo-A, as miRNA-mediated neuronal knock-down reproduced this phenotype in rats [53]. In several brain regions, including the hippocampus and

cerebellum, Nogo-A and the NgR1 but also S1PR2 are complementarily expressed in the pre- and postsynaptic elements [67, 70, 71]. Both Nogo-A receptors, NgR1 [52] and S1PR2 [67], have been shown to restrict LTP, most likely by converging on the RhoA-ROCK signaling pathway which is implicated in the LTP mediated effects on spine morphology [72]. The growth stabilizing function of Nogo-A might be also linked to the tonic down-regulation of growth-related genes and may involve retrograde signalosome transport along axons affecting the growth program in the opposite way than retrograde signaling of neurotropic factors [62].

In the visual system, Nogo-A/B and the receptor NgR1 are involved the closure of the critical period and restriction of adult OD plasticity [14]. Short time monocular deprivation (4 days) in the adult Nogo-A/B or NgR1 knock-out (KO) mice was sufficient to promote OD shift as detected by single unit recordings. However, the anatomical bases of this plasticity were not investigated. It has been reported that the increased number of the layer 5 pyramidal neuron apical dendritic spines in binocular cortex correlates with the increased responsiveness to the non-deprived eye [73]. Therefore, it is most likely that the effects of a short term deprivation in Nogo-A/B or NgR1 deficient mice are mediated by synaptic plasticity and not by large scale growth and reorganization of the circuit. PirB, the other Nogo-66 receptor, has been also observed to restrict OD plasticity during and after the critical period [74]. In this study, monocular enucleation (ME) for 5 to 10 days led to marked widening of the neuronal activity-associated *Ark* mRNA expressing region in the layer 4 of binocular visual cortex in the PirB KO mice as compared to wild-type controls. This suggests that growth and expansion of thalamocortical projections from the remaining eye may be increased in the absence of PirB.

Much less is known, about the role of Nogo-A during synaptic refinement at the early postnatal life. One of the model systems of developmental synaptic refinement is the elimination of surplus

climbing fibers (CF) innervating Purkinje cells (PC) in the cerebellum during the third postnatal week, leading to single CF innervation of a given PC. In Nogo-A deficient mice, the elimination of CF was transiently decreased but excessive fibers were eliminated by P28 [70]. Moreover, in the Nogo-A KO cerebellum, each CF appeared to make more vGLUT2 positive synapses on PC dendrites than in WT brains, suggesting that in the absence of Nogo-A CF had more complex terminal arbors. Whether Nogo-A is also involved in the refinement of retinogeniculate terminals is unknown.

3 Conclusions

In this chapter I have described the anatomical organization of the adult mouse subcortical visual system and some of the known mechanisms which underlie the retinotopic map formation and its developmental refinement. Spontaneous neuronal activity in the retina plays a fundamental role in the maturation of the retinal projections. The molecular mechanisms governing this process are not fully understood. After the maturation phase, the subcortical visual system has often been thought to be insensitive to sensory experience. However, recent studies indicate that retinogeniculate synapses are more plastic than previously assumed. The molecular mechanisms that limit subcortical plasticity in adult brains have not been investigated so far. I have also introduced the most widely used models of experience-dependent plasticity, the ocular dominance (OD) of neurons in the binocular visual cortex, as well as the optokinetic response which is mediated by cortical and subcortical structures and can undergo plastic changes upon monocular deprivation (MD). One of the factors that was shown to limit OD plasticity in the adult cortex is the Nogo-A protein and its receptor NgR1. Nogo-A has also been shown to influence the developmental refinement of climbing fibers in the cerebellum. Therefore we decided to investigate whether Nogo-A regulates developmental refinement and adult plasticity of retinogeniculate terminals as well as functional plasticity of the optokinetic response in the adult mouse brain.

4 Aims of the thesis

To be able to hypothesize about the possible role of Nogo-A and its receptors in the maturation and plasticity of subcortical visual system it is necessary to know their pattern of expression. Therefore, in the chapter 2, I have analyzed the expression profile of Nogo-A as well as its receptors NgR1 and S1PR2 in the developing and adult retina. Furthermore, I analyzed the cellular localization of the Nogo-A protein in the optic nerve, the lateral geniculate nucleus and in the visual cortex of adult mice. To determine whether Nogo-A regulates the developmental refinement of retinogeniculate terminals, in chapter 2, I have analyzed eye-specific terminal segregation in the dorsal lateral geniculate nucleus of Nogo-A deficient mice at postnatal day 10, just after the refinement.

To determine if Nogo-A restricts the anatomical plasticity of the adult subcortical visual system, in chapter 3 I have analyzed the eye-specific projection segregation in the dLGN of adult mice at postnatal day 60, well beyond the subcortical and cortical critical period. I further tested whether visual experience influences anatomical plasticity of retinal projections in the adult brain and whether Nogo-A is involved in the restriction of this plasticity. To answer whether Nogo-A deletion influences visual function of adult mouse, I measured the spatial frequency and contrast sensitivity using the optokinetic tracking response (OKR). Furthermore, to understand if Nogo-A can restrict plasticity on a functional level I promoted enhancement of the OKR by monocular deprivation and analyzed spatial frequency and contrast sensitivity in wild-type and Nogo-A knock-out mice.

References

1. Wang, Q. and A. Burkhalter, *Area map of mouse visual cortex.* J. Comp. Neurol., 2007. **502**(3): p. 339-57.
2. Simmons, P.A., V. Lemmon, and A.L. Pearlman, *Afferent and efferent connections of the striate and extrastriate visual cortex of the normal and reeler mouse.* J. Comp. Neurol., 1982. **211**(3): p. 295-308.
3. Gandhi, N.J. and H.A. Katnani, *Motor functions of the superior colliculus.* Annu. Rev. Neurosci., 2011. **34**: p. 205-31.
4. McLaughlin, T. and D.D. O'Leary, *Molecular gradients and development of retinotopic maps.* Annu. Rev. Neurosci., 2005. **28**: p. 327-55.
5. Pfeiffenberger, C., et al., *Ephrin-As and neural activity are required for eye-specific patterning during retinogeniculate mapping.* Nat. Neurosci., 2005. **8**(8): p. 1022-7.
6. Pfeiffenberger, C., J. Yamada, and D.A. Feldheim, *Ephrin-As and patterned retinal activity act together in the development of topographic maps in the primary visual system.* J. Neurosci., 2006. **26**(50): p. 12873-84.
7. Huberman, A.D., et al., *Ephrin-As mediate targeting of eye-specific projections to the lateral geniculate nucleus.* Nat. Neurosci., 2005. **8**(8): p. 1013-21.
8. Jaubert-Miazza, L., et al., *Structural and functional composition of the developing retinogeniculate pathway in the mouse.* Vis. Neurosci., 2005. **22**(5): p. 661-76.
9. McLaughlin, T., et al., *Retinotopic map refinement requires spontaneous retinal waves during a brief critical period of development.* Neuron, 2003. **40**(6): p. 1147-60.
10. Penn, A.A., et al., *Competition in retinogeniculate patterning driven by spontaneous activity.* Science, 1998. **279**(5359): p. 2108-12.
11. Gordon, J.A. and M.P. Stryker, *Experience-dependent plasticity of binocular responses in the primary visual cortex of the mouse.* J. Neurosci., 1996. **16**(10): p. 3274-86.
12. Gianfranceschi, L., et al., *Visual cortex is rescued from the effects of dark rearing by overexpression of BDNF.* Proc. Natl. Acad. Sci. U. S. A., 2003. **100**(21): p. 12486-91.
13. Antonini, A., M. Fagiolini, and M.P. Stryker, *Anatomical correlates of functional plasticity in mouse visual cortex.* J. Neurosci., 1999. **19**(11): p. 4388-406.
14. McGee, A.W., et al., *Experience-driven plasticity of visual cortex limited by myelin and Nogo receptor.* Science, 2005. **309**(5744): p. 2222-6.
15. Pernet, V., et al., *Nogo-A and myelin-associated glycoprotein differently regulate oligodendrocyte maturation and myelin formation.* J. Neurosci., 2008. **28**(29): p. 7435-44.
16. Dickendesher, T.L., et al., *NgR1 and NgR3 are receptors for chondroitin sulfate proteoglycans.* Nature Neurosci., 2012. **15**(5): p. 703-12.
17. Wagor, E., N.J. Mangini, and A.L. Pearlman, *Retinotopic organization of striate and extrastriate visual cortex in the mouse.* J. Comp. Neurol., 1980. **193**(1): p. 187-202.
18. Drager, U.C. and J.F. Olsen, *Origins of crossed and uncrossed retinal projections in pigmented and albino mice.* J. Comp. Neurol., 1980. **191**(3): p. 383-412.
19. Hayhow, W.R., C. Webb, and A. Jervie, *The accessory optic fiber system in the rat.* J. Comp. Neurol., 1960. **115**(2): p. 187-215.
20. Yonehara, K., et al., *Identification of retinal ganglion cells and their projections involved in central transmission of information about upward and downward image motion.* PLoS ONE, 2009. **4**(1): p. e4320.
21. Cassone, V.M., et al., *Comparative anatomy of the mammalian hypothalamic suprachiasmatic nucleus.* J. Biol. Rhythms, 1988. **3**(1): p. 71-91.

22. Harrington, M.E., *The ventral lateral geniculate nucleus and the intergeniculate leaflet: interrelated structures in the visual and circadian systems.* Neurosci. Biobehav. Rev., 1997. **21**(5): p. 705-27.
23. Hattar, S., et al., *Melanopsin-containing retinal ganglion cells: architecture, projections, and intrinsic photosensitivity.* Science, 2002. **295**(5557): p. 1065-70.
24. Pak, M.W., et al., *Retinopretectal and Accessory Optic Projections of Normal Mice and the Okn-Defective Mutant Mice Beige, Beige-J, and Pearl.* J. Comp. Neurol., 1987. **258**(3): p. 435-446.
25. Simpson, J.I., *The accessory optic system.* Annu. Rev. Neurosci., 1984. **7**: p. 13-41.
26. Hofbauer, A. and U.C. Drager, *Depth segregation of retinal ganglion cells projecting to mouse superior colliculus.* J. Comp. Neurol., 1985. **234**(4): p. 465-74.
27. Rodieck, R.W. and M. Watanabe, *Survey of the morphology of macaque retinal ganglion cells that project to the pretectum, superior colliculus, and parvicellular laminae of the lateral geniculate nucleus.* J. Comp. Neurol., 1993. **338**(2): p. 289-303.
28. Godement, P., J. Salaun, and M. Imbert, *Prenatal and Postnatal-Development of Retinogeniculate and Retinocollicular Projections in the Mouse.* J. Comp. Neurol., 1984. **230**(4): p. 552-575.
29. Ciossek, T., et al., *Eph receptor-ligand interactions are necessary for guidance of retinal ganglion cell axons in vitro.* Eur. J. Neurosci., 1998. **10**(5): p. 1574-80.
30. Yates, P.A., et al., *Topographic-specific axon branching controlled by ephrin-As is the critical event in retinotectal map development.* J. Neurosci., 2001. **21**(21): p. 8548-63.
31. Feldheim, D.A. and D.D. O'Leary, *Visual map development: bidirectional signaling, bifunctional guidance molecules, and competition.* Cold Spring Harb Perspect Biol, 2010. **2**(11): p. a001768.
32. Hindges, R., et al., *EphB forward signaling controls directional branch extension and arborization required for dorsal-ventral retinotopic mapping.* Neuron, 2002. **35**(3): p. 475-87.
33. Schmitt, A.M., et al., *Wnt-Ryk signalling mediates medial-lateral retinotectal topographic mapping.* Nature, 2006. **439**(7072): p. 31-7.
34. Feldheim, D.A., et al., *Topographic guidance labels in a sensory projection to the forebrain.* Neuron, 1998. **21**(6): p. 1303-13.
35. Godement, P., J. Salaun, and M. Imbert, *Prenatal and postnatal development of retinogeniculate and retinocollicular projections in the mouse.* J. Comp. Neurol., 1984. **230**(4): p. 552-75.
36. Chapman, B., *Necessity for afferent activity to maintain eye-specific segregation in ferret lateral geniculate nucleus.* Science, 2000. **287**(5462): p. 2479-82.
37. Demas, J., et al., *Failure to maintain eye-specific segregation in nob, a mutant with abnormally patterned retinal activity.* Neuron, 2006. **50**(2): p. 247-59.
38. Toychiev, A.H., C.W. Yee, and B.T. Sagdullaev, *Correlated spontaneous activity persists in adult retina and is suppressed by inhibitory inputs.* PLoS ONE, 2013. **8**(10): p. e77658.
39. Sernagor, E., C. Young, and S.J. Eglen, *Developmental modulation of retinal wave dynamics: shedding light on the GABA saga.* J. Neurosci., 2003. **23**(20): p. 7621-9.
40. Hooks, B.M. and C. Chen, *Distinct roles for spontaneous and visual activity in remodeling of the retinogeniculate synapse.* Neuron, 2006. **52**(2): p. 281-91.
41. Hooks, B.M. and C. Chen, *Vision triggers an experience-dependent sensitive period at the retinogeniculate synapse.* J. Neurosci., 2008. **28**(18): p. 4807-17.
42. Wiesel, T.N. and D.H. Hubel, *Single-Cell Responses in Striate Cortex of Kittens Deprived of Vision in One Eye.* J. Neurophysiol., 1963. **26**: p. 1003-17.
43. Hubel, D.H. and T.N. Wiesel, *The period of susceptibility to the physiological effects of unilateral eye closure in kittens.* J Physiol., 1970. **206**(2): p. 419-36.
44. Stevens, B., et al., *The classical complement cascade mediates CNS synapse elimination.* Cell, 2007. **131**(6): p. 1164-78.
45. Huberman, A.D., M.B. Feller, and B. Chapman, *Mechanisms underlying development of visual maps and receptive fields.* Annu. Rev. Neurosci., 2008. **31**: p. 479-509.

46. Hensch, T.K., et al., *Local GABA circuit control of experience-dependent plasticity in developing visual cortex.* Science, 1998. **282**(5393): p. 1504-8.
47. Harauzov, A., et al., *Reducing intracortical inhibition in the adult visual cortex promotes ocular dominance plasticity.* J. Neurosci., 2010. **30**(1): p. 361-71.
48. Maya Vetencourt, J.F., et al., *The antidepressant fluoxetine restores plasticity in the adult visual cortex.* Science, 2008. **320**(5874): p. 385-8.
49. Sale, A., et al., *Environmental enrichment in adulthood promotes amblyopia recovery through a reduction of intracortical inhibition.* Nat. Neurosci., 2007. **10**(6): p. 679-81.
50. Greifzu, F., et al., *Environmental enrichment extends ocular dominance plasticity into adulthood and protects from stroke-induced impairments of plasticity.* Proc. Natl. Acad. Sci. U. S. A., 2014. **111**(3): p. 1150-5.
51. Pizzorusso, T., et al., *Reactivation of ocular dominance plasticity in the adult visual cortex.* Science, 2002. **298**(5596): p. 1248-51.
52. Delekate, A., et al., *NogoA restricts synaptic plasticity in the adult hippocampus on a fast time scale.* Proc. Natl. Acad. Sci. U. S. A., 2011. **108**(6): p. 2569-74.
53. Tews, B., et al., *Synthetic microRNA-mediated downregulation of Nogo-A in transgenic rats reveals its role as regulator of synaptic plasticity and cognitive function.* Proc. Natl. Acad. Sci. U. S. A., 2013. **110**(16): p. 6583-6588.
54. Prusky, G.T., et al., *Rapid quantification of adult and developing mouse spatial vision using a virtual optomotor system.* Invest. Ophthalmol. Vis. Sci., 2004. **45**(12): p. 4611-6.
55. Sun, W., et al., *ON direction-selective ganglion cells in the mouse retina.* J Physiol., 2006. **576**(Pt 1): p. 197-202.
56. Dhande, O.S., et al., *Genetic dissection of retinal inputs to brainstem nuclei controlling image stabilization.* J. Neurosci., 2013. **33**(45): p. 17797-813.
57. Sugita, Y., et al., *Contributions of retinal direction-selective ganglion cells to optokinetic responses in mice.* Eur. J. Neurosci., 2013. **38**(6): p. 2823-31.
58. Cahill, H. and J. Nathans, *The optokinetic reflex as a tool for quantitative analyses of nervous system function in mice: application to genetic and drug-induced variation.* PLoS ONE, 2008. **3**(4): p. e2055.
59. Porciatti, V., T. Pizzorusso, and L. Maffei, *The visual physiology of the wild type mouse determined with pattern VEPs.* Vision Res., 1999. **39**(18): p. 3071-81.
60. Prusky, G.T., N.M. Alam, and R.M. Douglas, *Enhancement of vision by monocular deprivation in adult mice.* J. Neurosci., 2006. **26**(45): p. 11554-61.
61. Wada, N., K. Funabiki, and S. Nakanishi, *Role of granule-cell transmission in memory trace of cerebellum-dependent optokinetic motor learning.* Proc. Natl. Acad. Sci. U. S. A., 2014. **111**(14): p. 5373-8.
62. Joset, A., et al., *Pincher-generated Nogo-A endosomes mediate growth cone collapse and retrograde signaling.* J. Cell Biol., 2010. **188**(2): p. 271-85.
63. Huber, A.B., et al., *Patterns of Nogo mRNA and protein expression in the developing and adult rat and after CNS lesions.* J. Neurosci., 2002. **22**(9): p. 3553-67.
64. Buffo, A., et al., *Application of neutralizing antibodies against NI-35/250 myelin-associated neurite growth inhibitory proteins to the adult rat cerebellum induces sprouting of uninjured purkinje cell axons.* J. Neurosci., 2000. **20**(6): p. 2275-86.
65. Oertle, T., et al., *Nogo-A inhibits neurite outgrowth and cell spreading with three discrete regions.* J. Neurosci., 2003. **23**(13): p. 5393-406.
66. Fournier, A.E., T. GrandPre, and S.M. Strittmatter, *Identification of a receptor mediating Nogo-66 inhibition of axonal regeneration.* Nature, 2001. **409**(6818): p. 341-6.
67. Kempf, A., et al., *The sphingolipid receptor S1PR2 is a receptor for Nogo-a repressing synaptic plasticity.* PLoS Biol., 2014. **12**(1): p. e1001763.

68. Manns, R., et al., *Protein synthesis dependence of growth cone collapse induced by different Nogo-A-domains.* PLoS ONE, 2014. **9**(1): p. e86820.
69. Kempf, A. and M.E. Schwab, *Nogo-A represses anatomical and synaptic plasticity in the central nervous system.* Physiology (Bethesda), 2013. **28**(3): p. 151-63.
70. Petrinovic, M.M., et al., *Neuronal Nogo-A negatively regulates dendritic morphology and synaptic transmission in the cerebellum.* Proc. Natl. Acad. Sci. U. S. A., 2013. **110**(3): p. 1083-8.
71. Zagrebelsky, M., et al., *Nogo-A stabilizes the architecture of hippocampal neurons.* J. Neurosci., 2010. **30**(40): p. 13220-34.
72. Rex, C.S., et al., *Different Rho GTPase-dependent signaling pathways initiate sequential steps in the consolidation of long-term potentiation.* J. Cell Biol., 2009. **186**(1): p. 85-97.
73. Hofer, S.B., et al., *Experience leaves a lasting structural trace in cortical circuits.* Nature, 2009. **457**(7227): p. 313-7.
74. Syken, J., et al., *PirB restricts ocular-dominance plasticity in visual cortex.* Science, 2006. **313**(5794): p. 1795-800.

CHAPTER 2

EXPRESSION OF NOGO-A IN THE MOUSE VISUAL SYSTEM AND ITS INFLUENCE ON THE DEVELOPMENTAL REFINEMENT OF THE RETINOGENICULATE PROJECTIONS

Anna Guzik-Kornacka, Vincent Pernet, Flora Vajda, Martin E. Schwab

Manuscript in preparation

I contributed to the design of the study, performed anterograde and retrograde anatomical tracings, harvested and processed tissues, performed some of the immunohistochemical (IHC) stainings in retinae and optic nerves, acquired the microscopic images and analyzed the retinal projection patterns. I also performed qRT-PCR. I analysed all the data, wrote the manuscript and made figures.

1 Introduction

Retinal projections are produced in excess during perinatal period and the maturation of axonal terminals is required to sculpt the stereotypical retinotopic map. This process consists of the pruning of collateral branches in the terminals that overshoot their neuronal targets [1]. The retinogeniculate pathway of the visual system has been widely used as a model to study mechanisms of developmental circuits remodeling during early postnatal life [2-5]. In the mouse, retinal terminals from both eyes occupy overlapping territories in the dorsal lateral geniculate nucleus (dLGN) in thalamus during the first postnatal days, but before natural eye opening at P12-14 undergo extensive pruning which leads to the segregation of the two eye domains [6, 7]. Later in life, the segregated retinal terminals from both eyes in the dLGN were thought to be very stable and the visual system plasticity was assumed to be restricted to the higher, cortical level [8]. However, recent studies by Hooks and Chen [9, 10] brought this view into question, by showing that the retinogeniculate synapses are plastic and sensitive to visual experience around P20.

Nogo-A and its receptor NgR1 have been previously implicated in the restriction of the cortical ocular dominance plasticity beyond the developmental critical period [11].Whether Nogo-A is also involved in the regulation of developmental retinogeniculate refinement is unknown. Expression of Nogo-A protein has been reported in the retina and optic nerve of early postnatal mice [12] making it a plausible regulator of the maturation process. However, a detailed temporal profile of Nogo-A expression in the maturing visual system is still lacking.

Here we have analyzed the expression of Nogo-A in the retina of early postnatal and adult mice and looked at the expression profiles of the two main Nogo-A receptors, NgR1 and S1PR2, in the retina. Additionally, we have determined the pattern of Nogo-A expression in the subcortical and

cortical visual pathways. To determine whether Nogo-A influences the developmental refinement of the retinogeniculate projections we have analyzed the degree of eye-specific terminal segregation in the dLGN in Nogo-A knock-out (KO) and wild-type (WT) mice at postnatal day 10 (P10) when the majority of excessive terminals are already pruned.

We observed that the expression of Nogo-A protein is developmentally regulated and its receptors are expressed in the retina. Nogo-A is also expressed in the dLGN and in the visual cortex. The systemic deletion of Nogo-A did not influence the eye-specific terminal segregation in the dLGN. Our results indicate that Nogo-A is not involved in the developmental refinement of retinal terminals.

2 Material and methods

2.1 Animals

Retinal and brain tissues from postnatal (P1-P15) female and male mice and young adult (P30 or P60) male C57BL/6 wild-type (WT) mice were used for immunohistochemistry or mRNA expression studies. Analysis of retinogeniculate projection refinement was conducted on brain tissues from P10 C57BL/6 WT and Nogo-A knock-out (KO) mice of the same genetic background. Nogo-A KO mice were generated in our laboratory as described previously [13]. Animal experiments were carried out with acceptance and in agreement with the guidelines of the Cantonal Veterinary Office in Zurich.

2.2 Retrograde tracing

To visualize the cell bodies of retinal ganglion cells (RGCs) for immunohistochemistry of Nogo-A we retrogradely labeled them with cholera toxin β-subunit (CTb) conjugated to Alexa 488. At P8, WT pups were anesthetized with isoflurane and 1 µl of CTb-488 (0.5% in PBS, Molecular Probes) was injected through the intact skull to the surface of the left superior colliculus using NanoFil 10 µl syringe (WPI) with 33 gauge needle. Animals were sacrifice at P10 and retinae were collected after perfusion.

2.3 Anterograde tracing

To visualize retinal projections from two eyes to the brain, CTb tracers conjugated either to Alexa 594 (red, left eye) or Alexa 488 (green, right eye) were injected intraocularly. P8 pups WT (n=6) and Nogo-A KO (n=6) were anesthetized with isoflurane, superior surface of sclera was exposed by making incision in the upper eyelid and 0.5 µl of CTb was injected to each eye at a 45° angle using NanoFil syringe with 35G needle taking care not to damage the lens and the

ciliary bodies. Animals were sacrificed 2 days later. For immunohistochemistry in adult WT brain, retinal projections from the left eye were traced with CTb-594 as previously described [14].

2.4 Tissue collection

Tissues for immunohistochemistry and tracing experiments were collected from perfused mice. Mice were terminally anesthetized with Nembutal (100 mg/kg body weight) and transcardially perfused with PBS followed by 4% PFA. Tissues were postfixed in 4% PFA overnight and cryoprotected with 30% sucrose in PBS (brains, retinae and optic nerves for cryosectioning). Brains were sectioned in the coronal plane at 40 µm, retinae cross-sectioned and optic nerves with chiasm longitudinally sectioned at 14 µm using a cryostat. Retinae with retrogradely labeled RGCs and adult retinae for NgR1 staining were flat-mounted after postfixation by doing 4 radial incisions to create petal shape and were used immediately for immunostaining. For mRNA expression study of Nogo-A receptors we collected retinae from P4, P10, P15, P30 and P60 WT mice (3 mice per time point). Postnatal mice (P4-P15) were sacrificed by decapitation and P30-P60 mice by cervical dislocation. Eyes were immediately enucleated and retinae were quickly dissected in ice cold, sterile PBS, taking care to remove lens, sclera and hyaloids vessels, snap-frozen in liquid nitrogen and stored in -80°C.

2.5 Immunohistochemistry

The expression of Nogo-A in the retina of early postnatal mice (P1-P6) mice was visualize on retinal cross-sections using rabbit antiserum (1:200, Laura (Rb173A) raised against aa 174-979 fragment of rat Nogo-A, produced in our laboratory [15]) together with RGC marker β-3 tubulin (1: 1000, mouse Ab, Promega, #G712A). Primary and secondary antibodies were diluted in PBS containing 0.3% of Triton-X-100 and 5% of normal goat serum. For staining of Nogo-A on the

retinal flat-mount, P10 retinae were incubated with primary antibodies for one week at 4°C (anti-Nogo-A Laura AS, 1:200; anti-Brn3a - nuclear RGC marker, 1:100, mouse Ab, Santa Cruz Biotech., #sc-8429) followed by 2 days of incubation at 4°C with corresponding secondary antibodies in the same buffer as for Nogo-A staining on sections. The staining of NgR1 (1:200, goat Ab, R&D Systems, #AF1440) was performed on adult (P60) WT retina cross-sections using PBS with 0.3% of Triton-X-100 and 5% of BSA as a blocking and antibody buffer. For double staining for NgR1 (1:100) and Nogo-A (1:200) on adult retinal flat-mounts, incubations with primary and secondary antibody were performed as for P10 retinae using the same buffer as for NgR1 staining on sections. On optic nerve sections from adult WT mice (P60), we detected Nogo-A (Laura AS, 1:200) and Adenomatus Polyposis Coli, a mature oligodendrocytes marker (mouse anti-APC; 1:250; Calbiochem Ab-7) using the same protocol as for retinal cross-sections. For the staining of Nogo-A in the adult WT brain we first incubated sections in 50mM glycine in 0.1M Tris buffer pH 8, and performed heat-induced antigen retrieval for 30 s in a microwave to increase Nogo-A immunoreactivity. Following primary antibodies were used: rabbit anti-Nogo-A Laura AS (1:200) and mouse anti-NeuN (1:500, Milipore, #MAB377).

2.6 Semi-quantitative real-time PCR

Total RNA was isolated from retinal tissues of WT mice (P4-P60) using RNeasy Mini Kit (Qiagen) including a DNase I treatment to digest the residual genomic DNA. Reverse transcription was performed using oligoT primers as previously described [16]. When possible, primers were designed to span exon-exon junction to prevent genomic DNA amplification. Sequences of primers can be found in Table 1. qPCRs were performed in LightCycler480 using SYBR Green I MasterMix (Roche Diagnostics). Each reaction was done in triplicate with 3 biological replicates. Expression levels of *Ngr1* or *S1pr2* were normalized to 2 housekeeping

genes (*Gapdh* and *Rpl19*) using comparative threshold method ($\Delta\Delta C_T$) [17] and one sample from P4 mouse was used as a calibrator.

Table 1

Gene	Forward primer	Reverse primer	Annealing temp (°C)	Product size (bp)
Ngr1	CTCGACCCCGAAGATGAAG	TGTAGCACACACAAGCACCAG	60	116
S1pr2	CATCGCCATCGAGAGACAAG	TCAGACAATTCCAGCCCAGG	62	146
Gapdh	CAGCAATGCATCCTGCACC	TGGACTGTGGTCATGAGCCC	58	96
Rpl19	TGAGTATGCTCAGGCTACAG	GAATGGACAGTCACAGGCTT	62	175

2.7 Image acquisition

Images of retinal stainings were acquired using Leica SPE-II confocal microscope at 40X (NA 1.25 with step size of 0.2 µm and are presented as maximum intensity projections. Nogo-A stainings in the optic nerve and in the brain were acquired using Leica DM550B epi-fluorescence microscope with a 20X objective (NA 0.5) in automatic mosaic mode. Pictures of retinal projections in the dLGN were visualized with a Zeiss Axioskop 2 Plus epi-fluorescence microscope (Carl Zeiss) using 10X objective (NA 0.3) with the same exposure setting for both tracers.

2.8 Analysis of eye-specific projections segregation in the dLGN

The segregation of eye-specific projections in the dLGN of P10 WT and Nogo-A KO mice was determined for different contralateral thresholds on a 0-255 grayscale as described by Muir-Robinson and colleagues [18]. Background fluorescence was subtracted from the images using a rolling ball filter of 200 pixels radius and histograms were normalized to 8-bit intensity range (NIH ImageJ). Ipsilateral gray value thresholds were kept constant and adjusted consistently for

each picture. For each animal, we analyzed three sections from the middle of the dLGN containing the largest ipsilateral patch using custom-written NIH ImageJ plugins and routines (by van der Burg A. Brain Research Institute, Zurich). In the segregation and the dLGN size analysis we determined borders of dLGN based on contralateral tracing excluding the optic tract and the intergeniculate leaflet. Size of dLGN was measured on the same 3 central sections which were used in the segregation analysis and is represented for each animal as an average of those 3 sections.

2.9 Statistical analysis

All numerical data are presented as a mean ± standard error of the mean (SEM). Threshold depended segregation data were compared between WT vs. KO using the two-way repeated measures (RM) analysis of variance ANOVA with post-hoc Bonferroni's tests ($\alpha = 0.05$). Size of dLGN was compared between WT and KO group using Student's t-test using the GraphPad Prism software.

3. Results

3.1 Expression of the Nogo-A protein in the retina is developmentally regulated

To understand if the Nogo-A signaling may play a role in the postnatal maturation of the mouse visual system we decided to first determine the expression pattern of Nogo-A and its receptors. In the adult mouse retina, Nogo-A is expressed in the ganglion cell layer (GCL) however the expression is limited to the endfeet of Müller glia and absent in the retinal ganglion cells (RGCs) [12, 14]. In early postnatal retina (P1 [12] and P4 [19]) Nogo-A was reported to be strongly expressed by RGCs. To determine when the pattern of expression exactly changes, we performed immunohistochemical stainings for Nogo-A and the RGC marker β-3 tubulin on cross-sections of early postnatal retina from P1 to P6 mice (Fig. 1a). At P1 (Fig. 1a') and P4 (Fig. 1a'') Nogo-A signal was present in β-3 tubulin-positive RGC cell bodies and axons. However, in P6 retina (Fig. 1a''') the expression pattern changed dramatically and Nogo-A signal was mainly present around RGC cells in the endfeet of Müller glia. To better visualize the RGC cell bodies and Müller glia endfeet we decided to retrogradely trace RGCs and performed stainings on a flat-mounted retinae. The retrograde tracing was performed at P8 by a single injection of cholera toxin β-subunit conjugated to Alexa 488 (CTb-488) into the left superior colliculus; the right retina was harvested at P10. In P10 retinae the CTb-488 tracer fully filled cell bodies of RGCs (Fig. 1b; green) and the RGC nuclei were additionally visualized by staining against the RGC-specific transcription factor Brn3a (Fig. 1b; blue). CTb-488-positive RGC cells were devoid of Nogo-A signal; however, Nogo-A was clearly expressed around RGC cell bodies in Müller glia processes forming a typical honeycomb pattern (Fig. 1b; red).

Figure 1 Nogo-A expression in RGCs is down-regulated by P6 whereas the expression of NgR1 stays high in RGCs until adulthood

a The Nogo-A protein (red) is strongly expressed in the β-3 tubulin-positive (green) retinal ganglion cell bodies and axons at postnatal day 1 (P1) and P4 but is down-regulated by P6, when the expression increases in Müller glia endfeet (arrowheads). **b** On retinal flat-mounts from P10 mice, Nogo-A (red) is present in Müller glia endfeet around retrogradely labeled RGC bodies (CTb-488 tracing; green) expressing Brn3a nuclear marker (blue); maximal intensity projection of 5-µm serial confocal optical sections. **c** In the adult retina, NgR1 is exclusively expressed in the ganglion cell layer and in the fiber layer corresponding to RGC bodies and axons. Abbreviations: **ONL**: outer nuclear layer; **OPL**: outer plexiform layer; **INL**: inner nuclear layer; **IPL**: inner plexiform layer, **GCL**: ganglion cell layer; **FL**: fiber layer. **d** On flat-mounted adult WT mouse retinae, NgR1 staining (green) is present in RGC bodies and axonal fascicles whereas Nogo-A is exclusively expressed around RGC bodies in Müller glia endfeet; see higher magnification picture of the region marked with dotted line in **d'**. Scale bars in **a-d,** 50 µm; **d',** 10 µm. **e,f** Developmental regulation of Nogo-A receptors mRNA expression in the retina. **e** *Ngr1* mRNA is expressed in the retina across different developmental ages (P4-P60). **f** *S1pr2* mRNA expression is strongly down-regulated in the retina after P4.

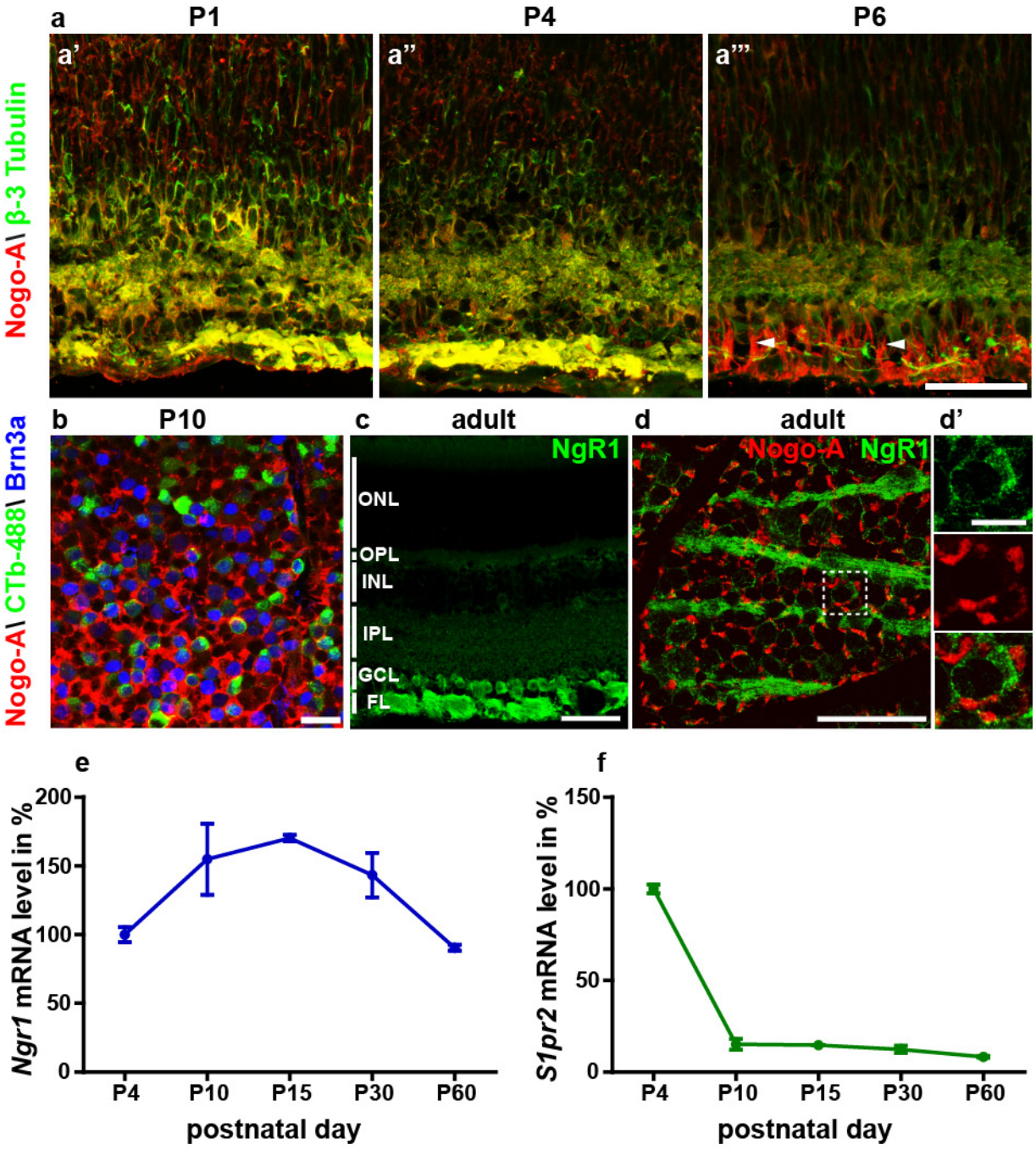
a
P1
P4
P6
a'
a''
a'''
Nogo-A\ β-3 Tubulin
b
P10
c
adult
d
adult
d'
Nogo-A\ CTb-488\ Brn3a
NgR1
Nogo-A NgR1
ONL
OPL
INL
IPL
GCL
FL
e
Ngr1 mRNA level in %
200
150
100
50
0
P4
P10
P15
P30
P60
postnatal day
f
S1pr2 mRNA level in %
150
100
50
0
P4
P10
P15
P30
P60
postnatal day

Taken together, our results show that Nogo-A is strongly expressed by mouse retinal ganglion cells during first postnatal days and is strongly down-regulated between P4 and P6. After P6 in the retina, Nogo-A is predominantly expressed in Müller glia.

3.2 Nogo-A receptors are expressed in the mouse retina

Nogo-A exerts its inhibitory functions mainly through two domains called Nogo-66 and Nogo-A-Δ20 [14]. The C-terminal Nogo-66 domain binds predominantly to the Nogo-66 receptor 1 (NgR1) [21], whereas the Nogo-A specific Nogo-A-Δ20 domain binds to the newly identified sphingosine 1-phosphate receptor 2 (S1PR2) [22]. The two Nogo-A receptors, have been reported to be expressed in the adult mouse RGCs [20-22]. However, their developmental profile of expression in the retina is unknown. In adult mouse retinal cross-sections, we detected NgR1 protein expression (Fig. 1c) exclusively in ganglion cell layer (GCL) and in the fiber layers (FL) corresponding to RGC bodies and axonal fascicles. NgR1 staining was negative in the inner plexiform layer (IPL) with the RGC dendrites and the inner nuclear layer (INL) containing the cell bodies of bipolar, amacrine and horizontal cells. NgR1 was also not detected in the outer plexiform layer (OPL) with the horizontal and bipolar cell dendrites and in the nuclear layer (ONL) containing photoreceptors. To further compare the pattern of Nogo-A and NgR1 expression in adult mice we performed double immunostainings on retinal flat-mounts. On confocal images at the level of RGC bodies and axons (Fig. 1d, close-up in d'), the NgR1 staining (green) was localized in the RGC cytoplasm and at the cell surface and in axonal fascicles of RGCs. In contrast, the Nogo-A signal (red), as in P10 retinae, was present in Müller glia endfeet and undetectable in RGCs.

To determine if the expression of NgR1 and S1PR2 in the retina is developmentally regulated we analyzed their mRNA expression profiles using qPCR. *Ngr1* mRNA was detectable in retinal

samples from early postnatal (P4) to adult (P60) ages (Fig. 1e) and the expression was more elevated between P10 to P30 (at P15 70% higher than at P4). The expression of *S1pr2* mRNA in the retina was highest at P4 and decreased by P10 to around 15% of the P4 level and stayed at the same level in older ages (P15-P60; Fig. 1f). Overall, the two Nogo-A receptors are expressed in the retina; however *S1pr2* mRNA is down-regulated by postnatal day 10.

3.3 Nogo-A expression in the adult mouse brain

We have demonstrated that Nogo-A expression in the RGCs is down-regulated by the sixth postnatal day and that NgR1 is expressed in postnatal and adult RGCs. Therefore, to determine if NgR1 expressing RGC axons could interact with the Nogo-A in the visual pathway, we decided to analyze expression of Nogo-A in the optic nerve and the brain. In the optic nerve, Nogo-A has been reported to be expressed in typical rows of interfascicular oligodendrocytes already at the eighth postnatal day and, at the mRNA level, to strongly increase during myelination of the optic nerve [12]. As expected, in the adult WT optic nerve we detected Nogo-A protein in APC-expressing oligodendrocyte cell bodies and processes (Fig. 2a). Therefore, Nogo-A expressed in the optic nerve oligodendrocytes, may interact with NgR1 receptor present in RGC axons. At P8, a time of maturation of retinogeniculate projections, Nogo-A has been reported to be mainly expressed by neurons throughout the brain [19] while the myelination of retinal projections is just starting at this time [23]. We further wanted to analyze the expression of Nogo-A protein in the lateral geniculate nucleus (LGN), in the thalamus of adult mouse. To visualize retinal projections to the LGN, we traced them anterogradely by injection of CTb-594 in the left eye. After antigen retrieval, we performed immunohistochemistry against Nogo-A and the neuronal marker NeuN and could detect strong Nogo-A expression in NeuN positive neurons in the thalamus and hippocampus (Fig. 2b,c).

Figure 2 Expression of Nogo-A protein in the adult mouse visual system

a In the adult mouse optic nerve, Nogo-A (green) is expressed by APC-positive (red) oligodendrocytes. **a'** Magnification of the optic nerve region marked at **a** with the dotted line. **b** In the thalamus and the hippocampus, Nogo-A is strongly expressed by neurons but also by oligodendrocytes. Inset **b'** represents 5x magnification of the dLGN region marked with dotted line. **c** Retinal projections to the LGN were traced with the CTb-594 tracer (red). Nogo-A is expressed in the majority of NeuN-positive neurons (blue) and in some putative oligodendrocytes (arrowheads). **c**' Region of inset as in **b'**. **d** Nogo-A is also expressed by cortical neurons including the primary visual cortex (V1) and by oligodendrocytes in the corpus callosum (arrowheads). **d'** Nogo-A (green) is strongly expressed in the NeuN positive neurons (blue) in layer II/III and V/VI of V1. Scale bars: **a** 100 μm; **a'** 50 μm; **b-c** 200 μm; **b'-c'** 20 μm; **d** 500 μm and **d'** 100 μm.

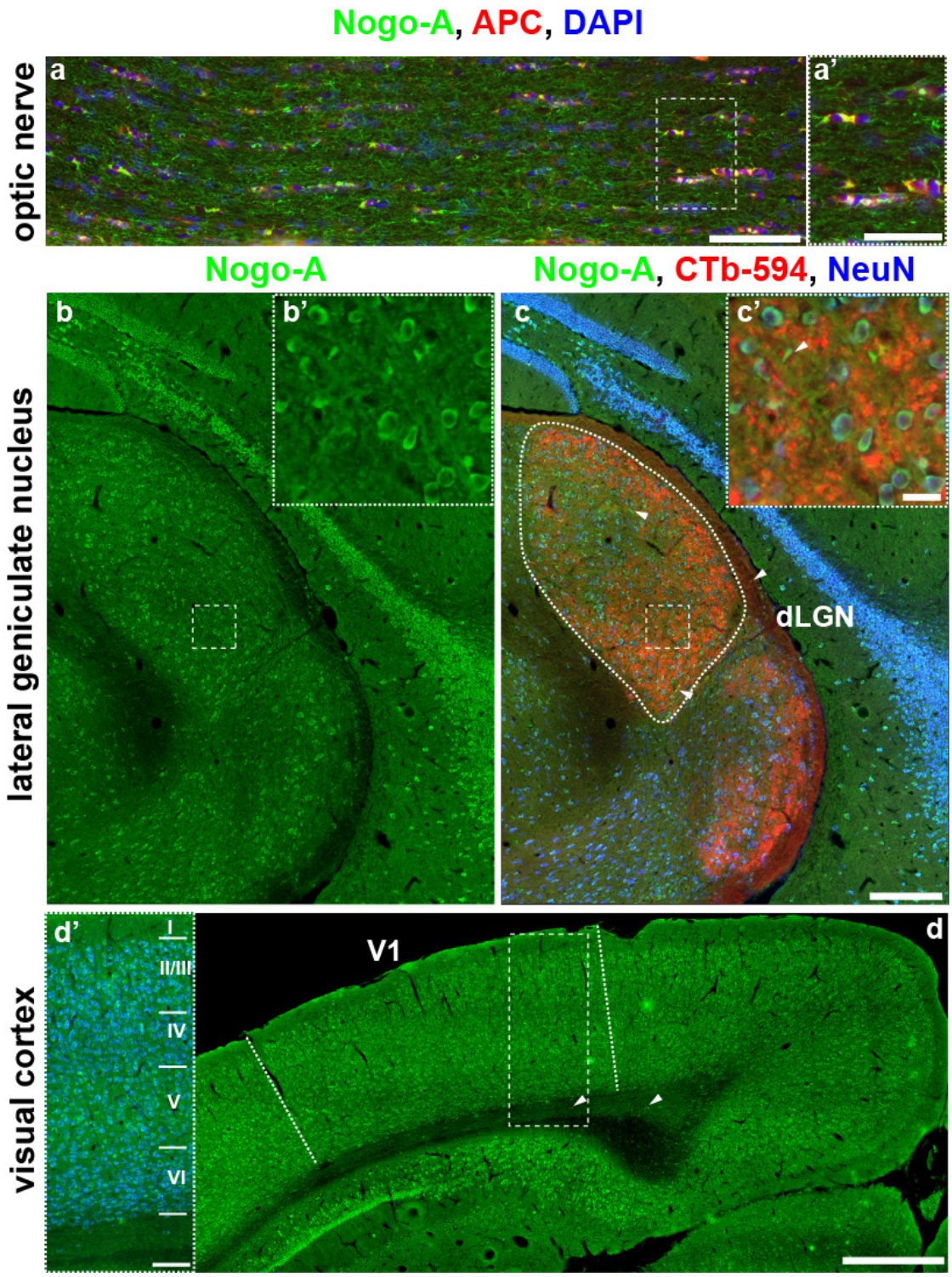
Nogo-A, APC, DAPI
optic nerve
a
a'
Nogo-A
Nogo-A, CTb-594, NeuN
lateral geniculate nucleus
b
b'
c
c'
dLGN
visual cortex
d'
I
II/III
IV
V
VI
V1
d

In the dLGN, Nogo-A was uniformly expressed in both ipsi- and contralateral eye projection-receiving areas (CTb-594; red) by most of the NeuN positive neurons (Fig. 2b,c). Interestingly, the dLGN is the only rodent relay thalamic nucleus, which next to excitatory relay neurons contains also GABAergic interneurons [24]. Apart from NeuN-positive neurons, we could observe Nogo-A expression in NeuN-negative, smaller cells in the dLGN and optic tract, possibly oligodendrocytes (Fig. 2c).

We have also analyzed Nogo-A protein expression in the adult mouse primary visual cortex. In the adult WT mouse cortex we could detect Nogo-A protein signal in neurons and also oligodendrocyte cell bodies (Fig. 2d). The Nogo-A expression looked uniform across different cortical areas (data not shown) and in the primary visual cortex Nogo-A was expressed in NeuN-positive neurons in layer II to VI (Fig. 2d'). Consistently with the previous report for Nogo-A mRNA [25], the strongest Nogo-A staining was detected in layers II/III and V-VI. Taken together, our immunostainings showed that Nogo-A is widely expressed in neurons of the adult mouse visual system.

3.4 Nogo-A does not influence the developmental segregation of retinogeniculate terminals

Nogo-A and NgR1 are both expressed in the visual system during the developmental refinement of the retinogeniculate projection which in mice take place between P4-P8 [26, 27]. Therefore we investigated whether systemic deletion of Nogo-A would influence this process. To visualize the retinal projections from both eyes we intravitreally injected CTb tracers of different colors in the two eyes of P8 WT and Nogo-A KO mice (Fig. 3a; left eye CTb-594, red; right eye CTb-488, green). At P10, after course-scale refinement, we analyzed eye-specific segregation of retinogeniculate terminals in the dLGN (Fig. 3b). As expected, in P10 WT mice, eye-specific projections to the dLGN from ipsi- and contralateral eyes were well segregated, with only a small

rim of overlapping projections at the border of the two eye-specific domains (Fig. 3b; close-up Fig. 3c) corresponding to the typical pattern of segregation reported for this age [7]. In Nogo-A KO mice at P10, eye-specific projections were segregated to a similar extent as in WT mice (Fig. 3b,c). Quantitatively, the percentage of non-overlapping pixels could be determined by subtraction of binarised images of the green and the red channels. To avoid subjective determination of the threshold, the extent of segregation was represented not as a single value but rather as a function of the contralateral threshold as previously reported [18]. The analysis confirmed that at P10 the eye-specific projection segregation in the left and right dLGN was comparable and not significantly different between WT and Nogo-A KO mice (Fig. 3d; at contralateral threshold 30, right dLGN WT 64.8±3.3% vs. KO 69.4±4.4%, RM-ANOVA $p>0.99$; left dLGN WT 61.3±2.5% vs. KO 62.9±4.8%; $p>0.99$). We also measured the size of the dLGN at P10 on brain sections. In the two hemispheres, the dLGN size did not differ significantly between WT and Nogo-A KO animals (Fig. 3e; right dLGN $p=0.64$; left dLGN $p=0.18$; t-test). Thus, the systemic deletion of Nogo-A does not seem to interfere with the developmental refinement of retinogeniculate terminals.

Figure 3 Nogo-A does not influence the developmental refinement of retinogeniculate projection

a Scheme of the anterograde tracing procedure. Eye retinal ganglion cell projections to the LGN were traced in Nogo-A KO and WT mice at P8 by intravitreal injection of cholera toxin β-subunit (CTb) tracers; (green, CTb-488 right eye; red, CTb-594 left eye). For each animal, the degee of the two-eye projection segregation in the dLGN was analyzed at P10 on 3 coronal brain sections in the center of the dLGN. **b** At P10 in WT mice, retinal terminals in the dLGN appeared segregated into central ipsilateral eye and surrounding contralateral eye territories. In Nogo-A KO mice at P10, the eye-specific segregation in the dLGN resembled that of WT mice at this age. **c** Higher magnification from panel **b** of the border between ipsilateral and contralateral eye territories in the dLGN. **d** Quantitatively, the eye-specific projection segregation in the left and right dLGN did not differ significantly between P10 Nogo-A KO and WT mice. Two-way RM ANOVA with Bonferroni's post-hoc tests, Nogo-A KO and WT n=6 mice. NS (not significant) $p > 0.05$. Scale bars: **b** 200 μm, **c** 100 μm.

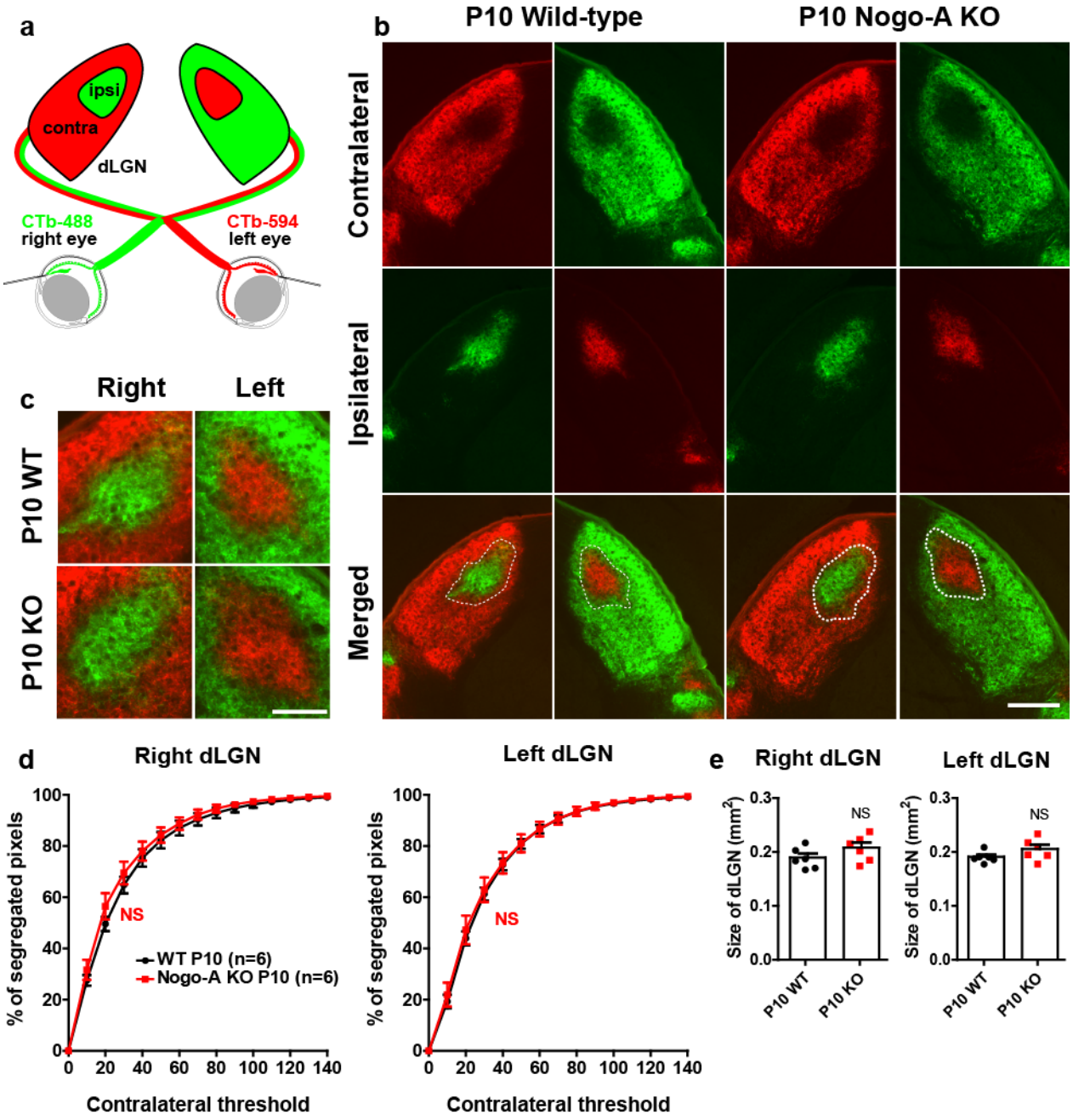
a
ipsi
contra
dLGN
CTb-488
right eye
CTb-594
left eye
b
P10 Wild-type
P10 Nogo-A KO
Contralateral
Ipsilateral
Merged
c
Right
Left
P10 WT
P10 KO
d
Right dLGN
Left dLGN
% of segregated pixels
NS
WT P10 (n=6)
Nogo-A KO P10 (n=6)
Contralateral threshold
e
Right dLGN
Left dLGN
Size of dLGN (mm²)
NS
P10 WT
P10 KO

4. Discussion

In the present study, we analyzed the expression pattern of Nogo-A protein in the early postnatal and adult mouse visual system and determined whether systemic deletion of Nogo-A influences the developmental refinement of the eye-specific retinogeniculate projection. The Nogo-A protein expression in the retinal ganglion cells is developmentally regulated and decreases before postnatal day 6, whereas Nogo-A receptor NgR1 is expressed in RGC cell bodies and axons in young and adult mice. In the optic nerve, Nogo-A is expressed by oligodendrocytes, whereas in the LGN and visual cortex Nogo-A is also present in neurons in addition to oligodendrocytes. Systemic deletion of Nogo-A did not influence the developmental refinement of the anatomical distribution of the terminals of axons from left and right eye in the dLGN.

4.1 Nogo-A and NgR1 are expressed in complementary patterns in the visual system

Nogo-A is strongly expressed in prenatal RGCs [28] and during the first postnatal days but is down-regulated before the sixth postnatal day, when the expression switches to Müller glia. The role of Nogo-A in Müller glia is unknown. Müller glia differentiate in the mouse retina around P3 and reach maturity at P20 [29]; morphologically, Müller glia process density and radial orientation seemed normal in the Nogo-A KO mice (data not shown), but more subtle effects of the absence of Nogo-A on the biochemical or functional maturation of Müller cells cannot be excluded. However, in the adult Nogo-A KO mice retinae expression of the glial structural proteins, vimentin and GFAP [14] and the expression of the mature Müller glia markers, Kir 4.1 and aquaporin 4, (Pernet.V.;data not shown) was not significantly different from the WT retinae.

Neuronal Nogo-A expression might be involved in axonal growth and fasciculation [30, 31] as the timing of RGC axonal growth correlates with the high Nogo-A expression in those cells. In

the mouse, retinal axons crossing at the chiasm innervate the LGN at around embryonic day 15-16, whereas uncrossed projections reach their target postnatally around P0-P2 [6]. Nogo-A and its receptors have been also implicated in the axonal guidance at the optic chiasm. During the optic chiasm decussation, acute blockage of the NgR1 receptor with blocking peptide NEP1-40 led to guidance errors [32]. However, using the DiI tracing of the RGC axons at the embryonic day 15 and at P1 we did not observe any guidance errors at the optic chiasm of Nogo-A KO mice (Pernet. V.; data not shown).

The Nogo-A receptors NgR1 and S1PR2 are both expressed in the retina but *S1pr2* mRNA is down-regulated to a lower level before postnatal day 10. On the other hand, *Ngr1* mRNA is expressed in young and adult retinae. In adult mouse retinae, NgR1 protein is specifically expressed in retinal ganglion cell bodies and axons.

So far, there was not detailed study on the Nogo-A protein expression in the thalamus. In the Allen Institute adult mouse brain resources [33] Nogo-A mRNA appears to be moderately to strongly expressed in the LGN neurons and in oligodendrocytes in the optic tract. A similar expression is described in other thalamic nuclei and hippocampus. Previous studies reported that in adult rat brains Nogo-A mRNA expression in the neocortex was the strongest in layer II/III and layer V-VI [25, 26]; the protein was mainly detected in oligodendrocytes in the corpus callosum [25]. In the adult brain, including the visual system, we detected Nogo-A in both oligodendrocytes and neurons. The staining intensity was stronger in neurons; however, the myelin pool of Nogo-A is probably underestimated, since we did not use organic solvents that would improve detection of myelin proteins but hinder neuronal signal [25]. These localizations suggest that NgR1 and S1PR2 expressed in retinal axons may interact with Nogo-A expressed by

oligodendrocytes in the optic nerve and the optic tract and by neurons and oligodendrocytes of the LGN.

4.2 Retinotopic map formation is not affected by Nogo-A deletion

Several guidance molecules including Slit, Shh and Ephrin-B [34-36] are involved in the RGC growth cone guidance at the optic chiasm. Recently, Nogo-A expressed by radial glia at the optic chiasm has been suggested to be involved in the repulsion of the NgR1 expressing RGC growth cones especially from ventrotemporal retina which projects ipsilaterally [32]. However, in P10 Nogo-A mice, the ipsilateral eye projections appear to form normally and to innervate the appropriate region of the dLGN.

4.3 The refinement of the retinogeniculate projection is normal in the absence of Nogo-A

Eye-specific segregation of retinal synaptic terminals in the mouse dLGN occurs based on the spontaneous retinal activity at the time when photoreceptors are still immature and eyelids are closed [37, 38]. As the spontaneous activity of two eyes is not synchronous, synaptic terminals from one eye ending on a given LGN neuron get selectively strengthened and those from the other eye eliminated based on the burst-time-dependent plasticity leading finally to a monocular innervation [39]. Nogo-A and its receptor NgR1 have been recently shown to restrict long term potentiation (LTP) in hippocampus and motor cortex [40-42]. Therefore, it is tempting to speculate that the developmental down-regulation of Nogo-A expression in the RGCs before postnatal day 6 might be required for a proper synaptic strengthening and refinement of retinal terminals which occurs around this time. In line with this hypothesis, the stabilization of the synaptic contacts between Purkinje and deep cerebellar nuclei neurons has been shown to require developmental Nogo-A down-regulation [43]. The genetic deletion of Nogo-A in the present study could have enhanced this process. Thus, it would be interesting to investigate whether

ectopic overexpression of Nogo-A in RGCs during LGN segregation would interfere with this process and, on the other hand, if systemic deletion of Nogo-A would accelerate the refinement at P4 when the Nogo-A level is still high in WT RGCs. Moreover, systemic deletion of Nogo-A was shown to induce up-regulation of other repulsive and inhibitory factors and their receptors, in particular semaphorin 3F and 4D, plexin B2, ephrin A3 and EphA4 in the mouse spinal cord and neocortex [44]. It would be therefore interesting to know the expression pattern of these factors in the developing visual system, but one should also analyze whether Nogo-A deletion affects spontaneous and visually-evoked retinal and retinogeniculate activity. Finally, cell-specific Nogo-A KO mice, which are coming available now, should be used to determine the role of myelin vs. neuronal Nogo-A in the different aspects of retinal pathway development and refinement.

References

1. McLaughlin, T. and D.D. O'Leary, *Molecular gradients and development of retinotopic maps.* Annu. Rev. Neurosci., 2005. **28**: p. 327-55.
2. Chen, C. and W.G. Regehr, *Developmental remodeling of the retinogeniculate synapse.* Neuron, 2000. **28**(3): p. 955-66.
3. Mooney, R., et al., *Thalamic relay of spontaneous retinal activity prior to vision.* Neuron, 1996. **17**(5): p. 863-74.
4. Pham, T.A., et al., *The CRE/CREB pathway is transiently expressed in thalamic circuit development and contributes to refinement of retinogeniculate axons.* Neuron, 2001. **31**(3): p. 409-420.
5. Pfeiffenberger, C., et al., *Ephrin-As and neural activity are required for eye-specific patterning during retinogeniculate mapping.* Nat. Neurosci., 2005. **8**(8): p. 1022-7.
6. Godement, P., J. Salaun, and M. Imbert, *Prenatal and postnatal development of retinogeniculate and retinocollicular projections in the mouse.* J. Comp. Neurol., 1984. **230**(4): p. 552-75.
7. Jaubert-Miazza, L., et al., *Structural and functional composition of the developing retinogeniculate pathway in the mouse.* Vis. Neurosci., 2005. **22**(5): p. 661-76.
8. Hubel, D.H. and T.N. Wiesel, *The period of susceptibility to the physiological effects of unilateral eye closure in kittens.* J Physiol., 1970. **206**(2): p. 419-36.
9. Hooks, B.M. and C. Chen, *Distinct roles for spontaneous and visual activity in remodeling of the retinogeniculate synapse.* Neuron, 2006. **52**(2): p. 281-91.
10. Hooks, B.M. and C. Chen, *Vision triggers an experience-dependent sensitive period at the retinogeniculate synapse.* J. Neurosci., 2008. **28**(18): p. 4807-17.
11. McGee, A.W., et al., *Experience-driven plasticity of visual cortex limited by myelin and Nogo receptor.* Science, 2005. **309**(5744): p. 2222-6.

12. Pernet, V., et al., *Nogo-A and myelin-associated glycoprotein differently regulate oligodendrocyte maturation and myelin formation.* J. Neurosci., 2008. **28**(29): p. 7435-44.
13. Simonen, M., et al., *Systemic deletion of the myelin-associated outgrowth inhibitor Nogo-A improves regenerative and plastic responses after spinal cord injury.* Neuron, 2003. **38**(2): p. 201-11.
14. Pernet, V., et al., *Neuronal Nogo-A upregulation does not contribute to ER stress-associated apoptosis but participates in the regenerative response in the axotomized adult retina.* Cell Death Differ., 2012. **19**(7): p. 1096-108.
15. Oertle, T., et al., *Nogo-A inhibits neurite outgrowth and cell spreading with three discrete regions.* J. Neurosci., 2003. **23**(13): p. 5393-406.
16. Pernet, V., et al., *Misguidance and modulation of axonal regeneration by Stat3 and Rho/ROCK signaling in the transparent optic nerve.* Cell Death Dis., 2013. **4**: p. e734.
17. Livak, K.J. and T.D. Schmittgen, *Analysis of relative gene expression data using real-time quantitative PCR and the 2(-Delta Delta C(T)) Method.* Methods, 2001. **25**(4): p. 402-8.
18. Muir-Robinson, G., B.J. Hwang, and M.B. Feller, *Retinogeniculate axons undergo eye-specific segregation in the absence of eye-specific layers.* J. Neurosci., 2002. **22**(13): p. 5259-64.
19. Wälchli, T., et al., *Nogo-A is a negative regulator of CNS angiogenesis.* Proc. Natl. Acad. Sci. U. S. A., 2013. **110**(21): p. E1943-52.
20. Park, J.B., et al., *A TNF receptor family member, TROY, is a coreceptor with Nogo receptor in mediating the inhibitory activity of myelin inhibitors.* Neuron, 2005. **45**(3): p. 345-51.
21. Dickendesher, T.L., et al., *NgR1 and NgR3 are receptors for chondroitin sulfate proteoglycans.* Nature Neurosci., 2012. **15**(5): p. 703-12.
22. Kempf, A., et al., *The sphingolipid receptor S1PR2 is a receptor for Nogo-a repressing synaptic plasticity.* PLoS Biol., 2014. **12**(1): p. e1001763.
23. Verity, A.N. and A.T. Campagnoni, *Regional expression of myelin protein genes in the developing mouse brain: in situ hybridization studies.* J. Neurosci. Res., 1988. **21**(2-4): p. 238-48.
24. Arcelli, P., et al., *GABAergic neurons in mammalian thalamus: a marker of thalamic complexity?* Brain Res. Bull., 1997. **42**(1): p. 27-37.
25. Huber, A.B., et al., *Patterns of Nogo mRNA and protein expression in the developing and adult rat and after CNS lesions.* J. Neurosci., 2002. **22**(9): p. 3553-67.
26. Godement, P., J. Salaun, and M. Imbert, *Prenatal and Postnatal-Development of Retinogeniculate and Retinocollicular Projections in the Mouse.* J. Comp. Neurol., 1984. **230**(4): p. 552-575.
27. Guido, W., *Refinement of the retinogeniculate pathway.* J Physiol., 2008. **586**(Pt 18): p. 4357-62.
28. Wang, J., et al., *Localization of Nogo and its receptor in the optic pathway of mouse embryos.* J. Neurosci. Res., 2008. **86**(8): p. 1721-33.
29. Cepko, C.L., et al., *Cell fate determination in the vertebrate retina.* Proc. Natl. Acad. Sci. U. S. A., 1996. **93**(2): p. 589-95.
30. Petrinovic, M.M., et al., *Neuronal Nogo-A regulates neurite fasciculation, branching and extension in the developing nervous system.* Development, 2010. **137**(15): p. 2539-50.
31. Richard, M., et al., *Neuronal expression of Nogo-A mRNA and protein during neurite outgrowth in the developing rat olfactory system.* Eur. J. Neurosci., 2005. **22**(9): p. 2145-58.
32. Wang, J., et al., *The growth-inhibitory protein Nogo is involved in midline routing of axons in the mouse optic chiasm.* J. Neurosci. Res., 2008. **86**(12): p. 2581-90.
33. Lein, E.S., et al., *Genome-wide atlas of gene expression in the adult mouse brain.* Nature, 2007. **445**(7124): p. 168-76.
34. Erskine, L., et al., *Retinal ganglion cell axon guidance in the mouse optic chiasm: expression and function of robos and slits.* J. Neurosci., 2000. **20**(13): p. 4975-82.
35. Trousse, F., et al., *Control of retinal ganglion cell axon growth: a new role for Sonic hedgehog.* Development, 2001. **128**(20): p. 3927-36.

36. Nakagawa, S., et al., *Ephrin-B regulates the Ipsilateral routing of retinal axons at the optic chiasm.* Neuron, 2000. **25**(3): p. 599-610.
37. Galli, L. and L. Maffei, *Spontaneous impulse activity of rat retinal ganglion cells in prenatal life.* Science, 1988. **242**(4875): p. 90-1.
38. Torborg, C.L., K.A. Hansen, and M.B. Feller, *High frequency, synchronized bursting drives eye-specific segregation of retinogeniculate projections.* Nat. Neurosci., 2005. **8**(1): p. 72-8.
39. Butts, D.A., P.O. Kanold, and C.J. Shatz, *A burst-based "Hebbian" learning rule at retinogeniculate synapses links retinal waves to activity-dependent refinement.* PLoS Biol., 2007. **5**(3): p. e61.
40. Delekate, A., et al., *NogoA restricts synaptic plasticity in the adult hippocampus on a fast time scale.* Proc. Natl. Acad. Sci. U. S. A., 2011. **108**(6): p. 2569-74.
41. Raiker, S.J., et al., *Oligodendrocyte-myelin glycoprotein and Nogo negatively regulate activity-dependent synaptic plasticity.* J. Neurosci., 2010. **30**(37): p. 12432-45.
42. Tews, B., et al., *Synthetic microRNA-mediated downregulation of Nogo-A in transgenic rats reveals its role as regulator of synaptic plasticity and cognitive function.* Proc. Natl. Acad. Sci. U. S. A., 2013. **110**(16): p. 6583-6588.
43. Aloy, E.M., et al., *Synaptic destabilization by neuronal Nogo-A.* Brain Cell Biol., 2006. **35**(2-3): p. 137-56.
44. Kempf, A., et al., *Upregulation of axon guidance molecules in the adult central nervous system of Nogo-A knockout mice restricts neuronal growth and regeneration.* Eur. J. Neurosci., 2013. **38**(11): p. 3567-79.

CHAPTER 3

NOGO-A DELETION INCREASES THE PLASTICITY OF THE OPTOKINETIC RESPONSE AND CHANGES RETINAL PROJECTION ORGANIZATION IN THE ADULT MOUSE VISUAL SYSTEM

Anna Guzik-Kornacka, Alexander van der Bourg, Flora Vajda, Sandrine Joly, Franziska Christ, Martin E. Schwab, Vincent Pernet.

Submitted and under review in, *Brain Structure and Function*

V.P., M.E.S. and A.G.K: designed the study. A.G.K. recorded and analyzed behavior, performed anatomical tracings (with help of V.P.), harvested and processed tissues, acquired microscopic images (with help of S.J. and F.C.), analyzed retinal projection segregation (with help of A.B.), made 3D brain reconstructions. V.P. performed viral tracing and visual cortex ablation, F.V. analyzed ectopic projections density. A.G.K. made all the figures (except Fig. 5 by V.P.) and wrote the manuscript (corrected by V.P. and M.E.S.).

1 Abstract

The inhibitory action of Nogo-A on axonal growth has been well described. However, much less is known about the effects that Nogo-A could exert on the plasticity of neuronal circuits under physiological conditions. We investigated the effects of Nogo-A knock-out (KO) on visual function of adult mice using the optokinetic head turning response (OKR) and the monocular deprivation (MD)-induced OKR plasticity and analyzed the anatomical organization of the eye-specific retinal projections. The spatial frequency sensitivity of the OKR was higher in intact Nogo-A KO than in wild-type (WT) mice. After MD, Nogo-A KO mice reached a significantly higher spatial frequency and contrast sensitivity. Bilateral ablation of the visual cortex did not affect the OKR sensitivity before MD but reduced the MD-induced enhancement of OKR by approximately 50 % in Nogo-A KO and WT mice. These results suggest that cortical and subcortical brain structures contribute to the OKR plasticity. The tracing of retinal projections to the dorsal lateral geniculate nucleus (dLGN) revealed that the segregation of eye-specific terminals was decreased in the adult Nogo-A KO dLGN compared with WT mice. Strikingly, MD of the right eye led to additional desegregation of retinal projections in the left dLGN of Nogo-A KO but not in WT mice. In particular, MD promoted ectopic varicosity formation in Nogo-A KO dLGN axons. The present data show that Nogo-A restricts visual experience-driven plasticity of the OKR and plays a role in the segregation and maintenance of retinal projections to the brain.

2 Introduction

The mammalian visual system is a well-established model to study the effects of lesions and experience on the CNS function and plasticity [1-4]. The ocular dominance (OD) plasticity of primary visual cortex neurons (V1) has been shown to be most prominent during the developmental critical period (in mouse postnatal day (P)19-P32) and to decline afterward upon maturation of inhibitory circuits [5, 6] and specific factors associated with myelin and perineuronal nets [7, 8]. In contrast to the visual cortex, the subcortical visual system is considered to be much less plastic [2, 9]. However, recent electrophysiological studies suggested that retinogeniculate synapses are sensitive to visual experience, and their plasticity is limited to the "sensitive period" overlapping with the cortical critical period [10, 11]. Factors limiting adult subcortical plasticity are largely unknown.

In this study, we investigated the potential role of the myelin-associated membrane protein Nogo-A in the plasticity of the adult mouse visual system. Nogo-A is best known as an inhibitor of neurite outgrowth and regeneration in the injured CNS [12, 13]. Recently, Nogo-A also emerged as a negative physiological regulator of neuronal plasticity in the intact adult CNS. Deletion of the Nogo-A/B or their receptor NgR1 gene maintained experience-dependent plasticity in the visual or the somato-sensory cortex beyond the end of the critical period [7, 14]. As oligodendrocytes mature and Nogo-A appears at the time of the normal maturational closure of the plastic time window, myelin Nogo-A was claimed to be a major modulator of this phenomenon [7]. Results from blockage experiments revealed that Nogo-A and NgR1 repressed LTP in the hippocampus and motor cortex [15-17].

To assess functional plasticity in the subcortical visual system we used the optokinetic head response (OKR) as described by Prusky and colleagues [18], measuring spatial frequency and

contrast sensitivity in adult Nogo-A knock-out (KO) mice before and after monocular deprivation (MD). This paradigm was previously used to demonstrate that vision plasticity can be enhanced in adult mice and is mediated by the visual cortex [19, 20]. Neither the role of subcortical circuits nor the molecular mechanisms influencing the increase of spatial frequency sensitivity in this system have been investigated so far.

Here we show that Nogo-A KO mice have improved spatial frequency sensitivity and increased spatial frequency and contrast sensitivity enhancement after MD-induced plasticity compared with WT mice. Additionally, upon bilateral visual cortex ablation, MD was still able to induce a significantly higher increase of spatial frequency sensitivity in Nogo-A KO than in WT mice, suggesting that cortical and subcortical visual regions participate in the OKR plasticity. At the anatomical level, Nogo-A deletion led to a decrease in the eye-specific segregation of retinal projections in the dLGN of adult mice. After ten days of right eye closure, the degree of retinal projections segregation in the left dLGN was additionally decreased in Nogo-A KO mice compared with intact mice. We observed significantly more ectopic terminals from the open eye into closed eye ipsilateral territory in Nogo-A KO vs. WT mice.

3 Materials and methods

3.1 Animals

Young adult (P60-P65) male C57BL/6 wild-type and Nogo-A knock-out (KO) mice [21] with the same genetic background were used for behavioral vision measurements or tissue analysis. Nogo-A KO mice were generated in our laboratory and were bred with C57BL/6 WT mice from the animal facility of the Brain Research Institute for more than 20 generations. Animal experiments were carried out with acceptance and in agreement with the guidelines of the Cantonal Veterinary Office in Zurich.

3.2 Visual deprivation

To test the functional and anatomical plasticity, we monocularly deprived adult Nogo-A KO and WT mice (the onset of deprivation, at P60-P65) by suturing the right eyelid as described previously [3]. Briefly, under isoflurane anesthesia the eyelid margins of the right eye were trimmed and antibiotic ophthalmic ointment was applied to the eye. The trimmed eyelids were closed with three mattress sutures using 9-0 silk. In behavioral experiments, the eyelids were re-opened after 7 days of deprivation under isoflurane anesthesia. Animals whose eyelids were not fully closed and animals that had corneal opacities after eye reopening were excluded from the experiments.

3.3 Measurements of spatial frequency and contrast sensitivity

Spatial frequency and contrast sensitivity thresholds of the OKR were measured with the virtual optomotor system in freely moving mice as described previously (Fig. 1a; [18]). Briefly, individual mice were placed on an elevated platform in the center of an arena surrounded by four computer screens, and moving gratings of increasing spatial frequency or decreasing contrast

were displayed on the monitors (OptoMotry, CerebralMechanics). As animals track only gratings moving in the temporal-to-nasal direction, it is possible to test the two eyes independently by changing the direction of the stimulus [22]. The OKR spatial frequency sensitivity threshold was determined by presenting full contrast gratings with increasing spatial frequency (starting from 0.042 cycle/degree (c/d)), until the maximum frequency that the mice were able to discriminate was reached. Contrast thresholds were determined at six spatial frequencies: 0.031, 0.064, 0.092, 0.103, 0.192, 0.272 c/d by decreasing the contrast of the gratings until the tracking behavior ceased. Contrast thresholds were re-calculated into contrast sensitivity (Michelson contrast) by taking into account the luminescence of the screens. The contrast sensitivity (the reciprocal of the threshold) was then plotted against spatial frequencies on a log–log graph. For example, a contrast sensitivity of value 20 corresponds to 5.1 % of contrast and contrast sensitivity of 4 corresponds to 25.1 % of contrast.

3. 4 Ablation of the visual cortices

To test the importance of the subcortical visual system for the plasticity of the OKR sensitivity, we bilaterally ablated the visual cortex using a modified protocol described by Prusky and colleagues [19]. Under isoflurane anesthesia, two small craniotomies were made above both striate cortices (2 to 3 mm lateral from the midline; 3 to 4 mm posterior from the bregma); and the cortices were aspirated down to the white matter according to the following stereotactic coordinates: 1.5 mm lateral to 4.0 mm lateral from the midline; 2.5 to 5.0 mm posterior from the bregma. The cavities were filled with gelfoam soaked with sterile saline, and the scalp was suture-closed. Operated animals were injected with an analgesic (Temgesic (Buprenorphin) 0.1 mg/kg of body weight) and were placed on a warm blanket until recovery. Visual function tests were started one day after the surgery. At the end of the behavioral testing, animals were

sacrificed using an overdose of Nembutal and were perfused with solution of PBS followed by 4 % PFA. Brains were coronally sectioned, and 3 dimensional (3D) reconstructions were created using Neurolucida software (MBF Bioscience). The volumes of the lesions were measured in the same software.

3.5 Anterograde tracing of retinal projections

To anterogradely trace retinal projections, cholera toxin β-subunit (CTb) conjugated to different fluorophores (Alexa 488, Alexa 594 or Alexa 647; 1.5 µl, 0.5 % in PBS, Molecular Probes) or adeno-associated virus serotype 2 (AAV2) containing eGFP cDNA under CAG promoter was intravitreally injected as previously described [23]. The AAV2.GFP vector (10^{14} vg/ml) was produced as described before [24] and was kindly provided by Dr. Deniz Dalkara (Institut de la Vision, Paris). CTb injections were made one day before sacrificing the animals, and the virus was injected into the left eye three weeks before the monocular deprivation in order to allow for optimal GFP expression. In monocularly deprived animals, the tracing was performed without exposing the cornea to light by making an incision in the upper eyelid above the sclera. Mice were sacrificed by an overdose of Nembutal and were perfused with PBS followed by a 4 % PFA solution. Brain coronal cryosections were cut at 40 µm and visualized with a Zeiss Axioskop 2 Plus epi-fluorescence microscope (Carl Zeiss) or for mosaic image reconstruction with Leica DM550B microscope using a 10X objective (NA 0.3). For the analysis of ectopic open eye projections images were acquired with a Leica SPE-II confocal microscope at 40X (NA 1.25), at a step size of 0.5 µm (Fig. 4) or 0.2 µm (Fig. 5) and a resolution of 1024 x 1024 pixels (0.27 µm/pixel).

3.6 Image analysis

Segregation between eye-specific projections in the dLGN was determined for different contralateral thresholds on a 0-255 grayscale as described by Muir-Robinson et al. [25]. Background fluorescence was subtracted from the images using a rolling ball filter of 200 pixels radius and histograms were normalized to 8-bit intensity range (NIH ImageJ). Ipsilateral gray value thresholds were kept constant and adjusted consistently for each picture. For each animal, we analyzed three sections from the middle of the dLGN containing the largest ipsilateral patch using custom-written NIH ImageJ plugins and routines. The size of the dLGN was measured in NIH ImageJ for the 3 sections used in the segregation analysis and is reported for each animal as an average from these 3 sections.

The analysis of the nucleus of the optic tract (NOT) was done on 3 coronal sections in the rostral region of the superior colliculus (SC). To measure the size of the nucleus we defined its borders in similar way for all pictures by excluding the optic tract and preoptic nuclei. The fiber density in the NOT was calculated by measuring the area occupied by the tracer on binarised images after background subtraction with a rolling ball filter of 200 pixels radius (NIH ImageJ).

To analyze the occurrence of the ectopic open eye projections in the middle of the closed eye ipsilateral territory, we acquired confocal pictures of three central sections of the right dLGN and created maximum intensity projections from 20 µm image stacks. On binarised pictures, we analyzed the percentage of area occupied by the ectopic left eye projections (CTb-594 Fig. 4f or CTb-594 and GFP Fig. 5e) in a 100 x 100 µm region of interest (ROI) placed in the center of the right eye ipsilateral territory. The ROI was automatically positioned at the center of mass of the right eye ipsilateral region (NIH ImageJ).

3.7 Statistical analysis

All numerical data are presented as a mean ± standard error of the mean (SEM). Spatial frequency and contrast sensitivity as well as eye-specific segregation data were analyzed between groups using the two-way repeated measures (RM) analysis of variance ANOVA. The lesion volume, the ectopic projections and size of the NOT were analyzed by applying a one-way ANOVA test. In all cases we applied Bonferroni's post-hoc tests with $\alpha = 0.05$. Sizes of dLGNs were compared between WT and KO groups using a Student's t-test.

4 Results

4.1 Nogo-A ablation increases the plasticity of the optokinetic response after monocular deprivation

The optokinetic response (OKR) to moving gratings allows a non-invasive assessment of spatial frequency sensitivity in mice [18]. Monocular deprivation (MD) induces plasticity in the OKR that is reflected by an increase in spatial frequency sensitivity of the non-deprived eye [19]. At the molecular level, the mechanisms of the OKR plasticity have not been studied. In order to determine if systemic Nogo-A deletion influences experience-driven plasticity of vision, we followed the MD-induced enhancement of OKR thresholds (Fig. 1a) mediated by the non-deprived eye in adult Nogo-A KO and WT mice (Fig. 1b). In intact Nogo-A KO mice, the OKR sensitivity threshold of the left (Fig. 1b; 0.416 ± 0.001 cycle/degree, mean ± SEM) and right (Fig. S1a; 0.417 ± 0.009 c/d) eye was significantly higher than in WT animals (WT left eye: 0.395 ± 0.0007 c/d; WT right eye: 0.397 ± 0.0008 c/d). The OKR sensitivity steadily increased in the non-deprived, left eye and plateaued at 5 days in the two groups subjected to 7 days of MD (Fig. 1b). After 7 days of MD, Nogo-A KO responded to higher spatial frequencies (0.595 ± 0.005 c/d; representing a 43 % increase above the baseline) than WT mice (0.530 ± 0.006 c/d; 34 % increase above baseline). After eye reopening, the sensitivity gradually returned to baseline within 6-7 days in both Nogo-A KO and WT mice. In the two mouse genotypes, the OKR threshold of the deprived eye showed no deficit after eye reopening (Fig. S1a). The spatial frequency sensitivity changes induced by MD in WT mice are consistent with previous reports [19, 20]. Repeated measurements of OKR sensitivity have been reported to influence the maximal spatial frequency that can be reached after MD [19]. Therefore, in another group of animals we measured the OKR sensitivity threshold one time before MD and another time at day 5 of MD (Fig. S1b). WT mice

tested only once at day 5 reached a lower OKR sensitivity threshold than that observed in the animal group measured daily (0.493 ± 0.004 vs. 0.527 ± 0.006 c/d; p = 0.001). However, in Nogo-A KO mice the difference between single and daily measurements was not significant (0.571 ± 0.003 vs. 0.589 ± 0.006 c/d; p = 0.103), suggesting perhaps a stronger plastic capacity than in WT visual system. We also measured contrast sensitivity that has previously been reported to increase after MD [19]. Contrast sensitivity was measured for six different spatial frequencies (0.031, 0.064, 0.092, 0.103, 0.192 and 0.272 c/d) before, during the 7-day period of MD and after eye reopening (Fig. 1c, d and Fig. S 1c, d). At the baseline, there was no difference in contrast sensitivity between WT and Nogo-A KO mice for the two eyes. The contrast sensitivity curves showed typical bell shapes with higher sensitivity for intermediate spatial frequencies (Fig. 1c and Fig. S1c, d). Upon MD, contrast sensitivity of the non-deprived eye strongly increased in both genotypes (Fig. S1c, d). The contrast sensitivity plateaued after 4 days of deprivation. Four intermediate spatial frequencies reached significantly higher values in Nogo-A deficient mice (Fig. 1c). In agreement with previous reports, both groups of mice showed their highest contrast sensitivity at a spatial frequency of 0.064 c/d [18, 19]. After 7 days of MD, Nogo-A KO mice reached a maximum sensitivity of 39.03 ± 0.462 whereas WT mice reached 33.64 ± 0.744, corresponding to 2.62 % and 3.04 % of contrast, respectively (Fig. 1d). One day after right eye reopening, contrast sensitivity of the left eye started decreasing although it remained significantly higher in the Nogo-A KO group, and went back to baseline after 7 days in both genotypes (Fig. S1e). At the behavioral level, our results revealed that Nogo-A ablation potentiates the MD-induced increase in visual plasticity.

Figure 1 Nogo-A deletion potentiates monocular deprivation-induced enhancement in visual performance of adult mice

a The virtual reality optokinetic response (OKR) test was applied to assess spatial frequency and contrast sensitivity. Mouse head tracking was elicited by temporal-to-nasal stimulation. Spatial frequency and contrast sensitivity of adult (P60) WT and Nogo-A KO mice was measured before, during closure and after reopening of the right eye. **b** Spatial frequency sensitivity was higher in Nogo-A KO than in WT mice at the baseline and after right eye MD. **c** The contrast sensitivity of the left eye (represented as a Michelson contrast) was measured at six different spatial frequencies, before and during MD. The right eye MD induced a stronger increase in contrast sensitivity in Nogo-A KO than in WT mice. **d** The time course of the contrast sensitivity measured at a spatial frequency of 0.064 c/d showed stronger increase upon MD in the Nogo-A KO group. (WT n = 5, KO n = 6 mice; two-way repeated measures (RM) analysis of variance (ANOVA), Bonferroni's post-hoc tests, ***$p < 0.001$, **$p < 0.01$, $p^* < 0.05$).

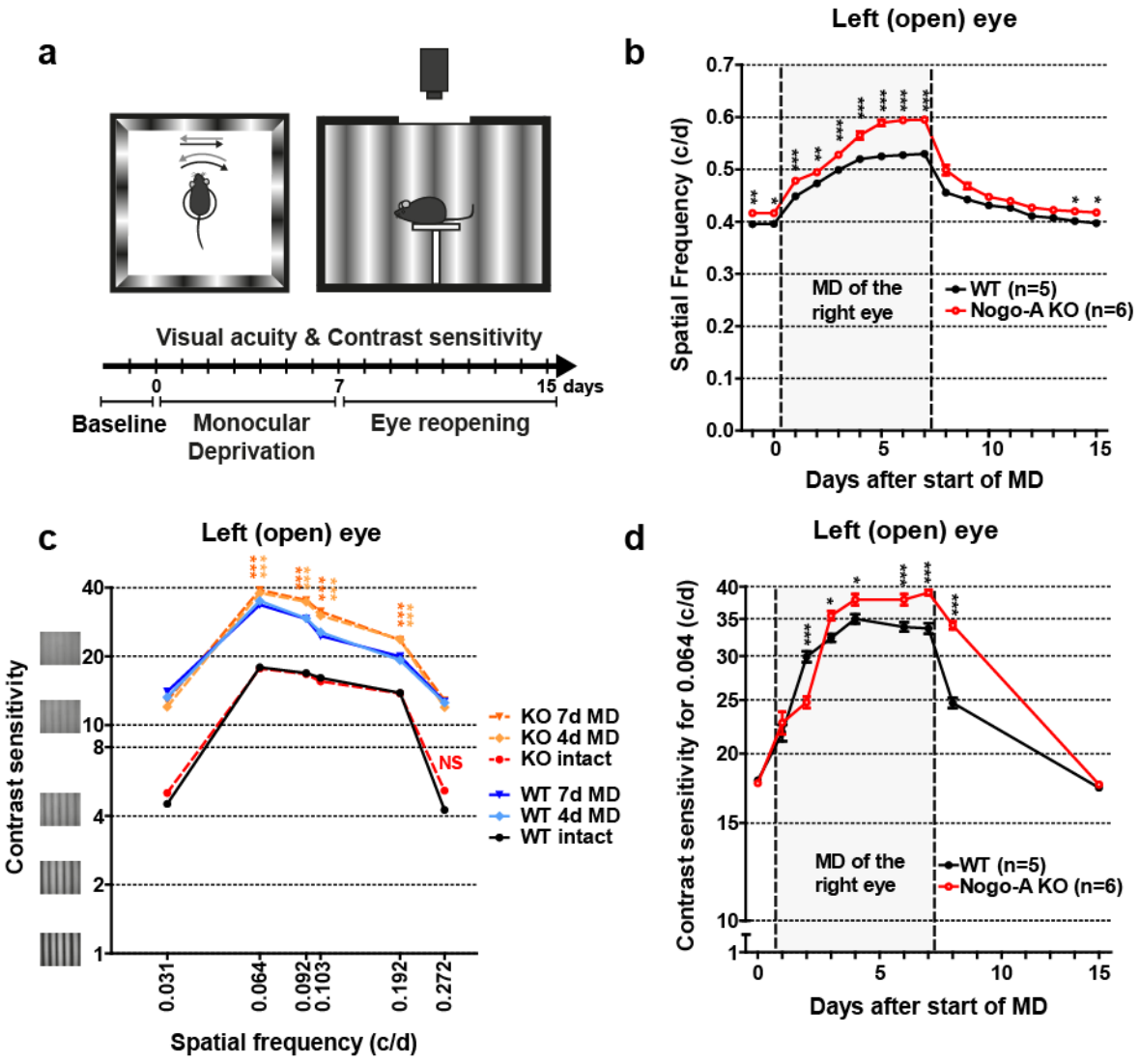
a
Visual acuity & Contrast sensitivity
0
7
15 days
Baseline
Monocular Deprivation
Eye reopening
b
Left (open) eye
Spatial Frequency (c/d)
MD of the right eye
WT (n=5)
Nogo-A KO (n=6)
Days after start of MD
c
Left (open) eye
Contrast sensitivity
KO 7d MD
KO 4d MD
KO intact
WT 7d MD
WT 4d MD
WT intact
NS
Spatial frequency (c/d)
d
Left (open) eye
Contrast sensitivity for 0.064 (c/d)
MD of the right eye
WT (n=5)
Nogo-A KO (n=6)
Days after start of MD

Supplementary figure 1 Spatial frequency and contrast sensitivity measurements
a The right eye OKR sensitivity was not affected by MD but was higher in Nogo-A KO than in WT mice (***$p < 0.001$; two-way RM ANOVA, between groups). **b** Comparison between daily (from Fig. 1b) and single OKR testing after 5 days of MD. In the WT group single measurement of OKR sensitivity at day 5 led to weaker MD-induced OKR enhancement whereas the sensitivity of Nogo-A KO group was increased as strongly as after daily testing. **c, d** Contrast sensitivity of the non-deprived eye increased strongly during 7d of MD in both WT and Nogo-A KO mice. Contrast sensitivity in both groups stabilized after 3-4 days of MD and reached higher values in Nogo-A deficient mice. **e** After reopening of the right eye, contrast sensitivity of the left eye started to decrease after one day but was significantly higher for Nogo-A KO group and went back to baseline by day 7 in both groups. **f** Contrast sensitivity of the right eye was only slightly decreased for WT mice one day after eye reopening but not distinguishable from the baseline for both groups at day 7.

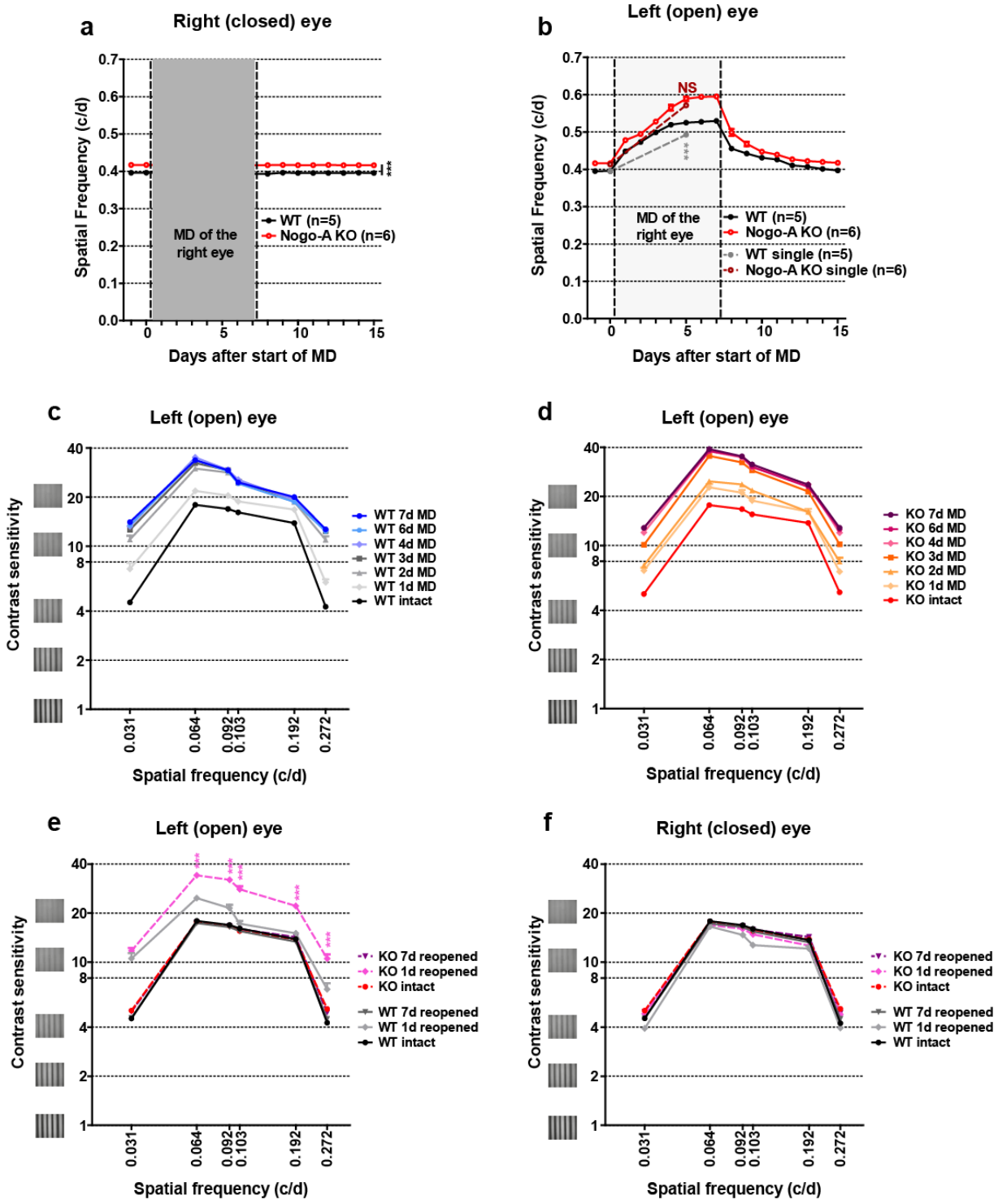
a
Right (closed) eye
Spatial Frequency (c/d)
Days after start of MD
MD of the right eye
WT (n=5)
Nogo-A KO (n=6)
***
b
Left (open) eye
NS
WT single (n=5)
Nogo-A KO single (n=6)
c
Left (open) eye
Contrast sensitivity
Spatial frequency (c/d)
WT 7d MD
WT 6d MD
WT 4d MD
WT 3d MD
WT 2d MD
WT 1d MD
WT intact
d
KO 7d MD
KO 6d MD
KO 4d MD
KO 3d MD
KO 2d MD
KO 1d MD
KO intact
e
KO 7d reopened
KO 1d reopened
KO intact
WT 7d reopened
WT 1d reopened
WT intact
f
Right (closed) eye

4.2 Cortical and subcortical visual regions are involved in the optokinetic response plasticity

Visual plasticity is thought to occur mainly at the cortical level. Prusky and colleagues [19] observed a 72 % reduction in MD-induced OKR elevation after bilateral V1 ablation. In order to determine the relative importance of cortical vs. subcortical structures in the MD-induced OKR increase, we monitored the OKR plasticity before and after bilateral V1 aspiration in WT and Nogo-A KO mice. Three dimensional brain reconstructions allowed to confirm the lesion of V1 (Fig. 2a) and that the lesion volume did not differ between WT and KO groups (Fig. 2b). As previously reported for WT mice [19], before MD, the spatial frequency sensitivity threshold was not affected by V1 cortex aspiration in Nogo-A KO or WT mice (Fig. 2c, d), suggesting that the slight, but significant OKR elevation found in intact KO mice is not a result of cortical plasticity. Under MD conditions, the OKR sensitivity increased significantly more in Nogo-A KO (after 7 days of MD: 0.495 ± 0.003 c/d, 20 % above baseline) than in WT mice (0.460 ± 0.003 c/d, 16 % above baseline), suggesting that ~50 % of MD-induced plasticity occurred in subcortical regions. Taken together, our functional results suggest an important contribution of cortical and subcortical brain regions to the visual plasticity in Nogo-A KO mice.

4.3 Eye-specific segregation of retinal projections is decreased in adult Nogo-A KO mice

We observed that functional plasticity was partially cortex independent. Therefore, we evaluated if Nogo-A deletion influences the retinal projections in subcortical regions. The OKR to horizontal stimuli is mediated by the nucleus of the optic tract (NOT) and the dorsal terminal nucleus (DTN) in the pretectum and the accessory optic system, respectively, receiving projections from the contralateral eye [26, 27]. To visualize retinal ganglion cell (RGC) projections in the brain, we anterogradely traced optic nerve axons by injecting cholera toxin β-

subunit (CTb) conjugated to either Alexa 488 (green; right eye) or Alexa 594 (red; left eye) in the intraocular space (Fig. 3a). We did not observe differences between Nogo-A KO and WT mice in the size (Fig. S2a, b, e, f) or fiber density (Fig. S2a, b, g, h) of the NOT. We then used the two-eye terminal segregation paradigm in the dorsal lateral geniculate nucleus (dLGN) to evaluate the distribution and possibly plasticity of retinal axons (Fig. 3a). Indeed, the dLGN receives projections from the two eyes in well-defined, non-overlapping territories [28, 29]. In adult coronal brain sections of intact WT mice, the projections from the two eyes were well segregated into central ipsilateral and surrounding contralateral eye territories (Fig. 3b, c). However, in adult Nogo-A deficient mice the border between the two eye projections showed a higher overlap (Fig. 3b, c). We quantified the segregation of the two eye projections in the dLGN using a method previously described by Muir-Robinson and colleagues [25]. The eye-specific projections to the dLGN were significantly less segregated in intact adult Nogo-A KO mice than in WT mice and the difference was apparent in the left and right dLGN (Fig. 3d; at contralateral threshold 30, right dLGN: WT 85.6 ± 1.6 vs. KO 70.6 ± 4.2 %; left dLGN WT 80.3 ± 7.5 vs. KO 60.3 ± 7.4 %). The overall size of the dLGN was not different between WT and KO mice (Fig. 3e). These results suggest that the segregation of retinogeniculate terminals is altered in the absence of Nogo-A.

4.4 Monocular deprivation enhances anatomical plasticity in the dorsal lateral geniculate nucleus of Nogo-A KO mice

After normal segregation, eye-specific retinogeniculate projection can destabilize and present more overlap due to abnormal retinal activity [30, 31]. Therefore we decided to investigate whether Nogo-A influences the retinal projection stability in the dLGN after MD monocularly

Figure 2 Cortical and subcortical brain regions contribute to the MD-induced visual acuity enhancement

a Representative dorso-ventral (left) and rostro-caudal projections of the 3D brain reconstruction (scale bar 2 mm). The superior colliculi are marked in yellow. Three weeks after bilateral V1 ablation, the size and position of the lesion was systematically analyzed in 3D reconstructions obtained from coronal brain sections. **b** The volume of cortical lesions was not significantly different between WT and Nogo-A KO mice (n = 5 and 6 mice respectively; One-way ANOVA with Bonferroni's post-hoc tests; NS > 0.05; WT left vs. KO left $p = 0.673$; WT right vs. KO right $p > 0.999$). **c** The spatial frequency sensitivity of the left eye was not affected by bilateral V1 ablation compared with intact animals, and stayed significantly higher in Nogo-A KO than in WT mice (e.g. at BL1 $p = 0.0023$). During right eye MD, the elevation of the spatial frequency sensitivity of the left eye was more modest than in intact conditions, but remained significantly higher in Nogo-A KO than in WT mice (at 7 days of MD WT 0.460 ± 0.003 vs. KO 0.495 ± 0.003 c/d; $p < 0.001$; Two-way RM ANOVA with Bonferroni's post-hoc tests; ***$p < 0.001$). **d** The spatial frequency sensitivity of the right eye was not changed by cortical lesions before and after eye reopening (WT n = 5, KO n = 6 mice; $p < 0.001$; Two-way RM ANOVA, between groups).

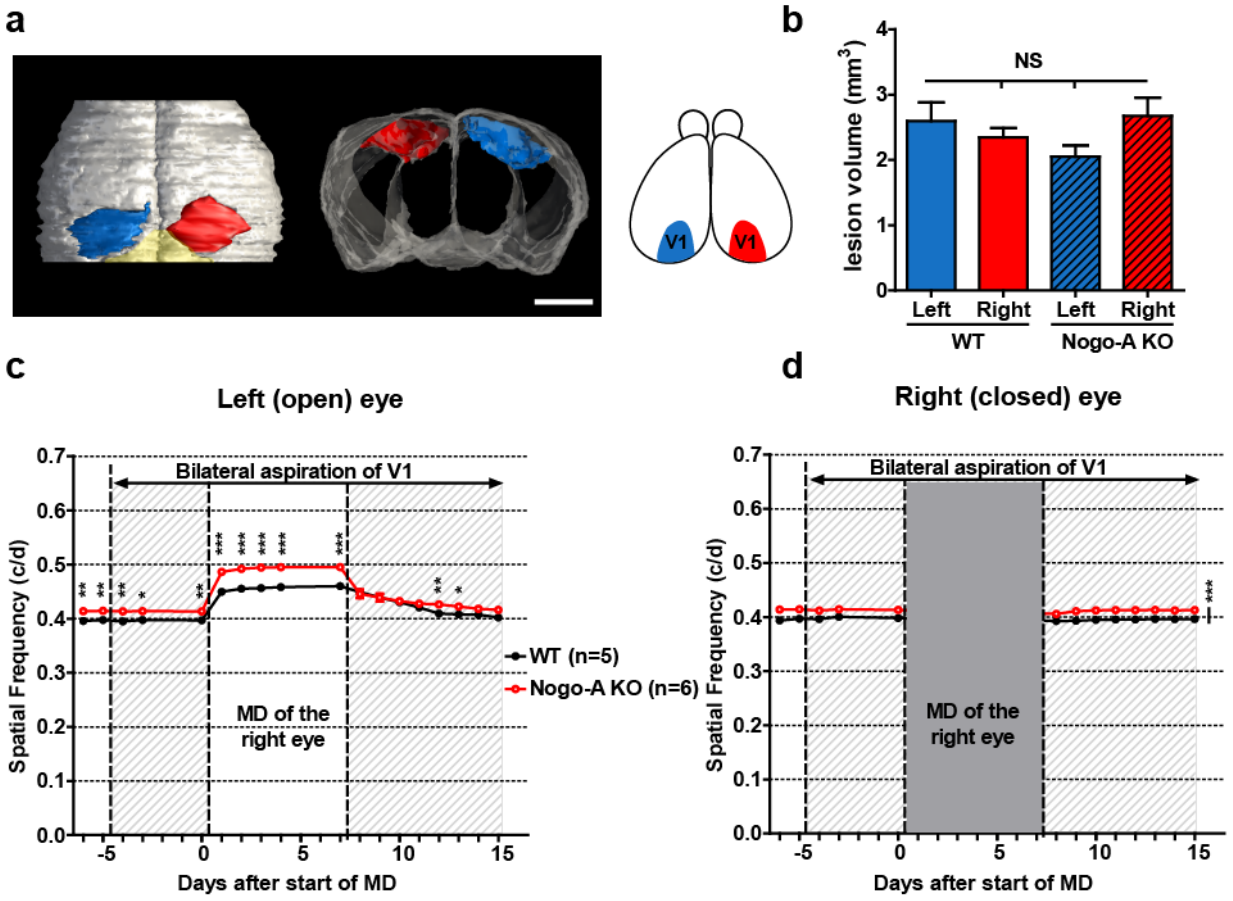
a
V1
V1
b
NS
lesion volume (mm3)
Left
Right
Left
Right
WT
Nogo-A KO
c
Left (open) eye
Bilateral aspiration of V1
MD of the right eye
Spatial Frequency (c/d)
Days after start of MD
WT (n=5)
Nogo-A KO (n=6)
d
Right (closed) eye
Bilateral aspiration of V1
MD of the right eye
Spatial Frequency (c/d)
Days after start of MD

Figure 3 Nogo-A deletion decreases eye-specific segregation of retinogeniculate terminals in adult mice

a Eye-specific projections to the dLGN were visualized by anterograde tracing of RGC projections with cholera toxin β-subunit tracers conjugated to either Alexa 488 (right eye) or Alexa 594 (left eye). The two tracers were intravitreally injected 1 day prior to brain collection. **b** On central dLGN sections, the segregation of ipsi- and contralateral retinal terminals appeared incomplete in adult (P60) Nogo-A KO compared to WT mice (dotted white line indicates the ipsilateral territory; scale bar 200 μm). **c** Magnified image from the ipsilateral eye territory shown in **b** (scale bar 100 μm). **d** Quantitative analysis of terminal segregation represented by the percentage of segregated ipsilateral pixels as a function of the contralateral signal threshold. For the Nogo-A KO group the segregation curves of the right and left dLGN were shifted to the right-hand side, indicating a significantly lower degree of segregation than in WT brains (WT n = 5, KO n = 8 mice; two-way RM ANOVA with Bonferroni's post-hoc tests, ***$p < 0.001$, **$p < 0.01$). **e** Size of the dLGN was not different between the two groups (t-test, right dLGN $p = 0.69$, left dLGN $p = 0.31$).

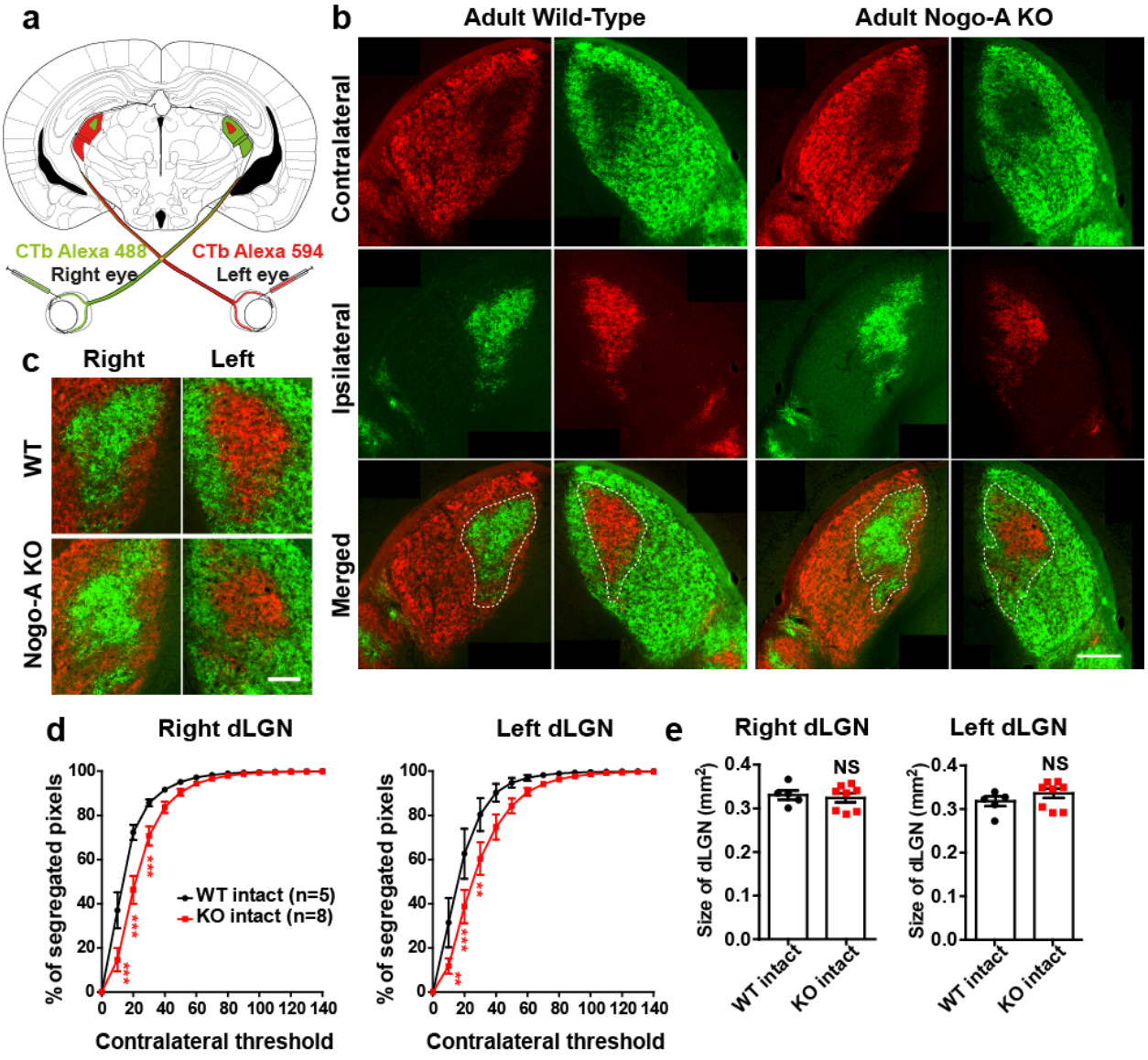
a
CTb Alexa 488
Right eye
CTb Alexa 594
Left eye
b
Adult Wild-Type
Adult Nogo-A KO
Contralateral
Ipsilateral
Merged
c
Right
Left
WT
Nogo-A KO
d
Right dLGN
Left dLGN
% of segregated pixels
Contralateral threshold
WT intact (n=5)
KO intact (n=8)
e
Right dLGN
Left dLGN
Size of dLGN (mm²)
NS
WT intact
KO intact

Supplementary figure 2 Retinal projections in the nucleus of the optic tract
a-d Representative images of the midbrain coronal sections containing the nucleus of the optic tract (NOT; dashed line), rostral end of the superior colliculi (SC) and pretectal nuclei (OPT olivary, PPT posterior and MPT medial pretectal nucleus). CTb tracing of retinal projections from left (red) and right (green) eye did not reveal anatomical changes in the organization of retinal projections in the NOT in the intact or MD Nogo-A KO mice (scale bar 200 μm). **e, f** The size of the NOT was measured on 3 consecutive sections in the rostral part of the superior colliculus. The size did not differ significantly between groups. **g, h** The density of the retinal terminals in NOT did not differ significantly between groups, $p>0.05$.

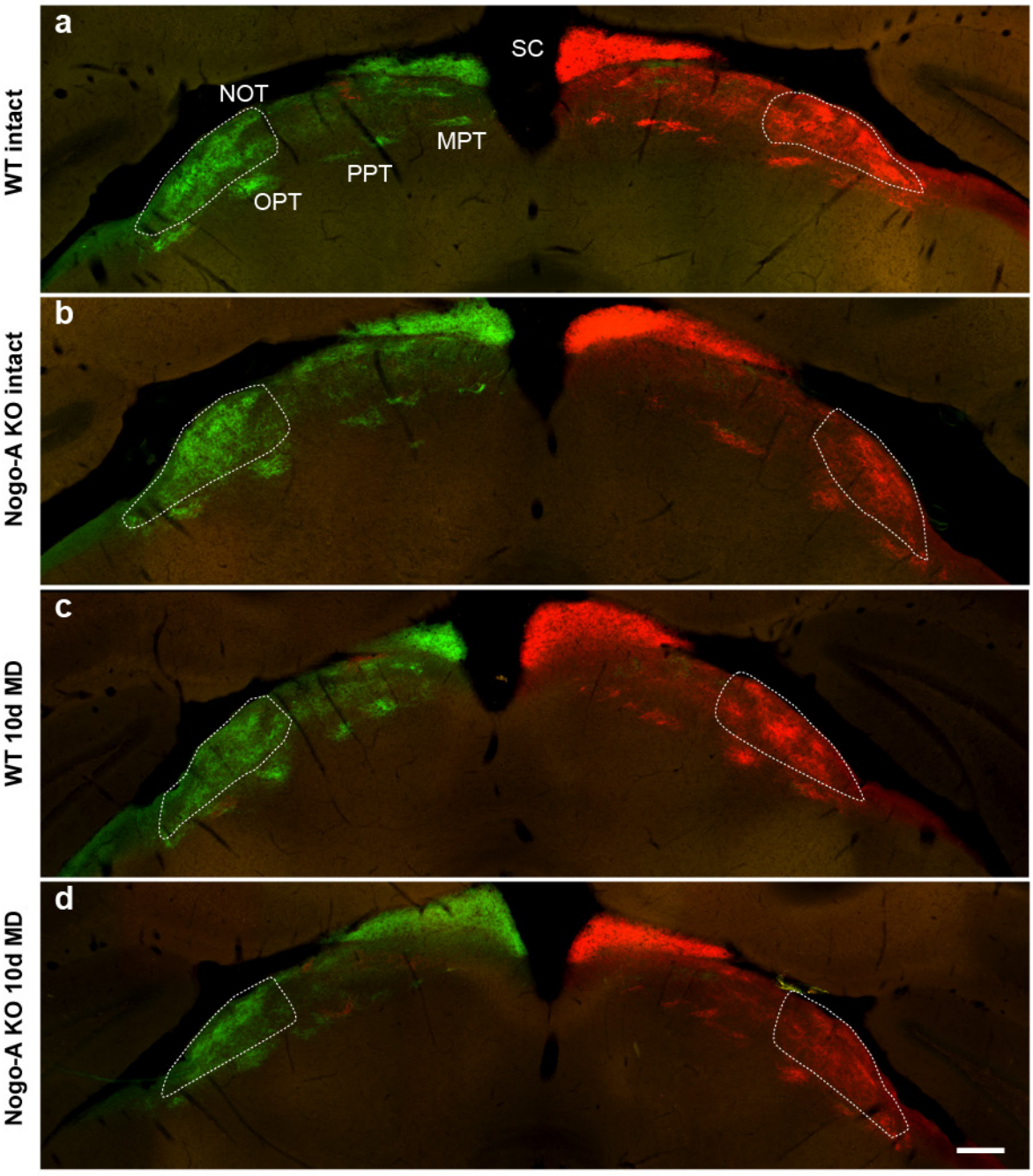
a
WT intact
SC
NOT
MPT
PPT
OPT
b
Nogo-A KO intact
c
WT 10d MD
d
Nogo-A KO 10d MD

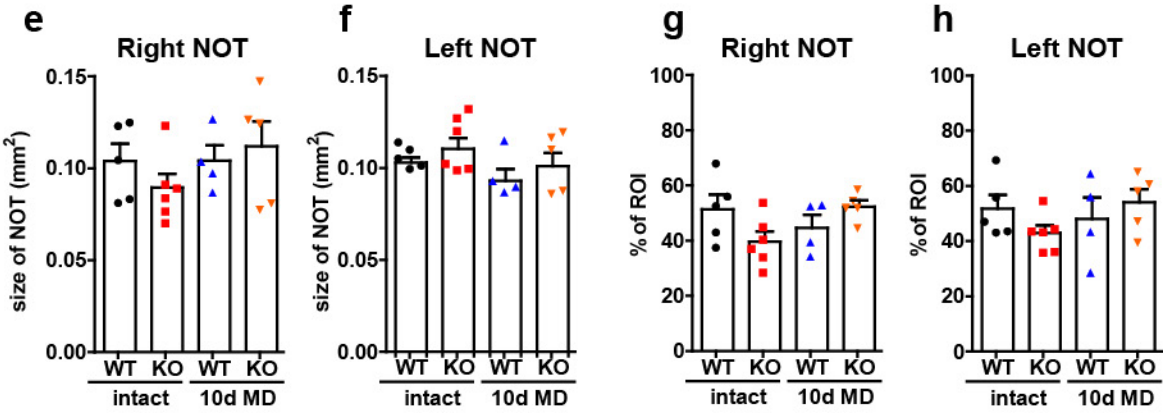
e
Right NOT
size of NOT (mm²)
0.15
0.10
0.05
0.00
WT KO WT KO
intact 10d MD
f
Left NOT
size of NOT (mm²)
0.15
0.10
0.05
0.00
WT KO WT KO
intact 10d MD
g
Right NOT
% of ROI
100
80
60
40
20
0
WT KO WT KO
intact 10d MD
h
Left NOT
% of ROI
100
80
60
40
20
0
WT KO WT KO
intact 10d MD

To test this, we deprived the right eye of adult WT and Nogo-A KO mice for 10 days, and traced retinal projections from both eyes with CTb without reopening the MD eye (Fig. 4a). After MD, the quantification of eye-specific projection segregation in the left dLGN revealed a non-significant shift in the segregation curve of the WT group (Fig. 4b, c; at contralateral threshold of 30: WT+MD: 68.079 ± 7.193 %). However, in the Nogo-A KO mice, MD significantly increased the overlap between the open eye and closed eye projections in the left dLGN when compared to the intact KO group (Fig. 4b, c; at threshold 30; KO+MD: 44.424 ± 9.924 %). In the right dLGN, MD did not cause detectable change in retinal projections segregation (Fig. 4d). However, in the right dLGN we noticed unusual occurrences of open eye projections in the middle of the ipsilateral territory of the closed eye. We therefore analyzed the ectopic open eye projections on higher resolution confocal images. In the intact condition, the density of contralateral terminals in the center of the ipsilateral eye territory was low and not significantly different between WT and KO mice (Fig. 4f; WT: 3.789 ± 0.547 % of ROI; KO: 5.644 ± 0.685 % of ROI; $p = 0.473$). However, compared with non-deprived animals, ectopic terminals from the open eye were significantly increased in this area of the dLGN in Nogo-A KO mice and covered 8.687 ± 0.710 % of the selected region (Fig. 4e, f; $p = 0.036$). In contrast, in WT mice only a trend toward an increase in the density of ectopic projections was observed after MD (5.257 ± 0.805 % of ROI; $p = 0.881$). After MD, we did not observe size (Fig. S2c, d, e, f) or fiber density changes (Fig. S2c, d, g, h) in the NOT of Nogo-A KO or WT mice. These results suggest that Nogo-A inactivation promotes ectopic terminal formation in the dLGN in the MD plasticity paradigm.

4.5 Formation of ectopic eye terminals in the Nogo-A KO dorsal lateral geniculate nucleus

In order to determine how ectopic terminals from the open eye developed in the Nogo-A KO dLGN after MD, RGC axons were labeled by transducing retinal ganglion cells with AAV2.GFP

(Fig. 5). MD of the right eye was performed three weeks after intravitreal injection of the AAV2.GFP vector in the left eye, and the terminals of the two eyes were visualized by injecting CTb-594 in the open eye and CTb-647 in the closed eye, one day before tissue collection (Fig. 5a). On coronal brain sections, a high density of GFP-filled axons was observed in the contralateral (right) and ipsilateral (left) dLGN receiving inputs from the open eye (Fig. 5b). Some of the GFP-labeled axons crossing the ipsilateral territory of the closed eye (blue) showed CTb-594-containing terminals (Fig. 5c). The superimposition of the three signals revealed the distribution of the CTb-594-positive varicosities and bouton-like structures on the course of GFP-filled fibers (Fig. 5d). Often several CTb-594-stained swellings appeared on the same axonal segment, indicating that ectopic terminals from the open eye may stem from contralateral axons normally passing through the closed eyes ipsilateral territory. Moreover, the density of the CTb-594-labeled open eye terminals was found to increase along with the density of GFP-labeled axons in the center of the closed eye ipsilateral territory in monocularly deprived Nogo-A KO mice compering with intact Nogo-A mice (Fig. 5e). These results suggest that Nogo-A gene deletion facilitates the formation of *en passant* varicosities and possibly also axon terminal sprouting from the open eye after monocular deprivation.

Figure 4 Monocular deprivation induces anatomical plasticity of retinal terminals in the dLGN of adult Nogo-A deficient mice

a The right eye of adult (P60) WT and Nogo-A KO mice was suture-closed for 10 days (MD). One day before brain fixation, both eyes were traced with CTb (right eye 488, left eye 594) without reopening the MD eye. **b** Coronal brain sections showing CTb-labeled retinal projections after ten days of MD in the dLGN of WT and Nogo-A KO mice (scale bar 200 μm). **c** Threshold-dependent quantification after MD revealed a decrease in eye-specific projection segregation in the left dLGN of Nogo-A KO but not in WT mice relative to intact mice. **d** The eye-specific projections segregation in the right dLGN was not affected by monocular deprivation (Two-way RM ANOVA with Bonferroni's post-hoc tests, ***$p < 0.001$, **$p < 0.01$, NS > 0.05). **e** In the right dLGN of Nogo-A KO mice, MD induced ectopic open eye projections (red) in the ipsilateral field innervated by the closed eye (green) as shown on merged confocal microscopy image stacks (20 μm) of the right dLGN ipsilateral territory. Ectopic projections from the open eye were more numerous in Nogo-A KO than in WT mice in the center of the closed eye ipsilateral territory (scale bar 50 μm). **f** The percentage of area occupied by ectopic projections was automatically calculated with the ImageJ software on binarised images (**e**; right-hand side) in a 100 x 100 μm region of interest (red box) placed in the center of mass of the closed eye ipsi territory. This quantification confirmed a significantly higher number of ectopic projections from the open eye of Nogo-A KO mice ($p = 0.036$) after MD, whereas in WT mice MD had no effect ($p = 0.88$); one-way ANOVA, Bonferroni's post-hoc tests).

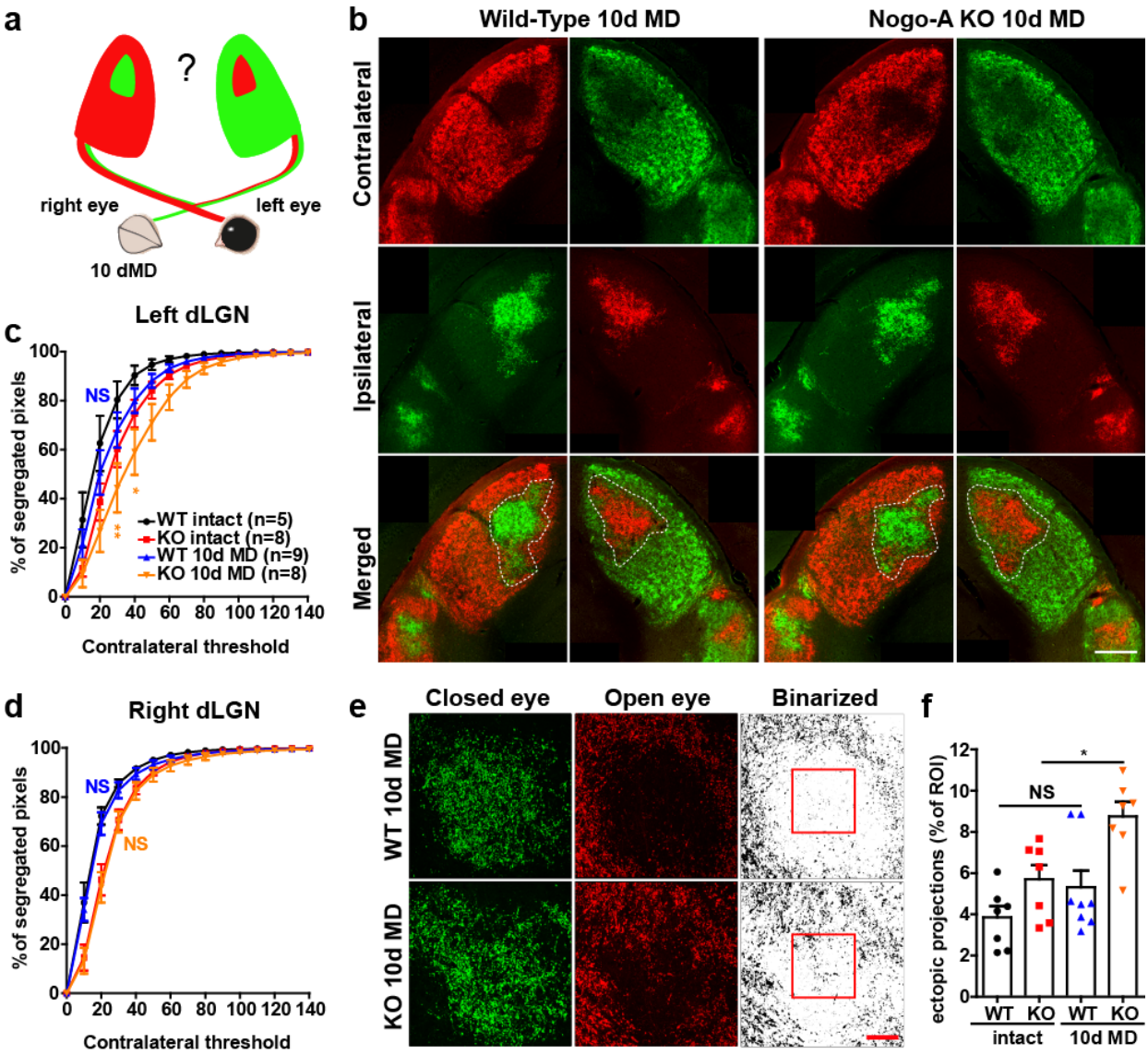
a
?
right eye
left eye
10 dMD
b
Wild-Type 10d MD
Nogo-A KO 10d MD
Contralateral
Ipsilateral
Merged
c
Left dLGN
% of segregated pixels
NS
WT intact (n=5)
KO intact (n=8)
WT 10d MD (n=9)
KO 10d MD (n=8)
Contralateral threshold
d
Right dLGN
% of segregated pixels
NS
NS
Contralateral threshold
e
Closed eye
Open eye
Binarized
WT 10d MD
KO 10d MD
f
ectopic projections (% of ROI)
NS
*
WT
KO
WT
KO
intact
10d MD

Figure 5 Open eye ectopic projections form as *en passant* varicosities in the dLGN of Nogo-A mice after MD

a AAV2.GFP vector was intraocularly injected in the left eye 3 weeks before deprivation of the right eye. CTb-594 or CTb-647 were injected in the vitreous the day preceding tissue fixation. The same injections time course was used for intact Nogo-A KO mice. **b** The GFP signal and the CTb fluorescence were imaged by confocal microscopy. Low magnification images show high densities of GFP-positive open eye axons in the contralateral (right) and ipsilateral (left) dLGN. **c** At high magnification, many GFP-labeled axons crossed the ipsilateral territory of the closed eye **d** Examples of single fiber labeling. The merge of the 3 fluorescent signals revealed CTb-594-positive varicosities on the course of GFP filled axons (scale bars, **b**: 200 µm, **c**: 100 µm, **d**: 25 µm). **e** Monocular deprivation in Nogo-A KO mice increased the density of CTb-594-positive varicosities and GFP-positive fibers in the center of the closed eye ipsilateral territory. The quantification of the percentage of area occupied by CTb-594 signal as a function of GFP signal, was calculated in a 100 x 100 µm ROI in the center of the right dLGN as in Fig. 4 f. Single data points represent individual brain sections, shades of color represent individual animals (n = 3 mice).

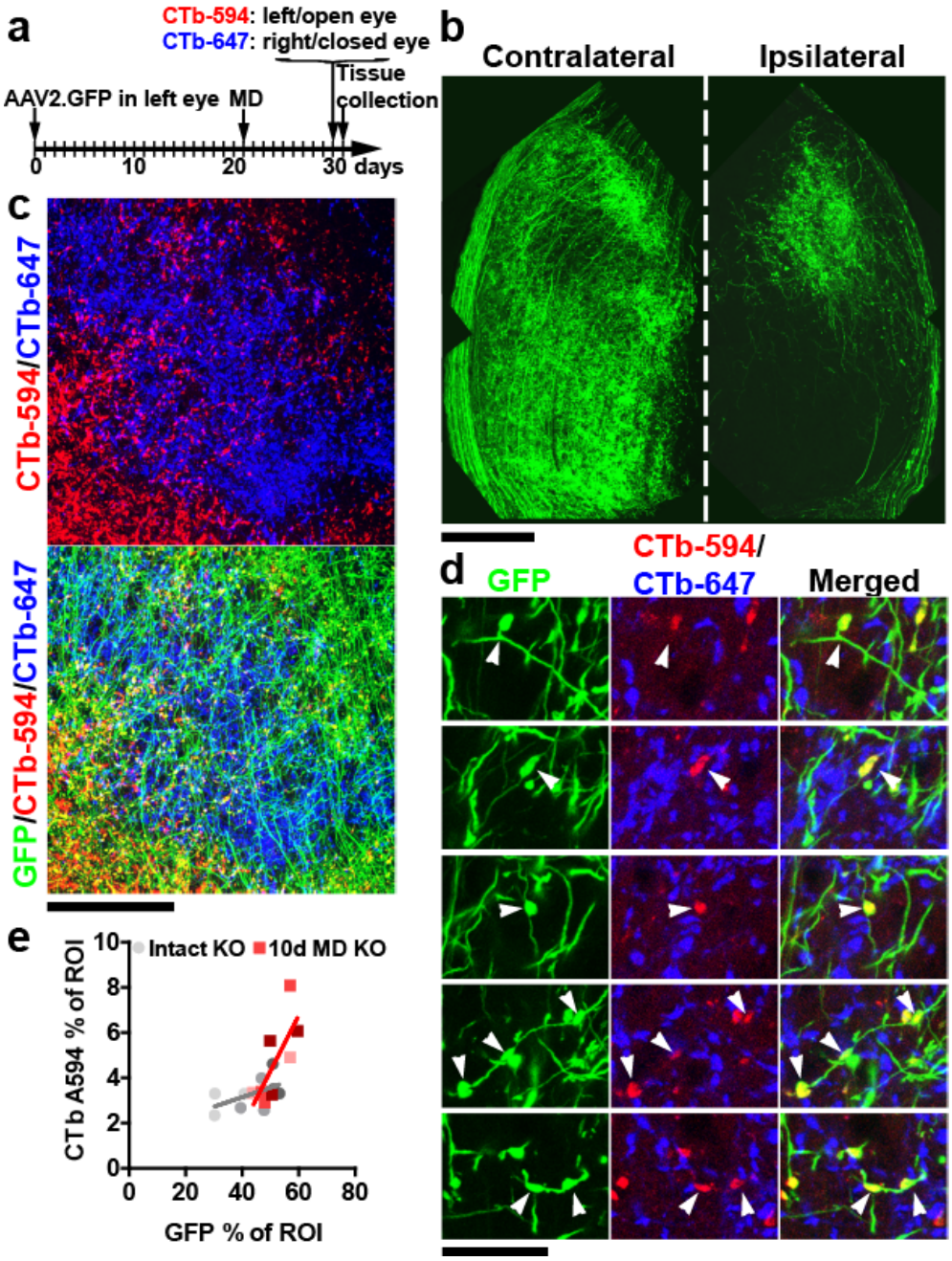
a
CTb-594: left/open eye
CTb-647: right/closed eye
AAV2.GFP in left eye
MD
Tissue collection
0
10
20
30 days
b
Contralateral
Ipsilateral
c
CTb-594/CTb-647
GFP/CTb-594/CTb-647
d
GFP
CTb-594/ CTb-647
Merged
e
Intact KO
10d MD KO
CTb A594 % of ROI
GFP % of ROI
0
2
4
6
8
10
0
20
40
60
80

5 Discussion

In the present study, we showed that genetic deletion of Nogo-A potentiated the MD-induced enhancement of the OKR spatial frequency and contrast sensitivity in adult mice, in part independently of the visual cortex, demonstrating that the OKR plasticity can be improved by removing the neurite growth inhibitory protein Nogo-A. In the dLGN, Nogo-A KO mice showed decreased eye-specific segregation of retinal projections. This feature was potentiated by MD, suggesting that Nogo-A can modulate visual experience-induced plasticity in subcortical regions of the adult mouse brain.

The visual cortex is thought to be the most plastic structure in the visual system. Modulation of visual experience can induce ocular dominance shift, during the critical period and to a lower extent as well beyond P30 and in adult mice [32-34]. Our data suggest that ~50 % of the enhancement in the OKR sensitivity induced by MD in Nogo-A KO mice was due to cortical plasticity. It has been previously shown by McGee and colleagues [7] that cortex myelination, and therefore increased Nogo-A expression, played a key role in the closure of the critical period. The genetic removal of the Nogo receptor NgR1 or of Nogo-A/B greatly enhanced the ocular dominance shift after brief MD in adult mice (P45 and older), suggesting that Nogo-A inhibits neuronal plasticity via NgR1 activation. Moreover, the neutralization of PirB, another receptor for Nogo-A increased cortical plasticity in adult animals [35]. In addition, proteoglycans present around neurons can restrict plasticity; enzymatic digestion of chondroitin sulfate proteoglycans (CSPGs) in the perineuronal nets restored ocular dominance shifts after MD in adult rats [8]. Interestingly, a recent study reported that NgR1 binds not only Nogo-A but also CSPGs suggesting signaling convergence of those inhibitors on the same transduction mechanisms [36].

We found that MD could still induce spatial frequency sensitivity increase after cortex ablation in WT and Nogo-A KO animals, suggesting that subcortical brain regions play an important and so far underestimated role in the OKR plasticity. Two important nuclei, the nucleus of the optic tract (NOT) and the dorsal terminal nucleus (DTN) in the subcortical visual system control the OKR in response to horizontally moving stimuli independently of the visual cortex [37-39]. Accordingly, the ablation of the visual cortices did not change the baseline of the OKR sensitivity. It was previously reported that cortical aspiration strongly but not fully diminished the elevation of OKR sensitivity after MD [19]. Our results further substantiate that the OKR sensitivity increase is partially due to subcortical nuclei that could involve direct retinal projections to the DTN and NOT. A LTP-like strengthening of synaptic contacts by Nogo-A removal may take place in this process [15, 16]. It is not clear how the eyelid closure of the right eye could influence the synaptic contacts of the left open eye terminals in these nuclei, as they receive mostly if not exclusively contralateral projections [40, 41]. In addition, we did not find any deficits in visual acuity of the deprived eye after eye reopening. Therefore, the increased OKR sensitivity in the open eye during MD unlikely involves direct competition between the two eye projections in the same nuclei, contrary to what has been described during postnatal maturation of the lateral geniculate nucleus [42]. Anatomically, we could not observe detectable changes in size or in retinal fiber density in the NOT after MD (Fig. S2).

However, in the Nogo-A KO dLGN the degree of eye-specific axon segregation was significantly lower than in WT animals. This phenotype may result from the alteration of terminal maturation that normally occurs during the first two postnatal weeks in mice [43]. However, it could also reflect the decreased stabilization of the visual circuit in adult mice [14]. The weaker terminal stability hypothesis is supported by the changes observed here in Nogo-A KO mice after MD. In Nogo-A KO mice, eyelid closure decreased even more the segregation between open eye and

closed eye projections in the left dLGN. Furthermore, in Nogo-A deficient mice MD promoted ectopic terminal formation from open eye axons. The gain of ectopic terminals after MD in the Nogo-A KO dLGN could be related to the increased turnover of axonal varicosities that has been reported in the somato-sensory cortex of adult NgR1 KO and Nogo-A/B KO mice [14]. Importantly, in Nogo-A KO mice, 10 days of MD increased the density of ectopic fibers from the open eye, suggesting that axonal growth had occurred.

Although the retinogeniculate synapses of adult mammals have been considered as stable and insensitive to visual experience changes, recent studies by Hooks and Chen [10, 11] challenged this view. The authors demonstrated that initial visual experience is necessary to allow the plasticity of retinogeniculate synapses after dark rearing and that the plasticity is limited to a specific “sensitive period”. As shown in this study, Nogo-A is involved in the stabilization of retinal afferents in the dLGN of the adult mice.

In summary, the current study demonstrates that Nogo-A limits the plasticity of the adult mouse visual system not only at the cortical but also at a subcortical level. We propose that acute neutralization of Nogo-A with function blocking antibodies may be a new strategy to restore visual experience-driven plasticity in adult amblyopic patients and thereby aid in the treatment of visual dysfunction.

Acknowledgements: We thank Dr. Deniz Dalkara (Institut de la Vision, Paris) for providing us with the AAV2.GFP virus and Dr. Olivier Raineteau for allowing us to use his SPE-II confocal microscope. This work was supported by the Swiss National Science Foundation (SNF) grants no. 3100A0-1222527-2 and 31003A-149315-1 and the SNF National Center of Competence in Research 'Neural Plasticity and Repair' (to MES).

References

1. Wiesel, T.N. and D.H. Hubel, *Single-Cell Responses in Striate Cortex of Kittens Deprived of Vision in One Eye.* J. Neurophysiol., 1963. **26**: p. 1003-17.
2. Hubel, D.H. and T.N. Wiesel, *The period of susceptibility to the physiological effects of unilateral eye closure in kittens.* J Physiol., 1970. **206**(2): p. 419-36.
3. Gordon, J.A. and M.P. Stryker, *Experience-dependent plasticity of binocular responses in the primary visual cortex of the mouse.* J. Neurosci., 1996. **16**(10): p. 3274-86.
4. Eysel, U.T., et al., *Reorganization in the visual cortex after retinal and cortical damage.* Restor. Neurol. Neurosci., 1999. **15**(2-3): p. 153-64.
5. Hensch, T.K., et al., *Local GABA circuit control of experience-dependent plasticity in developing visual cortex.* Science, 1998. **282**(5393): p. 1504-8.
6. Hensch, T.K., *Critical period plasticity in local cortical circuits.* Nat Rev Neurosci, 2005. **6**(11): p. 877-88.
7. McGee, A.W., et al., *Experience-driven plasticity of visual cortex limited by myelin and Nogo receptor.* Science, 2005. **309**(5744): p. 2222-6.
8. Pizzorusso, T., et al., *Reactivation of ocular dominance plasticity in the adult visual cortex.* Science, 2002. **298**(5596): p. 1248-51.
9. Daw, N.W., et al., *Critical period for monocular deprivation in the cat visual cortex.* J. Neurophysiol., 1992. **67**(1): p. 197-202.
10. Hooks, B.M. and C. Chen, *Distinct roles for spontaneous and visual activity in remodeling of the retinogeniculate synapse.* Neuron, 2006. **52**(2): p. 281-91.
11. Hooks, B.M. and C. Chen, *Vision triggers an experience-dependent sensitive period at the retinogeniculate synapse.* J. Neurosci., 2008. **28**(18): p. 4807-17.
12. Schwab, M.E., *Functions of Nogo proteins and their receptors in the nervous system.* Nat. Rev. Neurosci., 2010. **11**(12): p. 799-811.
13. Pernet, V. and M.E. Schwab, *The role of Nogo-A in axonal plasticity, regrowth and repair.* Cell Tissue Res., 2012. **349**(1): p. 97-104.
14. Akbik, F.V., et al., *Anatomical plasticity of adult brain is titrated by Nogo Receptor 1.* Neuron, 2013. **77**(5): p. 859-66.
15. Delekate, A., et al., *NogoA restricts synaptic plasticity in the adult hippocampus on a fast time scale.* Proc. Natl. Acad. Sci. U. S. A., 2011. **108**(6): p. 2569-74.
16. Tews, B., et al., *Synthetic microRNA-mediated downregulation of Nogo-A in transgenic rats reveals its role as regulator of synaptic plasticity and cognitive function.* Proc. Natl. Acad. Sci. U. S. A., 2013. **110**(16): p. 6583-6588.
17. Raiker, S.J., et al., *Oligodendrocyte-Myelin Glycoprotein and Nogo Negatively Regulate Activity-Dependent Synaptic Plasticity.* J. Neurosci., 2010. **30**(37): p. 12432-12445.
18. Prusky, G.T., et al., *Rapid quantification of adult and developing mouse spatial vision using a virtual optomotor system.* Invest. Ophthalmol. Vis. Sci., 2004. **45**(12): p. 4611-6.
19. Prusky, G.T., N.M. Alam, and R.M. Douglas, *Enhancement of vision by monocular deprivation in adult mice.* J. Neurosci., 2006. **26**(45): p. 11554-61.
20. Lehmann, K., K.F. Schmidt, and S. Lowel, *Vision and visual plasticity in ageing mice.* Restor. Neurol. Neurosci., 2012. **30**(2): p. 161-78.
21. Simonen, M., et al., *Systemic deletion of the myelin-associated outgrowth inhibitor Nogo-A improves regenerative and plastic responses after spinal cord injury.* Neuron, 2003. **38**(2): p. 201-11.

22. Douglas, R.M., et al., *Independent visual threshold measurements in the two eyes of freely moving rats and mice using a virtual-reality optokinetic system.* Visual neuroscience, 2005. **22**(5): p. 677-684.
23. Pernet, V., et al., *Neuronal Nogo-A upregulation does not contribute to ER stress-associated apoptosis but participates in the regenerative response in the axotomized adult retina.* Cell Death Differ., 2012. **19**(7): p. 1096-108.
24. Pernet, V., et al., *Misguidance and modulation of axonal regeneration by Stat3 and Rho/ROCK signaling in the transparent optic nerve.* Cell Death Dis., 2013. **4**: p. e734.
25. Muir-Robinson, G., B.J. Hwang, and M.B. Feller, *Retinogeniculate axons undergo eye-specific segregation in the absence of eye-specific layers.* J. Neurosci., 2002. **22**(13): p. 5259-64.
26. Simpson, J.I., R.E. Soodak, and R. Hess, *The accessory optic system and its relation to the vestibulocerebellum.* Prog. Brain Res., 1979. **50**: p. 715-24.
27. Soodak, R.E. and J.I. Simpson, *The accessory optic system of rabbit. I. Basic visual response properties.* J. Neurophysiol, 1988. **60**(6): p. 2037-54.
28. Linden, D.C., R.W. Guillery, and J. Cucchiaro, *The dorsal lateral geniculate nucleus of the normal ferret and its postnatal development.* J. Comp. Neurol., 1981. **203**(2): p. 189-211.
29. Godement, P., J. Salaun, and M. Imbert, *Prenatal and postnatal development of retinogeniculate and retinocollicular projections in the mouse.* J. Comp. Neurol., 1984. **230**(4): p. 552-75.
30. Chapman, B., *Necessity for afferent activity to maintain eye-specific segregation in ferret lateral geniculate nucleus.* Science, 2000. **287**(5462): p. 2479-82.
31. Demas, J., et al., *Failure to maintain eye-specific segregation in nob, a mutant with abnormally patterned retinal activity.* Neuron, 2006. **50**(2): p. 247-59.
32. Sawtell, N.B., et al., *NMDA Receptor-Dependent Ocular Dominance Plasticity in Adult Visual Cortex.* Neuron, 2003. **38**(6): p. 977-985.
33. Hofer, S.B., et al., *Prior experience enhances plasticity in adult visual cortex.* Nat. Neurosci., 2006. **9**(1): p. 127-32.
34. Lehmann, K. and S. Lowel, *Age-dependent ocular dominance plasticity in adult mice.* PLoS ONE, 2008. **3**(9): p. e3120.
35. Syken, J., et al., *PirB restricts ocular-dominance plasticity in visual cortex.* Science, 2006. **313**(5794): p. 1795-800.
36. Dickendesher, T.L., et al., *NgR1 and NgR3 are receptors for chondroitin sulfate proteoglycans.* Nat. Neurosci., 2012.
37. Benassi, C., et al., *Correlation between Amount of Retinal Afferents to the Pretectal Nucleus of the Optic Tract and Dorsal Terminal Accessory Optic Nucleus and Performance of Horizontal Optokinetic Reflex in Rat.* Behav. Brain Res., 1991. **45**(1): p. 87-95.
38. Hayhow, W.R., C. Webb, and A. Jervie, *The accessory optic fiber system in the rat.* J. Comp. Neurol., 1960. **115**(2): p. 187-215.
39. Grasse, K.L., M.S. Cynader, and R.M. Douglas, *Alterations in response properties in the lateral and dorsal terminal nuclei of the cat accessory optic system following visual cortex lesions.* Exp. Brain Res., 1984. **55**(1): p. 69-80.
40. Pak, M.W., et al., *Retinopretectal and Accessory Optic Projections of Normal Mice and the Okn-Defective Mutant Mice Beige, Beige-J, and Pearl.* J. Comp. Neurol., 1987. **258**(3): p. 435-446.
41. Giolli, R.A., R.H. Blanks, and F. Lui, *The accessory optic system: basic organization with an update on connectivity, neurochemistry, and function.* Prog. Brain Res., 2006. **151**: p. 407-40.
42. Penn, A.A., et al., *Competition in retinogeniculate patterning driven by spontaneous activity.* Science, 1998. **279**(5359): p. 2108-12.
43. Jaubert-Miazza, L., et al., *Structural and functional composition of the developing retinogeniculate pathway in the mouse.* Vis. Neurosci., 2005. **22**(5): p. 661-76.

CHAPTER 4

CONCLUDING REMARKS

In this thesis, I addressed the influence of the nerve fiber growth inhibitory protein Nogo-A on the anatomical maturation and the functional and the anatomical plasticity of the visual system.

In chapter 2, I analyzed the expression pattern of Nogo-A and its receptors NgR1 and S1PR2 in the visual system. In the retina, Nogo-A protein was strongly expressed in early postnatal retinal ganglion cell bodies (RGCs) and their axons, but its expression was down-regulated by postnatal day 6 (P6), when Nogo-A started being predominantly expressed in Müller glia cells and the vitreal endfeet, surrounding the RGC bodies. This pattern of expression was also observed in the adult retina. Both Nogo-A receptors, NgR1 and S1PR2, were expressed in the retina, but the *S1pr2* mRNA was down-regulated to a lower level before P10, whereas the expression of *Ngr1* mRNA was moderately decreased until adulthood. In the retina, the NgR1 protein was exclusively expressed in the RGC bodies and axonal fascicles. In the brain, Nogo-A was strongly expressed in oligodendrocytes in the optic nerve and in neurons and oligodendrocytes in the dorsal lateral geniculate nucleus (dLGN) and in the primary visual cortex (V1) as well as in the non-visual brain regions. Therefore, the NgR1 receptor could sensitize RGCs to Nogo-A expressed in the subcortical visual system.

Furthermore, in chapter 2, I analyzed whether systemic Nogo-A deletion affects developmental refinement of retinogeniculate terminals, similarly to what has been described for climbing fibers in the cerebellum [1]. The Nogo-A down-regulation in the RGCs between P4 and P6 correlates with ongoing refinement of retinal projections, suggesting that Nogo-A down-regulation in axons might be required to allow the stabilization of terminals in the brain, similarly to what has been shown in the cerebellum [2]. At P10, just after refinement, the eye-specific segregation of retinal terminals in the dLGN was not affected by genetic ,Nogo-A deletion; however as I described in chapter 3, the eye-specific segregation of retinal terminals was lower in adult Nogo-A KO than in

WT mice suggesting a decreased stabilization of the circuit in the absence of Nogo-A. Alternatively, the complete segregation at later developmental stages of the eye-specific projections may fail to occur in Nogo-A KO mice between P10 and adulthood.

A desegregation of retinal terminals in the dLGN has been observed in two studies in which stage III retinal waves occurring after initial refinement of retinal terminals were pharmacologically [3] or genetically [4] blocked during the LGN plastic period. Therefore, it would be interesting to determine whether Nogo-A deletion affects retinal activity. Favoring the circuit stabilization hypothesis, Nogo-A and its receptor NgR1 have been shown to limit ocular dominance (OD) plasticity in adult brain, an effect that was attributed to Nogo-A expressed in myelin of the visual cortex, which matures at the time of the closure of the plastic period [5]. Up to now, the subcortical visual system was considered to be much less plastic than the visual cortex; however, at least at the functional level, altered visual experience has been shown to promote synaptic plasticity in retinogeniculate synapses during the developmental sensitive period starting at ~ P20 and finishing at ~ P32 [6, 7]. Whether this plasticity is also accompanied by structural changes had not been investigated. Therefore, to test whether abnormal visual experience caused by monocular deprivation can promote anatomical plasticity in the subcortical visual system, in chapter 3, I analyzed eye-specific terminal segregation after 10 days of MD. In adult Nogo-A KO mice, MD caused significant desegregation of retinal terminals as compared to intact Nogo-A KO mice. In adult WT mice, the MD effect was not significant, suggesting again that Nogo-A may limit axonal and synaptic sprouting in the subcortical visual system during adulthood. After MD in adult Nogo-A KO mice, we observed formation of ectopic open eye terminals in the ipsilateral territory innervated by the closed eye, a phenomenon which suggests increased plasticity of axonal branches and synapses. It would be interesting to test, whether monocular deprivation during the retinogeniculate sensitive period (P20-P32) would be associated with structural

rearrangements. In the study by Hayakawa and Kawasaki [8], long term MD starting before the sensitive period at P10 until P35 did not cause significant expansion of the open eye ipsilateral domain, contrary to the dramatic expansion observed after monocular enucleation (ME). When the ME was performed after the sensitive period at P34 and the anatomy examined at P60 the expansion was not apparent, suggesting that anatomical plasticity of the retinogeniculate terminals is limited to the sensitive period. Therefore, I propose that Nogo-A expression in myelin may be involved in the closure of the retinogeniculate sensitive period which would be then different from the down-regulation of Nogo-A in RGCs. It would also be interesting to know if in Nogo-A KO mice the relay LGN neurons at the border between two eye domains are innervated by both eyes and how the decreased segregation of retinal terminals is reflected in the visual cortex, on the anatomical and functional level. In the study by McGee and colleagues [5] the receptive field size and the cortical evoked and spontaneous activity was not affected by Nogo-A/B deletion.

Apart from anatomical plasticity in the subcortical visual system, we tested also the functional plasticity. The function of the subcortical visual system can be tested using the optokinetic tracking response (OKR) which is a reflexive head movement in response to large scale motion of the visual field. For the horizontally moving stimulus this behavior depends on the retinal projections to the pretectal and accessory optic system nuclei, that are the nucleus of the optic tract (NOT) and the dorsal terminal nucleus (DTN). As shown in chapter 3, in intact adult Nogo-A KO mice, we observed higher spatial frequency sensitivity which, together with contrast sensitivity, was more enhanced than in WT mice after MD. The initial higher sensitivity, before MD, was cortex-independent as it was not affected by the visual cortex ablation. The visual cortex seems to be involved in the plastic increase of OKR after MD; however subcortical structures might also contribute to this process, since MD was still able to induce moderate OKR

increase after bilateral visual cortex ablation. It is possible that this phenotype might involve also the cerebellum, which has been shown to play an important role for the OKR motor learning [9, 10]. Accordingly, adult Nogo-A KO mice show a higher density of innervation from both climbing (CF) and parallel fibers (PF) on Purkinje cells (PC) and increased synaptic transmission between PF and PC [1]. These anatomical changes may affect the vestibular and oculomotor performance and OKR learning. Accordingly, overexpression of Nogo-A in the Purkinje cells in adult mice has been shown to impair motor learning as assessed by the eye-blink conditioning test [2].

Finally, it would be interesting to assess whether acute blockage of Nogo-A in the adulthood e.g. by the administration of function blocking antibodies or by blockers of Nogo-A receptors would lead to similar OKR and anatomical retinogeniculate plasticity as that reported here after systemic Nogo-A deletion. Additionally, the role of Nogo-A and Nogo-A receptors in the plasticity could be addressed by cell type-specific knock-outs or knock-downs in oligodendrocytes, brain neurons or retinal ganglion cells. As we have shown that in the LGN and the visual cortex Nogo-A is expressed in both oligodendrocytes and neurons, distinguishing between the functions of Nogo-A in these two cell populations would be of great interest. In the CNS, myelination occurs at the final stage of neuronal circuit maturation and limits axonal growth and rearrangement [11]. It has been shown that the extent of myelination negatively correlates with the expression of growth-associated proteins such as GAP-43 [12]. On the other hand, neuronal Nogo-A and its receptor NgR1 have been shown to restrict long- term potentiation (LTP) without affecting the baseline synaptic transmission [13, 14]. To address the respective role of myelin and neuronal Nogo-A, one could take advantage of the cell-specific conditional Nogo-A KO mouse lines. All these approaches could help us to dissect the mechanism by which Nogo-A restricts plasticity in the adult visual system.

References

1. Petrinovic, M.M., et al., *Neuronal Nogo-A negatively regulates dendritic morphology and synaptic transmission in the cerebellum.* Proc. Natl. Acad. Sci. U. S. A., 2013. **110**(3): p. 1083-8.
2. Aloy, E.M., et al., *Synaptic destabilization by neuronal Nogo-A.* Brain Cell Biol., 2006. **35**(2-3): p. 137-56.
3. Chapman, B., *Necessity for afferent activity to maintain eye-specific segregation in ferret lateral geniculate nucleus.* Science, 2000. **287**(5462): p. 2479-82.
4. Demas, J., et al., *Failure to maintain eye-specific segregation in nob, a mutant with abnormally patterned retinal activity.* Neuron, 2006. **50**(2): p. 247-59.
5. McGee, A.W., et al., *Experience-driven plasticity of visual cortex limited by myelin and Nogo receptor.* Science, 2005. **309**(5744): p. 2222-6.
6. Hooks, B.M. and C. Chen, *Distinct roles for spontaneous and visual activity in remodeling of the retinogeniculate synapse.* Neuron, 2006. **52**(2): p. 281-91.
7. Hooks, B.M. and C. Chen, *Vision triggers an experience-dependent sensitive period at the retinogeniculate synapse.* J. Neurosci., 2008. **28**(18): p. 4807-17.
8. Hayakawa, I. and H. Kawasaki, *Rearrangement of retinogeniculate projection patterns after eye-specific segregation in mice.* PLoS ONE, 2010. **5**(6): p. e11001.
9. Wada, N., K. Funabiki, and S. Nakanishi, *Role of granule-cell transmission in memory trace of cerebellum-dependent optokinetic motor learning.* Proc. Natl. Acad. Sci. U. S. A., 2014. **111**(14): p. 5373-8.
10. Shutoh, F., et al., *Memory trace of motor learning shifts transsynaptically from cerebellar cortex to nuclei for consolidation.* Neuroscience, 2006. **139**(2): p. 767-77.
11. Schwegler, G., M.E. Schwab, and J.P. Kapfhammer, *Increased collateral sprouting of primary afferents in the myelin-free spinal cord.* J. Neurosci., 1995. **15**(4): p. 2756-67.
12. Kapfhammer, J.P. and M.E. Schwab, *Inverse patterns of myelination and GAP-43 expression in the adult CNS: neurite growth inhibitors as regulators of neuronal plasticity?* J. Comp. Neurol., 1994. **340**(2): p. 194-206.
13. Delekate, A., et al., *NogoA restricts synaptic plasticity in the adult hippocampus on a fast time scale.* Proc. Natl. Acad. Sci. U. S. A., 2011. **108**(6): p. 2569-74.
14. Tews, B., et al., *Synthetic microRNA-mediated downregulation of Nogo-A in transgenic rats reveals its role as regulator of synaptic plasticity and cognitive function.* Proc. Natl. Acad. Sci. U. S. A., 2013. **110**(16): p. 6583-6588.

Acknowledgments

I would like to express my gratitude to Prof. Martin E. Schwab for giving me the opportunity to conduct my PhD project in his excellent laboratory. I always felt his warm support and his door was always open for any spontaneous discussion. I would like to also thank the members of my committee, Prof. Stephan Neuhauss and Prof. Ulrich Suter for their valuable comments and suggestions.

I am very grateful to Dr. Vincent Pernet for being a great and helpful supervisor. I could always ask him for help or advice and at the same time he gave me the freedom to develop my own ideas.

I would like to acknowledge co-authors of my manuscript, Alex, Flora, Sandrine and Franzi, without your help and sometimes moral support it would be much harder to finish this project.

I would like to give my special thanks to Franzi and our animal “care givers” team for reliving me of the tedious task of animal care, breeding and genotyping.

Special thanks to Stella and Lukas for help with the German translation of the thesis summary.

I would like to thank all my good friends from the lab for sharing our sorrows and successes, for being there for me at and after the work, for our trips and for coming to my wedding. I hope we will stay in touch.

I always enjoyed the friendly atmosphere of HIFO, I will miss our scientific discussions, our lunch breaks, sport activities, and happy hours and even the hikes during our retreats.

My deep gratitude goes to my family and friends, for standing behind me in every situation.

My very special thanks and love to my best friend and husband, Lukasz, without whose love, encouragement and support for my decisions, I could have not accomplish it.

CURRICULUM VITAE

Personal data

Name:	**Anna Guzik-Kornacka**
Date of birth:	October 27th, 1983
Place of birth:	Radom, Poland
Citizenship:	Polish

Education

2009- present	**PhD in Neuroscience ETH, Zurich** with Prof. Martin Schwab Brain Research Institute, Zurich, Switzerland
2003-2008	**MSc in Biotechnology, Diploma grade 5 (very good)** Warsaw University of Life Sciences, Poland
2007-2008	**Master thesis** with Prof. Katarzyna Lukasiuk Laboratory of Epileptogenesis, Nencki Institute of Experimental Biology, Warsaw, Poland
Summer 2007	**Undergraduate research project** with Dr. David Henshall, Physiology & Medical Physics, RCSI, Dublin, Ireland
Summer 2006	**Undergraduate research project** with Prof. Wim G. Meijer, Molecular Microbiology, UCD, Dublin, Ireland
1998 - 2002	High School, Radom, Poland

Research articles:

Guzik-Kornacka A, van der Bourg A, Vajda F, Joly S, Christ F, Schwab ME, Pernet V.

Nogo-A deletion increases the plasticity of the optokinetic response and changes retinal projection organization in the adult mouse visual system. *Brain Struct. Func. 2014 (under review)*

Joly S, **Guzik-Kornacka A**, Schwab M.E, Pernet V. **New mouse retinal stroke model reveals direction-selective circuit damages linked to permanent optokinetic response loss.** *Invest. Ophthalmol. Vis. Sci. 2014 Jun 26. Epub ahead of print*

Pernet V, Joly S, Jordi N, Dalkara D, **Guzik-Kornacka A**, Flannery JG, Schwab ME.

Misguidance and modulation of axonal regeneration by Stat3 and Rho/ROCK signaling in the transparent optic nerve. *Cell Death Dis. 2013 Jul 18;4:e734.*

Wälchli T, Pernet V, Weinmann O, Shiu J, **Guzik-Kornacka A**, Decrey G, Yüksel D, Schneider H, Vogel J, Ingber DE, Vogel V, Frei K, Schwab ME. **Nogo-A is a negative regulator of CNS angiogenesis**. *Proc. Natl. Acad. Sci. U. S. A. 2013 May 21;110(21):E1943-52.*

Guzik-Kornacka A, Sliwa A, Plucinska G, Lukasiuk K. **Status epilepticus evokes prolonged increase in the expression of CCL3 and CCL4 mRNA and protein in the rat brain.** *Acta Neurobiol. Exp. (Wars) 2011 71(2):193-207.*

Posters:

Guzik-Kornacka A, Pernet V, Schwab ME. **Nogo-A influences the eye-specific segregation of retinogeniculate projections.** Neuroscience 2012, SfN's 42nd annual meeting, New Orleans, LA, USA.

Guzik-Kornacka A, Pernet V, Schwab ME. **Investigating the role of Nogo-A in the maturation of the visual system.** Cell Biology of the Neuron, EMBO Workshop, Heraklion, Greece

Guzik-Kornacka A, Pernet V, Joly S, Schwab ME. **Role of neuronal Nogo-A in retinal axon regrowth after optic nerve injury.** Neuroscience 2010, SfN's 40th annual meeting, San Diego, CA, USA.

Guzik A, Sliwa A, Lukasiuk K. **Expression of chemokine proteins in the rat model of temporal lobe epilepsy.** FENS Meeting 2008, Geneva, Switzerland.

Professional Memberships

2010-present Society For Neuroscience